CHALMERS
UNIVERSITY OF TECHNOLOGY

A brief introduction to Aeronautics

Tomas Grönstedt, Carlos Xisto, Xin Zhao, Marily Thoma
2024-08-01

Tomas Grönstedt, Professor, Turbomachinery

Foreword

Many excellent books on aviation are available for a beginning student. However, for those who wish to get a first introduction to the field, a study of multiple sources of extensive scope is needed. Furthermore, available texts require a background of fluid mechanics and often also compressible flow and turbomachinery. For this introductory text, only a basic knowledge of mechanics is required. The material brings knowledge together on the modelling of aircraft and the analysis of aero engines. It also touches upon aircraft and engine certification, emissions predictions and discusses how aviation affects climate. Several small but conscious steps have been taken to keep complexity to a minimum, for instance avoiding multiple definitions of thrust and efficiency and providing examples that are interconnected. The analysis of the cruise performance of a modern aero engine is included in the appendix together with a sample prediction on NO_x emissions and the use of the Schmidt-Appleman criteria to evaluate conditions for contrails formation. We predict aircraft performance using an aircraft model that matches the engine, hence the analysis is based on a state-of-the-art existing aircraft-engine-pair currently in commercial operation.

[1] Blue text is included but less important for MMS196 and green text is not included in the MMS196.

NOMENCLATURE

Variables

a	Speed of sound [m/s]
A	Area perpendicular to the flow direction [m^2]
c	Velocity [m/s], also coefficient for lift/drag but then always with a suffix (c_L or c_D).
c_D	Drag coefficient
c_L	Lift coefficient
c_p	Specific heat ratio [kJ/kg·K]
d	Differential
D	Drag [N]
F	Thrust [N]
g	Gravitational constant, 9.81 [m/s^2]
h	Enthalpy (u+pv)
L	Lift [N]
$\boldsymbol{m}$	Mass
$\dot{\boldsymbol{m}}$	Mass flow [kg/s]
M	Mach number
n	Degrees of freedom
p	Pressure [Pa]
P	Power [W/s]
q	Dynamic pressure [Pa]
$\dot{\boldsymbol{Q}}$	Heat transfer rates [W]
R	Gas constant [J/K·kg], but also aircraft Range [km] (should be clear from context what is meant)
RH	Relative humidity
s	Entropy [J/K·kg]
S	Aircraft reference area [m^2]
SFC	Specific Fuel Consumption [mg/Ns]
T	Temperature [K]
t	Time [s]
u	Internal energy
v	Specific volume (1/ρ) [m^3/kg]
$\boldsymbol{V}$	Flight velocity vector (v_x, v_y) [m/s, m/s]
V	Flight speed [m/s]
$\dot{\boldsymbol{W}}$	Mechanical power [W]
z	Elevation

Indices

0	Far upstream, free stream, ambient. Also used to denote stagnation condition (what is meant should be clear from context)
1	Entry for control volumes, inlet entry for engines.
13	Exit of fan (bypass stream) in turbofan
2	Exit for control volumes, fan entry for engines.
21	Exit of fan (core stream) in turbofan
26	High pressure compressor entry
3	Compressor exit
4	Turbine entry
45	Low pressure turbine entry
5	Turbine exit
8	Nozzle exit
18	Bypass duct exit
D	Drag
L	Lift
f	Fuel
grav	Gravimetric
i	Over ice (for relative humidity)
kin	Kinetic energy
o	Overall
p	Propulsive or polytropic. Polytropic refers to turbomachine components (compressors and turbines), whereas propulsive to exhaust jets
SL	Sea Level
vol	Volumetric
x	Axial direction

Greek

α	Angle of attack
$\boldsymbol{\gamma}$	Specific heat ratio of gas. For air $\boldsymbol{\gamma_a} = 1.4$ and $\boldsymbol{\gamma_g} = 1.333$ for gas with combustion products (see also below).
$\boldsymbol{\gamma}$	Climb gradient (see also above, clear from context which is meant).
η	Efficiency
$\boldsymbol{\Pi_{00}}$	Sea level overall pressure ratio set in type certificate. From station 2 to station 3 (see Figure 12)
$\boldsymbol{\rho}$	Density [kg/m^3]

Abbreviations

ATJ	Alcohol-To-Jet
BPR	Bypass ratio

$CAEP$	Committee on Aviation Environmental Protection
$\boldsymbol{E_I}$	Aircraft Energy Intensity [MJ/ASK]
$\boldsymbol{E_{IP}}$	Aircraft Energy Intensity for payload [MJ/tonne·km]
$\boldsymbol{EI_{NOx}}$	Emission index for NOx certification [gram/kN]
F_{00}	Sea level static thrust as set in type certificate [kN]
$HEFA$	Hydro-processed Esters and Fatty Acids
HPC	High Pressure Compressor
HPT	High Pressure Turbine
IPC	Intermediate Pressure Compressor
IPT	Intermediate Pressure Turbine
LPC	Low Pressure Compressor
LPT	Low Pressure Turbine
LTO	Landing-Take-Off cycle
LHV	Lower Heating Value
$MTOM$	Maximum Take-Off Mass [tonnes]
$MTOW$	Maximum Take-Off Weight [N]
OPR	Overall pressure ratio
RGF	Reference Geometric Factor [m^2]
RPK	Revenue passenger kilometer
SAR	Specific Air Range [km/kg fuel]
SFC	Specific Fuel Consumption [mg/Ns]
SIP	Synthesized Iso-Paraffinic Fuels
SOC	State Of Charge
TOC	Top-Of-Climb
TO	Take-Off
Cr	Cruise

Chemical substances

$C_{12}H_{23}$	Average composition representing Jet A
CO	Carbon monoxide
CO_2	Carbon dioxide
H_2	Hydrogen
HC	Unburnt hydrocarbons
O_2	Oxygen
NO_x	Nitrogen oxides

1. BASICS OF FLIGHT DYNAMICS

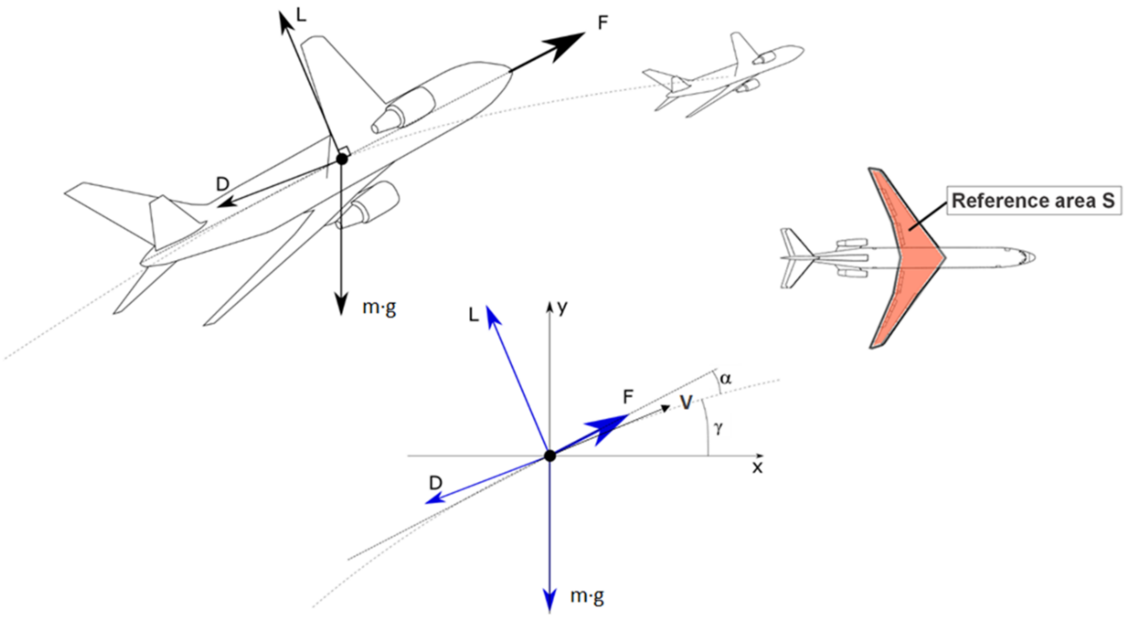

Figure 1: Basic nomenclature for flight mechanics modelling.

As an aircraft flies through the air, the relative speed V between the aircraft and the air creates a friction force that the aircraft must overcome. In addition, the relative velocity also creates a pressure distribution over the aircraft surface that will contribute to the reaction force that the air creates on the aircraft. To predict the performance of the aircraft, we simplify the complex 3-dimensional body that an aircraft represents into a point mass located at the center of gravity of the aircraft. We then study the motion of this point mass under the influence of the fluid forces, the earth's gravitational field and the thrust that the engines of the aircraft produce.

As illustrated in Figure 1, we define lift L and Drag D as reaction forces from the fluid on the aircraft acting in the center of gravity as the aircraft flies with a velocity $\boldsymbol{V}$=(v_x, v_y). The drag force D is acting in the parallel but opposite direction of $\boldsymbol{V}$ and L is directed orthogonal to $\boldsymbol{V}$. Notice that the flight direction, that is the motion of the center of gravity follows the direction of γ, but that the aircraft and engine is directed in the γ+α direction since the aircraft operates in an angle α > 0.0 relative to the direction of flight in order to develop an adequate lift.

The equations relating acceleration and flight motion in the x and y coordinate directions are:

$$\frac{d}{dt}(mv_x) = -L \cdot sin\gamma - D \cdot cos\gamma + F \cdot cos(\alpha + \gamma) \qquad (1.1a)$$

$$\frac{d}{dt}(mv_y) = L \cdot cos\gamma - D \cdot sin\gamma + F \cdot sin(\alpha + \gamma) - mg \qquad (1.1b)$$

where F is the engine thrust and m is the aircraft mass. As an alternative to the equations above, it is possible to formulate the equations in the flight direction:

$$\frac{d}{dt}(mV) = F \cdot cos(\alpha) - D - mg \cdot sin(\gamma) \quad (1.1c)$$

where the V in Equation (1.1c) is the aircraft speed, that is we have $V = \sqrt{v_x^2 + v_y^2}$. Do not confuse the speed V with the velocity vector $\boldsymbol{V}$. The three equations presented above are not independent, but as we will soon see equation (1.1c) may occasionally be preferable over (1.1a/1.1b) for reasons of simplicity. When working with (1.1c) it is possible to also define an equation orthogonal to the flight direction, requiring the definition of a centrifugal acceleration term.

Lift and drag forces are developed from the basic aerodynamic relations according to:

$$L = c_L(\alpha) \cdot q \cdot S \quad (1.2a)$$

$$D = c_D(\alpha) \cdot q \cdot S \quad (1.2b)$$

where S is the aircraft reference area, indicated in Figure 1 and q is the dynamic pressure $\frac{\rho v^2}{2}$. For high-speed flows it is possible to cast the dynamic pressure into a more convenient form depending on the pressure p and the Mach number M:

$$q = \frac{\rho V^2}{2} \overset{\substack{Mach\,number\,definition \\ +\,ideal\,gas\,law}}{\cong} \frac{p\left(M\sqrt{\gamma_a RT}\right)^2}{2RT} = \frac{\gamma_a p}{2} M^2 \quad (1.3)$$

The Mach number is properly introduced in the next chapter, here we simply state that it represents the ratio of the speed of the aircraft V and the speed of sound which is equal to $\sqrt{\gamma_a RT}$. As an example, if you fly twice the speed of sound then M = 2.0. The lift and drag coefficients $c_L(\alpha)$ and $c_D(\alpha)$ in (1.2a) and (1.2b) are aerodynamic parameters specific for the aircraft being studied. They depend primarily on the angle of attack α of the aircraft, but also on the Mach number and to a lesser degree on the Reynolds number. The Reynolds number broadly quantifies how important the friction forces are in relation to inertia forces in the fluid flow. Although the Reynolds number has a direct effect on skin friction, it will not be discussed further in this introductory text.

The first simplification we make is that we approximate the aircraft mass as constant, which allows us to factor out m in $\frac{d}{dt}(mv_x)$ and in $\frac{d}{dt}\left(mv_y\right)$. Actually, the mass drops slowly due to the combustion of the fuel, unless it is an electric aircraft which maintains its mass as constant. Although the velocity varies in a mission, it is customary to split the whole mission into different flight phases for which the flight speed is approximately constant. If we therefore assume that the aircraft velocity also remains constant, we get:

$$0 = -L \cdot sin\gamma - D \cdot cos\gamma + F \cdot cos(\alpha + \gamma) \qquad (1.4a)$$

$$0 = L \cdot cos\gamma - D \cdot sin\gamma + F \cdot sin(\alpha + \gamma) - mg \qquad (1.4b)$$

Equation (1.4a) can be used to eliminate F in equation (1.4b), to obtain:

$$0 = L \cdot cos\gamma - D \cdot sin\gamma + \frac{L \cdot sin\gamma + D \cdot cos\gamma}{cos(\alpha+\gamma)} \cdot sin(\alpha + \gamma) - mg \qquad (1.4c)$$

We usually set γ in (1.4c) to a fixed value to obtain a specific flight path. Solving (1.4c) then requires an iteration in α. For instance, we may assume $\gamma = -3$ degrees to model the aircraft performance during a descent phase. If we then guess α we can evaluate L and D from (1.2a) and (1.2b) using correlations on c_L and c_D, assuming that we have also prescribed the altitude and speed and ambient conditions for the aircraft. The values on L and D can then be fed into (1.4c) together with the current mass of the aircraft. If the α value assumption was correct the right-hand side in (1.4c) will evaluate to zero, otherwise the assumption needs updating to reach convergence. To approximate the aircraft mass variation the thrust F can be evaluated and the fuel flow need can then be estimated from the engine modelling. By discretizing flight legs such as climb, cruise and descent and updating the aircraft mass, an entire mission and its aircraft fuel burn and mass variation can be approximated.

Constant speed, constant altitude flight

From equation (1.4a/1.4b) we will now derive the special case of constant speed and constant altitude flight. This is a common flight phase, in which a commercial aircraft conducting a longer mission will spend most of its time.

Constant altitude flight means no climb gradient $\gamma = 0.0$. The α is on the other hand usually not zero, but a small positive value is typically needed to maintain a lift force that balances out the effect of gravity. We get:

$$D = F \cdot cos(\alpha)$$

$$0 = L + F \cdot sin(\alpha) - mg$$

From which we can eliminate the net force F.

$$mg = L + \frac{D}{cos(\alpha)} \cdot sin(\alpha) \quad \Longrightarrow \quad mg = L + D \cdot tan(\alpha)$$

Constant speed, constant altitude normally means that α is only a few degrees, so $sin(\alpha)$ and $tan(\alpha)$ are approximately zero, whereas $cos(\alpha)$ is approximately 1. Also, lift is usually much larger than drag, so we may often approximate the above relations with:

$$D = F \quad (1.5a)$$

$$mg = L \quad (1.5\text{b})$$

In conclusion, looking at (1.5a) and (1.5b), the net thrust is thus needed to overcome the aircraft drag, and the lift balances the gravity force on the aircraft.

Constant speed, constant climb gradient flight

For constant speed, constant climb gradient flight we need to use (1.4c) directly using the α iteration scheme described above. The procedure is the same for both climb and descent.

Sample correlation for C_L and C_D

Typical aero data, c_L and c_D as a function of the angle of attack α, for a high-performance propeller aircraft at cruise is found in Figure 2 below.

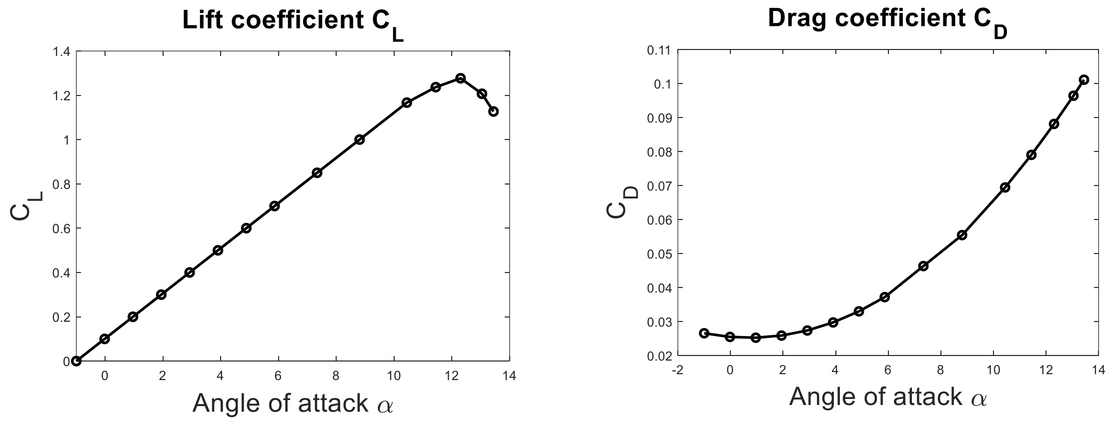

Figure 2: Aerodynamic data for typical high-performance propeller aircraft

As α increases $c_L$increases but so does c_D. Although the drag coefficient increases progressively with α, lift suddenly drops off, due to that the flow starts to separate over the aircraft. In basic texts on aerodynamics, you frequently see much higher lift coefficients in relation to drag than presented in the graphs above. This data is then based on 2D wing tests only, whereas the data given above is characteristic of the whole aircraft. For the above data set the best lift over drag happens at around an angle of attack α=6.0 degrees, with a c_L/c_D value close to 19.

Breguet range

A first understanding of an aircraft's range can be derived from something called the Breguet range. The Breguet range is derived for constant speed level flight using the ratio between how range changes with used fuel, or more simply put from the aircraft "milage". We observe:

$$\frac{Distance\ flown\ per\ unit\ time}{Aircraft\ mass\ change\ per\ unit\ time} = \frac{V}{-\dot{m}_f} \quad [m/kg]$$

To model the engine performance, we first introduce a metric called the SFC.

$$SFC = \frac{Fuel\ consumed\ per\ unit\ time}{Thrust\ developed\ by\ the\ engine} = \frac{\dot{m}_f}{F}$$

We also assume that constant speed constant altitude flight is taking place, that is that we can use equation (1.6a). The Breguet range can then be obtained:

$$\frac{V}{-\dot{m}_f} = -\frac{V}{F \cdot \frac{\dot{m}_f}{F}} = -\frac{V}{F \cdot SFC} = -\frac{V}{D \cdot SFC} = -\frac{V \cdot \frac{L}{D}}{L \cdot SFC} = -\frac{V \cdot \frac{L}{D}}{m_{aircraft} \cdot g \cdot SFC} \qquad (1.6)$$

Since the mass changes we need to integrate to establish the distance flown, referred to as the Breguet range R:

$$R = -\int_{m_{aircraft,start\ cruise}}^{m_{aircraft,end\ cruise}} \frac{V \cdot \frac{L}{D}}{m_{aircraft} g \cdot SFC} dm_{aircraft} = \frac{L}{D} \frac{V}{g \cdot SFC} \ln \frac{m_{aircraft,start\ cruise}}{m_{aircraft,end\ cruise}}$$

Example 1: A 19-passenger four engine turboprop aircraft has a cruise speed of V= 94 m/s. The mass of the aircraft at initial cruise is 8580 kg and at end of cruise it is 5300 kg. The lift over drag is estimated at 19.3 and the SFC of the engine is predicted at 7.2 mg/Ns.

The Breguet range is:

$$R_{Breguet} = \frac{L}{D} \frac{V}{g \cdot SFC} \ln \frac{m_{aircraft,start\ cruise}}{m_{aircraft,end\ cruise}} = 12500\ km \text{ !!!}$$

Example 1 above shows the enormous range that aircraft can achieve. Of course, this would correspond to a flight time of almost 37 hours, a horrendous experience for any passenger. Cruise milage for the same aircraft was estimated at 0,021 liter jet fuel per passenger kilometer.

State-of-the-art aircraft performance

Clearly range R is dependent on the amount of payload carried by the aircraft. This relation can be illustrated in a payload range diagram:

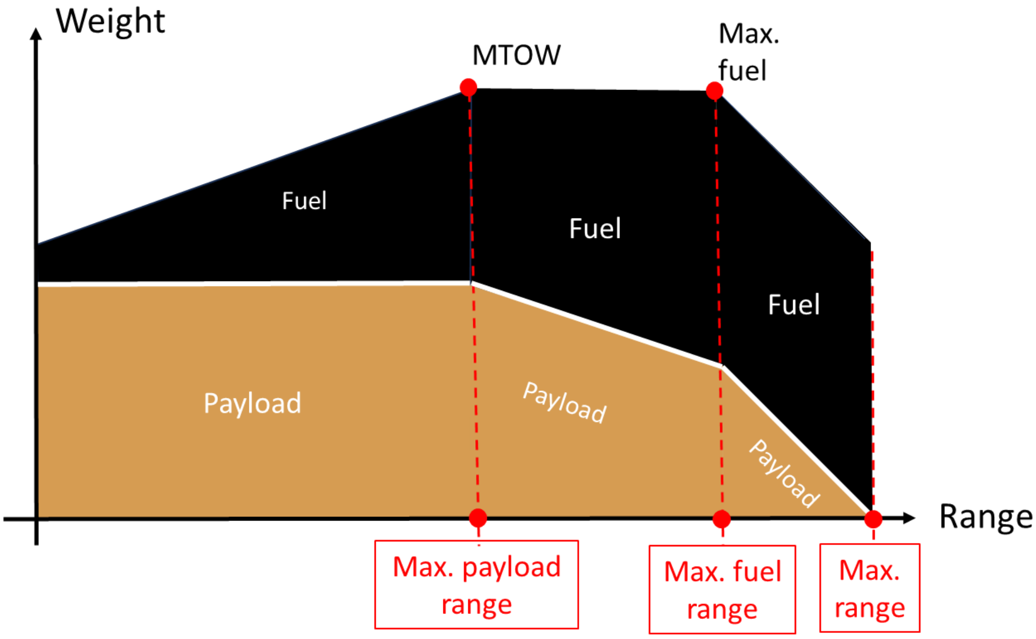

Figure 3: Payload range diagram.

Maximum payload range, see Figure 3, is the maximum range that the aircraft can achieve carrying the maximum payload. This condition coincides with the aircraft loading so much fuel that it reaches MTOW (Maximum Take-off Weight). MTOW is the maximum weight for which the pilot is allowed to take-off as set by the certification of the aircraft. When range is discussed for aircraft, without further specification, it is often the maximum fuel range that is referred to. This means the range that the aircraft can fly when taking off at the maximum weight allowed with all fuel tanks full. This means loading so much fuel that some of the payload cannot be carried. Finally, with no payload, the range is maximized achieving the max. range or "ferry range" of the aircraft.

To make comparisons possible across different transport modes and aircraft classes, it is quite useful to develop something called aircraft energy intensity, E_I. It is derived from the energy needed to move a passenger a certain distance.

$$E_I = \frac{LHV \cdot m_f}{Seats \cdot R} \quad \left[\frac{MJ}{ASK}\right] \qquad (1.7a)$$

$$E_{IP} = \frac{LHV \cdot m_f}{Total\ payload \cdot R} \quad \left[\frac{MJ}{tonne \cdot km}\right] \qquad (1.7b)$$

Where $Seats$ are the number of seats in the aircraft, m_f the mass of fuel used, LHV the fuel heating value, and R is the distance travelled. ASK is available seat kilometers. Here, data is presented for a typical modern medium range aircraft, the Airbus aircraft A321neo. The extension "neo" refers to "new engine option" allowing the PW1000G (Pratt & Whitney) and LEAP-1A (CFM International) to be fitted to the aircraft. The A321neo is available in several variants, but here the longest-range variant with three additional center tanks (ACTs) is given. See Table 1 for a compilation of data.

Table 1: some key performance parameters for a state-of-the-art aircraft (A321neo)

Aircraft type	**A321neo** (WV072)
Type of aircraft	Medium range
Max payload range	5651 km
Max fuel range	7414 km
Number of seats (economy seating)	220
LHV	43,0 [MJ/kg]
Fuel burn for max payload range	20,204 kg
Total payload	23,5 tonnes

E_I	0,70 [MJ/ASK] (from 1.8a)
E_{IP}	6,53 [MJ/tonne· km] (from 1.8b)
Max take-off mass	97,000 kg
F_{SL}	156 kN (per engine)
S	125.4 m^2 (authors estimate)
Wetted area	1129.0 m^2 (authors estimate)
$\frac{W_{TO}}{S}$	7619 N/ m^2 (authors estimate)
$\frac{F_{SL}}{W_{TO}}$	0.3265

Weight specific excess power

It is possible to develop a "master equation" for aircraft design by combing equation (1.1c) with assumptions on aircraft aerodynamics. If equation (1.1c) is multiplied by the speed V we get:

$$\frac{d}{dt}(mV) = F \cdot cos(\alpha) - D - mg \cdot sin(\gamma) \quad (1.1c)$$

Multiplying (1.1c) with the speed gives:

$$V\frac{d}{dt}(mV) = FV \cdot cos(\alpha) - DV - mgV \cdot sin(\gamma)$$

Re-writing the term on the left-hand side, approximating $cos(\alpha)$ = 1.0, and observing that $V \cdot sin(\gamma) = \frac{dh}{dt}$ where h is the altitude we get:

$$\frac{d}{dt}\left(\frac{mV^2}{2}\right) = FV \cdot cos(\alpha) - DV - mg\frac{dh}{dt}$$

Which can be changed into:

$$\frac{d}{dt}\overbrace{\left(\frac{mV^2}{2} + mgh\right)}^{W_{tot}} = \frac{dW_{tot}}{dt} = V(F - D)$$

showing how the total energy of the aircraft W_{tot} changes with thrust and drag. Thrust larger than the drag is converted to either increased kinetic or increased potential energy (or both). In aerospace, it is customary to use height rather than total energy, introducing the energy height as $z_e = h + \frac{V^2}{2g}$. This gives the equivalent form:

$$\frac{dz_e}{dt} = \frac{V(F - D)}{mg}$$

This relation shows how excess thrust, that is thrust larger than the drag, is used to increase either the altitude or the speed of the aircraft. The left-hand side of the equation above is frequently referred to as the weight specific excess power and is denoted P_s. Thus:

$$P_s = \frac{V(F - D)}{mg} \qquad (1.8)$$

Wing and thrust loading, constraint analysis

To relate sea-level / take-off performance with flying at altitude we introduce the thrust lapse factor α_{TL}. The thrust decreases at altitude and speed due to the variation of air density and the engine operating condition. We also introduce the fuel consumption parameter β which quantifies how much mass has been depleted by fuel combustion:

$$\alpha_{TL} = \frac{F}{F_{SL}}$$

$$\beta = \frac{m}{m_{TO}}$$

Where F_{SL} is the thrust delivered by the engine at sea level and m_{TO} is the take-off mass. Introducing the two relations above into equation (1.8) gives:

$$P_s = \frac{V(\alpha_{TL}F_{SL} - D)}{\beta m_{TO}g} = \frac{V\alpha_{TL}F_{SL}}{\beta m_{TO}g} - \frac{VD}{\beta m_{TO}g}$$

which can be re-written to:

$$\frac{F_{SL}}{m_{TO}g} = \frac{\beta}{\alpha_{TL}}\left(\frac{D}{\beta m_{TO}g} + \frac{P_s}{V}\right) \qquad (1.9)$$

By relating lift to drag, we can obtain an equation that allows us to understand how thrust and wing area are constrained by the specifications for the aircraft! A quite good approximation for how lift relates to drag is given by:

$$C_D = C_{D0} + K_1 C_L^2 \qquad (1.10)$$

Combining equation (1.2b) and (1.10) introducing them into (1.9) gives:

$$\frac{F_{SL}}{m_{TO}g} = \frac{\beta}{\alpha_{TL}}\left(\frac{qS}{\beta m_{TO}g}(C_{D0} + K_1 C_L^2) + \frac{P_s}{V}\right)$$

By specializing (1.9) to cases where $L = nmg$ (n is the number of g-loads orthogonal to V) and using equation (1.2a) we obtain the master equation by replacing C_L:

$$\frac{F_{SL}}{m_{TO}g} = \frac{\beta}{\alpha_{TL}}\left(\frac{qS}{\beta m_{TO}g}\left(C_{D0} + K_1\left(\frac{n\beta}{q}\frac{W_{TO}}{S}\right)^2\right) + \frac{P_s}{V}\right) \qquad (1.11)$$

The master equation, equation (1.11), can be used to predict performance of the aircraft in a large number of conditions. By specializing the master equation to a given flight condition, constraints can be formulated understanding how design choices limit the aircraft performance. In Figure 4 below constraints imposed on a fighter aircraft, denoted AAF, are used to illustrate how turn capability, a high speed requirement and the take-off field length limit the combination of possible wing loading $\frac{W_{TO}}{S}$ and thrust loading $\frac{T_{SL}}{W_{TO}}$. All points that fulfill all the constraints form a solution space, indicated by the green area in Figure 4.

The final choice for wing loading and thrust loading is a trade on cost and additional performance benefits that can be achieved from their variations. This is a characteristic trait for the art of aircraft design, showing that for a set of requirements much fewer choices of wing and propulsion system, than may have been initially viewed, would qualify as feasible designs. For this reason, certain aircraft types typically have similar values on thrust and wing loading, this is indicated in Figure 5 below.

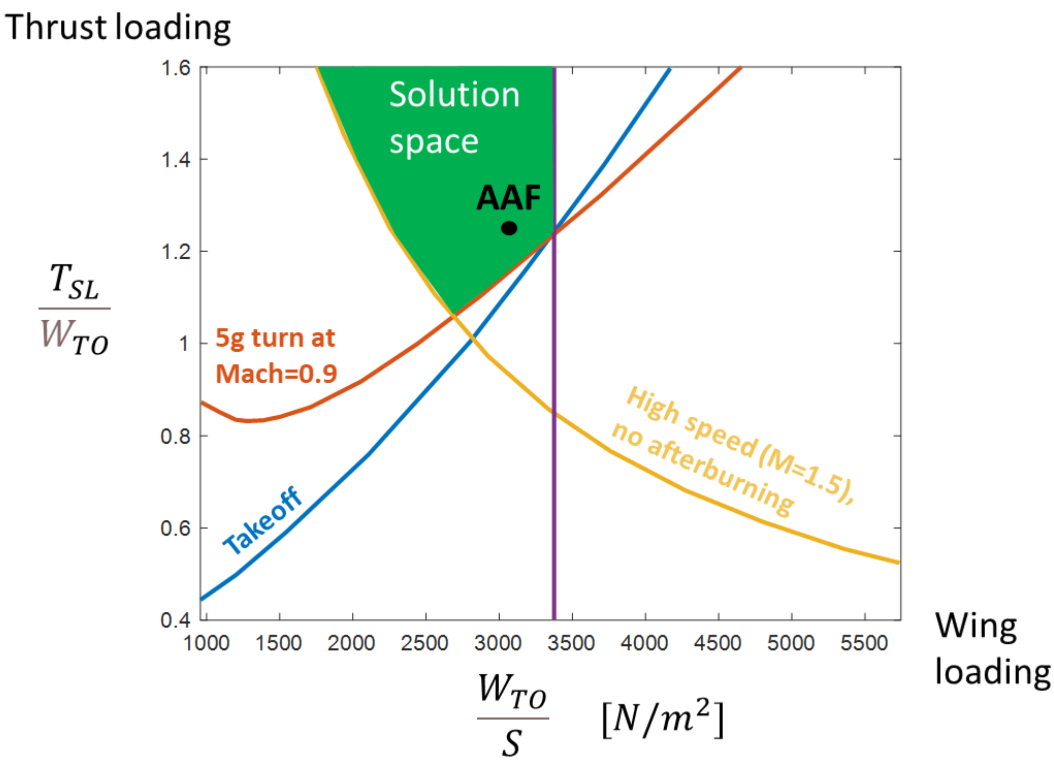

Figure 4: Constraint diagram giving an example of how aircraft performance requirements limit the solution space.

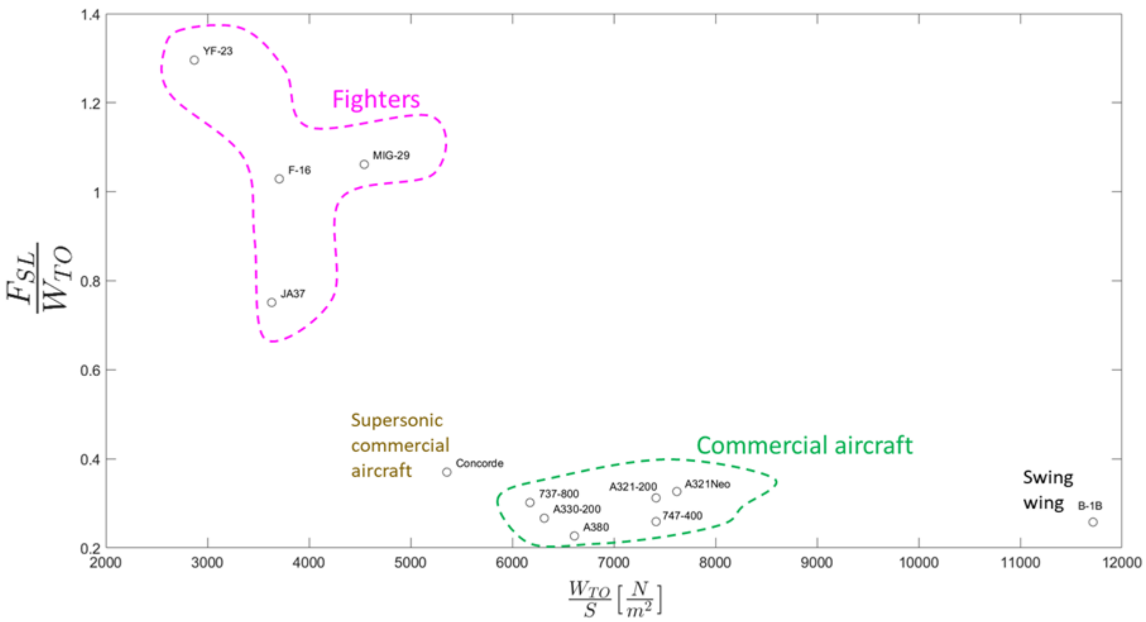

Figure 5: Wing and thrust loading for different aircraft types, re-worked form [1]

The most notable difference is the fighter aircraft having a much higher thrust to weight and lower wing loading than commercial aircraft. Commercial aircraft are all located in a quite small range. The supersonic transport aircraft Concorde lies between the Fighter and the commercial aircraft. The B-1B aircraft is interesting since it has a swing wing allowing it to take-off with a much smaller wing and still operate at very high speeds.

2. PROPULSION FUNDAMENTALS

The heat engine

A heat engine is simply a gadget which you put some heat into ($\dot{Q}$), to get some mechanical output ($\dot{W}$). In aerospace applications mechanical output usually means creating shaft work or performing fluid acceleration. In the usual academic manner, we illustrate a heat engine by a generalized process sketch as seen in Figure 6. We deliberately choose to have an inflow and an outflow to the engine since all interesting aerospace applications are open system flow machines.

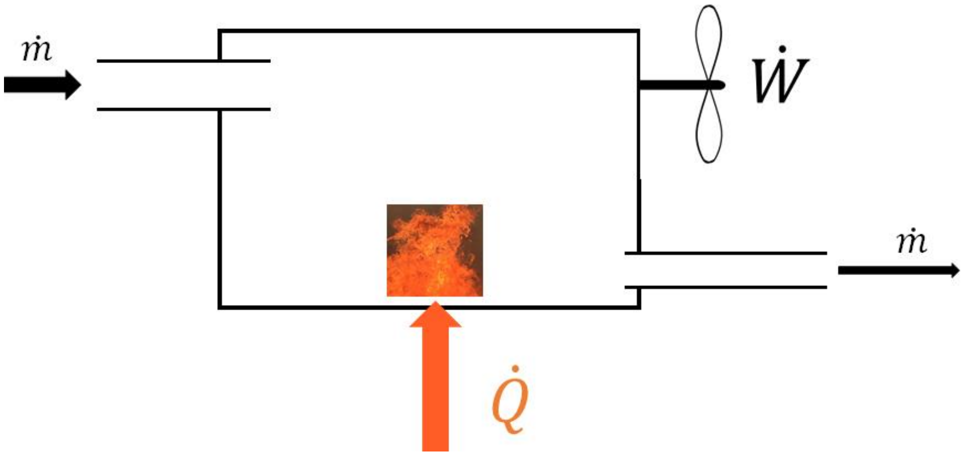

Figure 6: Heat engine developing work output $\dot{W}$ from added heat $\dot{Q}$ as a fluid is flowing through the system.

Applying the first law (energy conservation) for the open systems to our engine we get:

$$\dot{Q} - \dot{W} = \dot{m}\left[(h_2 - h_1) + \frac{1}{2}(c_2^2 - c_1^2) + g(z_2 - z_1)\right] \quad (2.1)$$

where h is fluid enthalpy, c is fluid velocity and z is fluid elevation. As you probably recall from your thermodynamics classes, enthalpy is a bureaucratically clever form of representing energy. It manages to get rid of the explicit need to use pressure in Equation (2.1). The pressure volume terms arising at the in- and outflow boundaries are elegantly hidden in the enthalpy terms.

Since speeds are high in aero engines and work input/output are as well, the third term on the right-hand side, the elevation term, is usually comparative small and can therefore be dropped. This simplifies equation (2.1) to:

$$\dot{Q} - \dot{W} = \dot{m}\left[(h_2 - h_1) + \frac{1}{2}(c_2^2 - c_1^2)\right] \quad (2.2)$$

The game plan for an aero engine is to increase the kinetic energy of the incoming fluid through fuel combustion ($\dot{Q}$) and thereby develop a reactive thrust as illustrated in Figure 7.

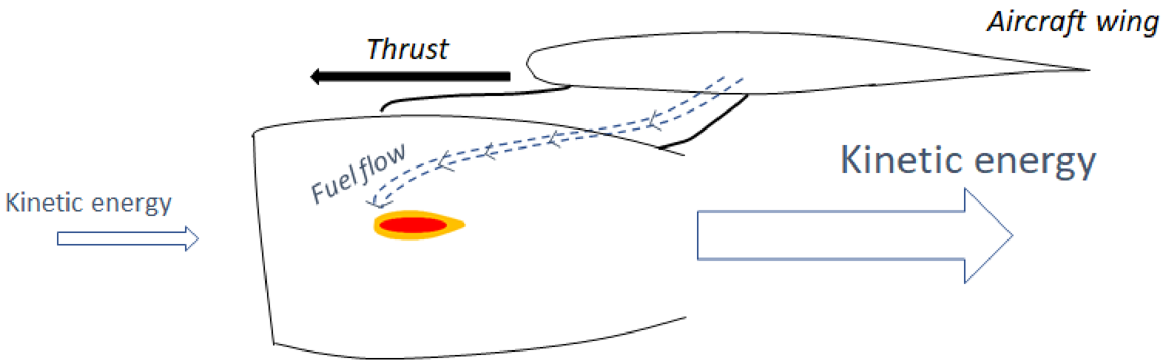

Figure 7: Typical underwing installation of an aero engine developing propulsive power by reaction

As an alternative to increasing the fluid energy content represented by the right-hand side of equation (2.2), the released energy can also be used to drive a propeller. Then, the heat $\dot{Q}$ is then instead used to mainly increase $\dot{W}$ in the form of shaft work. Such a propeller engine would then derive most of its thrust by accelerating another fluid stream of air around the engine.

Momentum conservation and thrust

To write down an expression for the developed thrust, we simply apply momentum conservation. The net thrust on a control volume is equal to the change in momentum. Hence,

$$\sum(\dot{m}c_x)_{out} - \sum(\dot{m}c_x)_{in} = \sum F_x \qquad (2.3)$$

The terms of the type $\dot{m}c$ in equation (2.3) represent the momentum of the in- and outflows, and the F terms are forces on the fluid directed in the axial direction. Momentum is a vectorial property, but as seen from Figure 7 the aero engine action is quite well aligned with a single coordinate axis. As a matter of fact, aero engines are often installed at a slight angle to compensate for the aircraft nose pointing upward during cruise making its action very close to axial.

To make the application of equation (2.3) more obvious we re-draw Figure 7, now with a control volume and the mass flow streams more clearly indicated. The refined figure is seen in Figure 8.The engine sucks in a mass flow $\dot{m}_0$ and out goes the same amount of air plus the fuel flow added $\dot{m}_0 + \dot{m}_f$. If the fluid is accelerated through the control volume, its momentum has been increased and according to equation (2.3) some forces F must have acted on the fluid to create that effect. According to Newtons law of action/reaction there must then also have been an equal and opposite force serving to push the aircraft forward, in the figure it is indicated as “Thrust”.

We follow aero engine conventions and denote the station upstream of the engine by 0 and the engine exit by 8. Hence, A_8 in refers to the cross-sectional area perpendicular to the flow direction of the fluid flowing out of the engine. The pressure surrounding the control volume is denoted p_0.

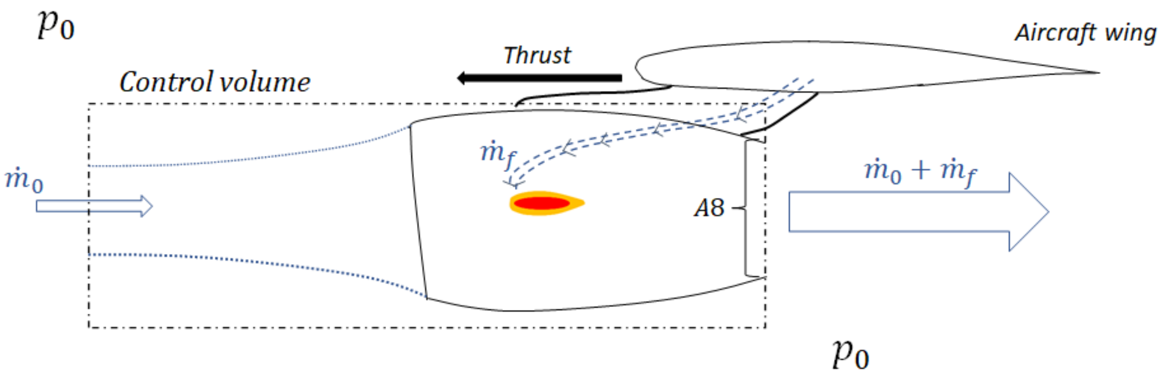

Figure 8: Aircraft engine with control volume

Simplifying equation (2.3) to our special case we get:

$$Thrust \ = \ F = (\dot{m}_0 + \dot{m}_f)c_8 - \dot{m}_0 c_0 \qquad (2.4)$$

Why are there no pressure terms in Equation (2.4)? Far upstream of the engine, the pressure is uniform and simply equal to p_0. This is why the control volume is extended so far upstream. When the mass flow gets closer to the engine the pressure in the fluid stream starts to change. The shape and values of the pressure contours around the engine depends both on the flow around the engine installation and how hard the engine is working. For example, if the engine runs at low power and the aircraft is flying at a high speed, the engine will not be able to ingest all the flow, but some flow “spills” around the engine creating additional installation drag.

For the exit the pressure, in station 8, the pressure is often quite well approximated by p_0. The air fuel mix that has been pressurized by the engine expands down to ambient pressure and the fluid is accelerated to its exit speed c_8. However, if the pressure upstream of the engine exit reaches sufficiently high values for the flow the exit flow will eventually reach the speed of sound. As we will soon show, after this speed is reached further engine exit pressure build-up will not result in further velocity increase. Instead, a pressure p_8 larger than ambient starts to build up giving a net addition to the thrust. To account for this effect a pressure thrust term, $(p_8 - p_0)A_8$, needs to be included in Equation (2.4):

$$\boldsymbol{F} = (\dot{\boldsymbol{m}}_0 + \dot{\boldsymbol{m}}_f)\boldsymbol{c}_8 + (\boldsymbol{p}_8 - \boldsymbol{p}_0)\boldsymbol{A}_8 - \dot{\boldsymbol{m}}_0\boldsymbol{c}_0 \qquad (2.5)$$

For common civil aero engines this normally does not happen at take-off, but it is frequently the case at cruise speeds.

Example 2: An aircraft is flying at 200 m/s and the mass flow through the engine is 100 kg/s. The flow velocity out of the engine c_8 is 400 m/s. The fuel flow is 2 kg/s. Compute the thrust. Assume that the pressure in the exhaust nozzle is lower than the limit when the pressure thrust term is established.

Solution: Since the speed of sound is not reached in the nozzle the pressure thrust term is not needed and we can write down the thrust using Equation (2.4). We get:

$$F = (\dot{m}_0 + \dot{m}_f)c_8 - \dot{m}_0 c_0 \ = (100 + 2.0) \cdot 400 \ - \ 100 \cdot 200 \ = 20800\ N$$

Developing the exhaust modelling for thrust

After our deceptively simple way to make a connection between the heat engine and reaction thrust, we will now develop the details needed to make thrust calculations for jet engine exhaust nozzles. Many readers may already have seen a lot of this material presented in basic texts on fluid mechanics and/or thermodynamics and you will then find this section a light read. Although many relations are derived from scratch, we avoid the most basic exercise of developing equations for mass, momentum, and energy conservation in fluids. We also inherit a number of key relations from thermodynamics.

The first task is to get to know how we predict the different variables in the thrust equation, as defined by equation (2.5). As we do this, we also develop a number of relations for high-speed flows. These expressions will then be used at least throughout this text, and should you follow the aerospace track you will use them a lot. The second task is then to go on to study the thermodynamics of the engine core components. We explain how the processes of compression, heat addition and expansion interrelate to the thrust equation.

Speed of sound and isentropic compression relations

The first and second law of thermodynamics are frequently combined into a very useful expression called the Gibbs's equation. It comes in two forms depending on if enthalpy h or internal energy u is preferred:

$$Tds = dh - \frac{dp}{\rho} \qquad (2.6a)$$
$$Tds = du + pdv \qquad (2.6b)$$

where the second form 2.6b follows from 2.6a and the definition of the enthalpy $h{=}u{+}pv$. Notice that Equation (2.6a/2.6b) do not contain any work or heat addition terms but they only interrelate the properties of the fluid. This makes them very useful! For instance, in thermodynamics we often study isentropic processes ($ds = 0$) since they represent reversible loss-less and, in that sense, ideal process which we strive to achieve.

Let's go ahead and explore the isentropic form of Equation (2.6a), that is when $ds = 0$:

$$dh = \frac{dp}{\rho} \quad (2.7)$$

For an ideal gas, we have:

$$\rho = \frac{p}{RT} \qquad (2.8)$$

Combining we get:

$$dh = \frac{RTdp}{p} \quad (2.9)$$

By replacing the enthalpy with the specific heat c_p we get:

$$\frac{c_p dT}{T} = \frac{Rdp}{p} \quad (2.10)$$

If we then integrate and neglect the temperature variation of c_p we arrive at:

$$c_p ln\frac{T_2}{T_1} = R\frac{p_2}{p_1} \quad (2.11)$$

Using the logarithm laws, we directly get:

$$\frac{T_2}{T_1} = \left(\frac{p_2}{p_1}\right)^{\frac{R}{c_p}} \quad (2.12)$$

The specific heat ratios c_p and c_v are defined as partial derivatives but these definitions simplify to normal derivatives for ideal gases:

$$c_p = \left(\frac{\partial h}{\partial T}\right)_p = \frac{dh}{dT} \quad (2.13)$$

$$c_v = \left(\frac{\partial U}{\partial T}\right)_V = \frac{dU}{dT} \quad (2.14)$$

From the definition of enthalpy, and the ideal gas law get:

$$h = u + pv \ = \ u \ + \ RT$$

Which by differentiation with respect to T gives:

$$\frac{dh}{dT} = \frac{du}{dT} \ + \ R \ \Longrightarrow \qquad c_p = c_v \ + \ R \quad (2.15)$$

The ratio of the two specific heats, the specific heat ratio, is defined as

$$\gamma = \frac{c_p}{c_v} \quad (2.16)$$

By some algebraic manipulation of 2.15 and 2.16 we update Equation (2.12) slightly to its more commonly used form:

$$\frac{T_2}{T_1} = \left(\frac{p_2}{p_1}\right)^{\frac{\gamma-1}{\gamma}} \qquad (2.17)$$

Using equation (2.17) and the ideal gas law to relate density ratios with pressure ratios gives:

$$\frac{P_2}{P_1} = \left(\frac{\rho_2}{\rho_1}\right)^{\gamma} \qquad (2.17b)$$

This can be seen by replacing the temperature ratio using the ideal gas law, and then group the pressure ratios together. This simplifies to equation (2.17b).

Apart from momentum conservation we often make use also of conservation of mass, here manifested by the continuity equation for steady flows:

$$\dot{m} = \rho A c \qquad (2.18)$$

The corresponding differential form of the continuity equation is:

$$\frac{dA}{A} + \frac{d\rho}{\rho} + \frac{dc}{c} = 0 \qquad (2.19)$$

We have already introduced momentum conservation for a control volume through equation (2.3). Another form of 2.3 can be obtained by replacing the mass flows using (2.18) and simplifying to a 1D single inflow, single outflow system. If the forces in the sum on the right-hand side of (2.3) arise solely from pressure terms we then get:

$$\rho_2 A c_2^2 - \rho_1 A c_1^2 = p_1 A_1 - p_2 A_2 \implies p_2 + \rho_2 c_2^2 = p_1 + \rho_1 c_1^2 \quad (2.3b)$$

Its corresponding differential form reads:

$$\rho c dc = -dp \qquad (2.20)$$

Perhaps somewhat unexpectedly, we now have enough information to predict the speed of sound! The derivation studies a planar wave *(dA=0)* using both the continuity and the momentum equations to develop the following result:

$$a^2 = \frac{dp}{d\rho} \qquad (2.21)$$

The details leading up to Equation (2.21) are found in Appendix A. We can use (2.17b) to progress beyond (2.21) by realizing that:

$$\frac{p_2}{p_1} = \left(\frac{\rho_2}{\rho_1}\right)^{\gamma} \implies p = const \cdot \rho^{\gamma}$$

where the constant simply groups the initial state 1 for the process. Since the final state 2 is arbitrary we can write the expression also in the form given to the right. A derivative of the expression to the right produces:

$$\frac{dp}{d\rho} = \frac{d(const \cdot \rho^{\gamma})}{d\rho} = const \cdot \gamma \rho^{\gamma-1} = \frac{const \cdot \gamma \frac{p}{const}}{\rho} = \gamma \frac{p}{\rho}$$

We then get:

$$a^2 = \gamma \frac{p}{\rho} = \gamma R T \implies a = \sqrt{\gamma R T} \qquad (2.22)$$

The speed of sound in a perfect gas can consequently be computed solely on gas properties and the local temperature. The speed is actually a lower bound for wave propagation speed in fluids, only valid for small isentropic waves such a sound. Stronger waves such as travelling shock waves and reacting shock always travel at higher speeds.

Example 3: For air at 300 K estimate the speed of sound.

Solution: For air, the average molecular weight is around $M_{w,air}$ = 28.96 g/mol. From the universal gas constant $R_u=8.314$ J/(kmol·K) we get R for air as:

$$R = \frac{R_U}{M_{w,air}} = 287.05\,J/kg\cdot K$$

Air is mostly diatomic and diatomic gases have 5 degrees of freedom at low temperatures, 3 translational and 2 rotational. From the theory of statistical physics, we might know that the number of degrees of freedom relate to the specific heat ratio γ by:

$$\gamma = \frac{n+2}{n} = \frac{5+2}{5} = 1{,}4$$

We get the speed of sound:

$$a = \sqrt{\gamma RT} = 347.2\,m/s$$

Nozzle flow theory and thrust

Now, that we know a little bit more about thermodynamics and have the speed of sound better explained, we are ready to go back to analyze thrust term for the aero engine exhaust. First, we define the Mach number as the ratio between the local velocity c and the speed of sound a:

$$M = \frac{c}{a} \qquad (2.23)$$

If M is larger than 1.0 we call the flow supersonic, and if smaller than 1.0 it is called subsonic. By using the above equations, we will now be able to derive a really interesting result about flows in converging and diverging ducts. Taking the momentum equation on differential form (2.20) and dividing it with $d\rho$ gives:

$$\frac{\rho c dc}{d\rho} = -\frac{dp}{d\rho} = -a^2$$

The last equality comes from Equation (2.21). Using this result in the continuity on differential form (2.19) gives:

$$\frac{dA}{A} - \frac{cdc}{a^2} + \frac{dc}{c} = 0$$

Which simplifies to:

$$(M^2-1)\frac{dc}{c} = \frac{dA}{A} \qquad (2.24)$$

We immediately realise that the flows behave quite differently depending on whether the Mach number is smaller or larger than 1.0 because the factor leading the left-hand side then changes sign. If for instance the area increases and the flow is subsonic, then $\frac{dA}{A} > 0$ and $(M^2-1) < 0$ and then $\frac{dc}{c} < 0$. Thus, the fluid slows down. The four cases are illustrated in Table 2 below.

Table 2: The four different cases as predicted by formula 2.24.

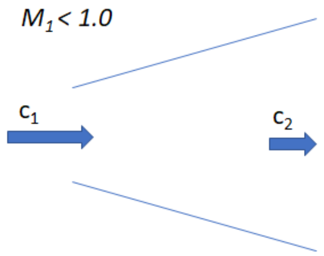 Subsonic flow in a divergent duct => fluid slows down	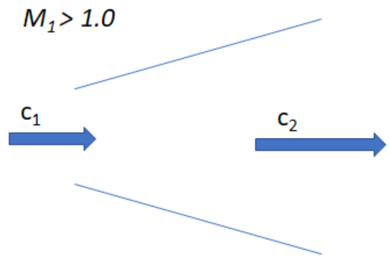 Supersonic flow in a divergent duct => fluid accelerates
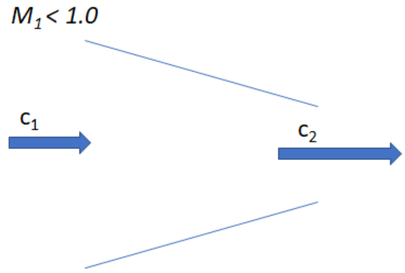 Subsonic flow in a convergent duct => fluid accelerates	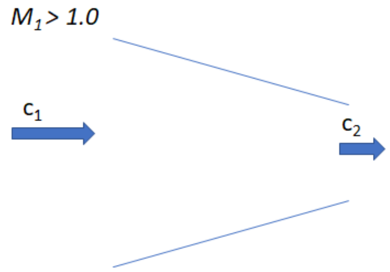 Supersonic flow in a convergent duct => fluid slows down

So, we can understand a little bit more of what happens in the exhaust nozzle of a jet engine. The flow goes through the convergent nozzle approaching the exit, the fluid accelerates increasing its Mach number towards 1.0.

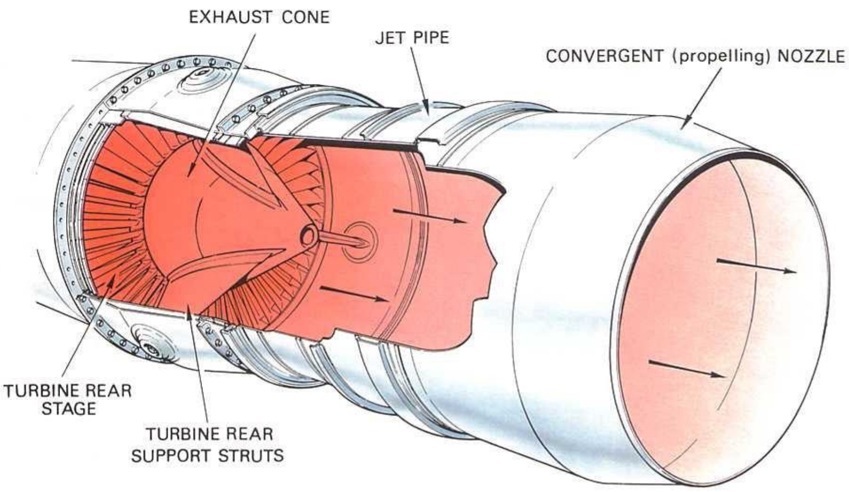

Figure 9: Jet engine exit, with converging nozzle [2]

In an engine the velocity at the nozzle entry is subsonic. Hence, equation (2.24) and the figure in the lower left of Table 2 show that the fluid will accelerate! This will of course help to develop the thrust since the exhaust momentum term reads $(\dot{m}_0 + \dot{m}_f)c_8$. The remaining bit of this section will be devoted to see how far this process can be driven, and to analyze what happens to other parameters such as pressure and temperature.

First, let us revisit the first law for open systems.

$$\dot{Q} - \dot{W} = \dot{m}\left[(h_2 - h_1) + \frac{1}{2}(c_2^2 - c_1^2)\right] \quad (2.2)$$

and group the velocity and enthalpies together, by using what we call the stagnation enthalpy h_0:

$$h_0 = h + \frac{c^2}{2} \qquad (2.25)$$

Equation (2.2) then simplifies to:

$$\dot{Q} - \dot{W} = \dot{m}(h_{02} - h_{01}) \quad (2.26)$$

Equation (2.26) is quite useful for most components using air in propulsion systems. Many times, we look at components that either have heat input/output or work input/output. For the "heat only" case we get:

$$\dot{Q} = \dot{m}(h_{02} - h_{01}) \qquad (2.26b)$$

And for the "work only" case we get:

$$-\dot{W} = \dot{m}(h_{02} - h_{01}) \; (2.26c)$$

Notice that Equation (2.2) and its forms (2.26, 2.26b, 2.26c) are very practical since they give you the freedom to choose control volume boundaries. So far, we have only discussed its use for the whole engine. In the upcoming discussion we will specialize the forms of Equation (2.26) to several different components of the aero engine.

The exhaust nozzle is actually a particularly simple case, because no mechanical work is transferred. Since the flow through the nozzle is quite rapid, the amount of transferred heat that we can expect is relatively modest. We therefore approximate the nozzle process by:

$$0 = (h_{02} - h_{01}) \quad (2.26d)$$

Let us now also use the component numbers according to the standard aero engine nomenclature, see Figure 10. The station number at the entry is denoted 5 and for the exhaust the station the number 8 is used.

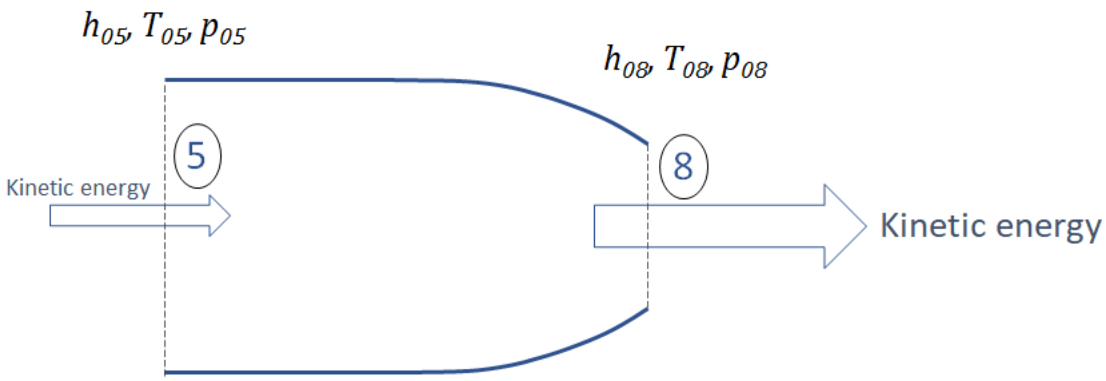

Figure 10: Nozzle with standard nomenclature, entry station denoted 5 and exit station 8.

Since, for a perfect gas, enthalpy relates proportionally to the temperature through c_p the relation for the stagnation temperature and stagnation enthalpy becomes:

$$h_0 = c_p T_0 \quad (2.27a)$$

For the enthalpy and temperature, we get:

$$h = c_p T \quad (2.27b)$$

By applying to the proper station numbering equation (2.26d) becomes:

$$h_{08} = h_{05}$$

Using (2.27b) we see that also the stagnation temperature in the nozzle remains constant.

$$T_{08} = T_{05}$$

As the fluid flows from station 5 to station 8 in the above expression, we showed that the stagnation enthalpy and stagnation temperature both remain constant, as long as we can neglect the heat transfer. In general, we cannot expect that the flow between station 5 and station 8 to be reversible, so we really do not know how to relate p_{05} with p_{08}. We only know that the stagnation pressure will decrease. The good news is that it does not drop too much, for a well-designed nozzle working close to its design condition it might drop with a few percent only. For simplicity, we will therefore neglect the stagnation pressure loss and assume an isentropic flow between 5 and 8, that is set $p_{08} \approx p_{05}$.

Since we often work with Mach numbers it is useful to relate the stagnation properties to the Mach number. This is now easily achieved re-using formulas derived above. From Equation (2.25) and (2.27a, 2.27b), the Mach number definition (2.23) and the ideal gas law (2.8) we get:

$$h_0 = h + \frac{c^2}{2} \quad \Leftrightarrow \quad T_0 = T + \frac{c^2}{2c_p} = T + \frac{M^2 \cdot \gamma RT}{2c_p} = \left[\frac{R}{c_p} = \frac{\gamma - 1}{\gamma}\right] = T + \frac{\gamma - 1}{\gamma} \cdot \frac{M^2 \cdot \gamma T}{2}$$

$$\Rightarrow \quad T_0 = T + \frac{\gamma - 1}{2} \cdot M^2 T \quad \Rightarrow \quad \frac{T_0}{T} = 1 + \frac{\gamma - 1}{2} \cdot M^2 \quad (2.28a)$$

Equation (2.17) is valid for any isentropic process that a perfect gas undergoes. Hence, it is valid for the particular isentropic process which we call stagnation. Thus,

$$\frac{p_0}{p} = \left(\frac{T_0}{T}\right)^{\frac{\gamma}{\gamma-1}} = \left(1 + \frac{\gamma - 1}{2} \cdot M^2\right)^{\frac{\gamma}{\gamma-1}} \quad (2.28b)$$

We now have everything we need to nail the nozzle theory! First, we ask ourselves how far can we drive the acceleration? If you take a close look at 2.24 you get a good feeling. If we have a convergent duct like the nozzle we study here, we can continue to accelerate until we reach Mach 1.0. To go beyond Mach 1.0, we would need to start increasing the area again as shown in the upper right of Table 2. Hence, if we set M=1.0, which we can easily evaluate the limit values. First, we derive the temperature in station 8. Since the stagnation temperature does not change through the nozzle, $T_{08} = T_{05}$, we can predict the temperature directly from 2.28a.

$$T_8 = \frac{T_{08}}{1 + \frac{\gamma - 1}{2} \cdot M^2} = \frac{T_{05}}{1 + \frac{\gamma - 1}{2} \cdot M^2} = \frac{T_{05}}{1 + \frac{\gamma - 1}{2} \cdot 1.0^2} = \frac{2}{1 + \gamma} T_{05}$$

Since we approximate the flow between 5 and 8 as isentropic $p_{08} \approx p_{05}$, Equation (2.28b) gives the limit pressure p_8:

$$p_8 = \frac{p_{05}}{\left(1 + \frac{\gamma - 1}{2} \cdot M^2\right)^{\frac{\gamma}{\gamma-1}}} = \left(\frac{2}{1 + \gamma}\right)^{\frac{\gamma}{\gamma-1}} p_{05}$$

Although the limit of acceleration in a convergent nozzle is set by M=1.0 it is much more practical to compare pressures to see if the nozzle has reached the M=1.0 condition.

In real engines γ would be lower than the previously stated value of 1.4. At the engine exhaust the temperature could be 1000 K and additional excitation modes then become statistically probable increasing the “degrees of freedom” of the gas. Thus, n in Example 3 above, would increase pushing γ towards lower numerical values. Also, at the exit the gas is no longer air but contains combustion products. The exact gamma depends on the concentration of the different species but for conventional jet fuel the γ will always drop further by the presence of combustion products. Specialized codes or data tables are needed to obtain accurate values for γ. The same is true for c_p which also depends both on temperature and gas composition. To keep things simple we will use two sets of γ: s and c_p:s. In Table 3 below we define one "cold" set for **air** and one "hot" set for **gas** in which fuel has been combusted.

Table 3: Property assumptions for perfect fluids (**air)** and air with combustion products (**gas**).

Air (a)	Air / combustion gas (g)
$\gamma_a = 1.4$	$\gamma_g = 1.333$
$c_{pa} = 1005\, J/K \cdot kg$	$c_{pg} = 1148\, J/K \cdot kg$

Applying the air value $\gamma_a = 1.4$ we get the limiting pressure ratio as:

$$\frac{p_{08}}{p_8} = \left(\frac{1+\gamma_a}{2}\right)^{\frac{\gamma_a}{\gamma_a - 1}} = 1.893$$

The corresponding value for gas with $\gamma_b = 1.333$ is:

$$\frac{p_{08}}{p_8} = \left(\frac{1+\gamma_b}{2}\right)^{\frac{\gamma_b}{\gamma_b - 1}} = 1.852$$

Hence, if the stagnation pressure entering the nozzle is more than 1.893 times larger than the ambient pressure the flow will reach $M=1.0$ in both instances and a pressure term will be present for the nozzle exit.

We can now summarize the procedure for modelling the thrust $(\dot{m}_0 + \dot{m}_f)c_8 + (p_8 - p_0)A_8$! If $\frac{p_{05}}{p_8}$ is above the limit, we simply use the above limit expressions to compute p_8 *and* T_8. From p_8 and T_8 we can determine the density using the ideal gas law. This also allows us to predict the area of the nozzle exit using Equation (2.18). When the nozzle reaches the limit condition of Mach 1.0, we refer to this as **the nozzle being choked**.

What if the pressure p_{05} is less than the choking limit? Then the exit pressure p_8 will reach the ambient pressure p_0 and there will be no pressure thrust term in the thrust equation. How do we then get the velocity? We can get the Mach number from 2.28b by approximating $p_{08} \approx p_{05}$ and setting $p_8 = p_0$:

$$\frac{p_{05}}{p_0} \approx \frac{p_{08}}{p_8} = \left(1 + \frac{\gamma - 1}{2} \cdot M_8^2\right)^{\frac{\gamma}{\gamma - 1}}$$

From the Mach number M_8 we get the temperature T_8, and again this allows us to estimate the density and the area needed for the flow.

Example 4: At the entry of the exhaust nozzle of an engine the stagnation temperature and stagnation pressure are P_{05}=193,2 kPa and T_{05}=1000 K. The aircraft is flying at 7000 meters altitude at a speed of 200 m/s. The engine entry mass flow $\dot{m}_0$ is 100 kg/s and the fuel flow $\dot{m}_f$ is 1.940 kg/s.

Predict the engine thrust!

Solution: From the above discussion we know that the nozzle will choke up at a pressure 1.852 times the ambient pressure (using the hot variant). Although we will discuss atmospheric data later, we can already now get the pressure at 7000 meters from the standard atmosphere given in Appendix B. At this condition the pressure p_0 is 41.06 kPa. The nozzle is clearly choked since accelerating to Mach 1.0 gives a pressure that is still larger than ambient:

$$p_{8,limit} = \frac{193,2}{1,852} = 104,3\ kPa\ >\ 41,06\ kPa$$

Since the nozzle is choked, we have sonic speed at the exit ($M_8 = 1.0$). This also means that the additional pressure term in the thrust expression $(p_8 - p_0)A_8$ is now greater than zero. The nozzle exit temperature T_8 becomes:

$$T_8 = \frac{2}{1+\gamma} T_{05} = 857,3\ K$$

The speed of sound at this temperature is:

$$a_8 = \sqrt{\gamma R T_8} = 572\ m/s$$

The exhaust velocity is then:

$$c_8 = M_8 \cdot a_8 = 1 \cdot a_8 = 572\ m/s$$

The pressure p_8 is (again) obtained directly from the choking limit:

$$p_8 = \left(\frac{2}{1+\gamma}\right)^{\frac{\gamma}{\gamma-1}} p_{05} = 104,3\ kPa$$

The density is now obtained from (2.8):

$$\rho_8 = \frac{p_8}{RT_8} = 0,4238\ kg/m^3$$

Finally, the needed area to fit this flow is obtained from Equation (2.18):

$$A_8 = \frac{\dot{m}_0 + \dot{m}_f}{c_8 \rho_8} = 0,420\ m^2$$

The thrust can now be computed from Equation (2.5) as:

$$F = \left(\dot{m}_0 + \dot{m}_f\right)c_8 + (p_8 - p_0)A_8 - \dot{m}_0 c_0 = 64942\ N$$

As a final note, it should be said that the most common engine type, the turbofan, has two separate exhaust nozzles. The equations above handle this problem equally well. The approach is to compute the thrust from the two separate streams using the above equations and then simply add them together!

Developing the engine core component modelling

Having the thrust generation in firm grip we now turn our attention to the core of a jet engine. See Figure 11 for a simple example of a jet engine. The air enters the engine inlet at station 1 and then flows on to station 2 and the compressor entry. Then, it is compressed from station 2 to station 3 before the combustion and heat addition occurs from station 3 to station 4. The turbine takes the hot air and expands it in the turbine from station 4 to station 5. This expansion generates power, which is transmitted to the compressor through the shaft, see Figure 11. The gases entering the turbine have so much energy that a lot remains at exit 5 allowing considerable thrust to be generated.

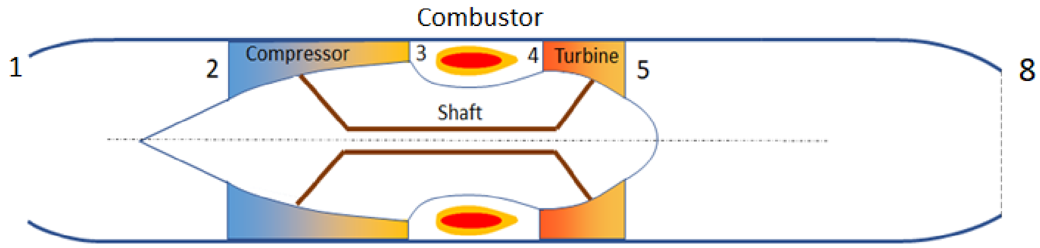

Figure 11: A jet engine (turbojet) with core components and station numbering.

We will now develop the basic principles for predicting the fuel use and efficiency of the core components (compressor, combustor and turbine).

To be able to predict the performance of aero engines the variation in the surrounding atmosphere has to be accounted for. Although temperature varies a lot over time, location and year a standard atmosphere has been defined, the international standard atmosphere or simply **the ISA standard**. The ISA standard temperature starts at 288.15 K at sea level and drops of by 6.5 degrees per 1000 meters up to 11000 meter after which the temperature remains constant. The pressure is defined to be 101325 Pa at sea level. Since the standard temperature drops linearly with altitude, the pressure variation with altitude is found by integration:

$$T_0 = T_{SL} - 6.5 \cdot 10^{-3} h \qquad (2.29a)$$

$$dP = -\rho g dh = [Ideal\ gas\ \ law] = -\frac{P}{RT} g dh \quad \Rightarrow$$

$$\int_{P_{SL}}^{P} \frac{dP}{P} = -\int_0^h \frac{g dh}{R(T_{SL} - 6.5 \cdot 10^{-3} h)} \quad \Rightarrow$$

$$P_0 = P_{SL} \cdot \left(\frac{T_{SL} - 6.5 \cdot 10^{-3} h}{T_{SL}} \right)^{\frac{g}{6.5 \cdot 10^{-3} \cdot R}} \qquad (2.29b)$$

Where $T_{SL} = 288.15$ K and h is the altitude in meters. P_{SL} =101325 Pa and g is the gravitational constant 9.81 m/s^2. Notice that the 0 in p_0 and T_0 represents the station number upstream of the engine, not stagnation. Equation (2.29a) and Equation (2.29b) are only valid up to 11,000 meters. A tabulation up to 25000 m is found in Appendix B. Frequently, the local temperature is presented as deviation from the ISA standard, rather than in absolute numbers. During engine design, provision is taken for hot days since this pushes the engines towards very high internal temperatures. “ISA+25” (313.15 K) at sea level take-off is a common “hot day” definition. Since pressure depends on altitude, see Equation (2.29b), high altitude airports may have much lower pressure than the sea level value. This reduces the thrust developed by the engines because the air density drops with pressure. In turn, this reduces the engine mass flow which lowers the thrust, as can be seen from Equation (2.5). For particular airports the combination of high temperatures and low pressures can be problematic during take-off[2].

The inlet performs no work, and the heat transfer is negligible. Hence, the inlet is thermodynamically very similar to the exhaust nozzle. Although a modest pressure loss is to expect through the inlet, it is a rather good approximation to assume that the flow is isentropic, that is $p_{02} \approx$

[2] A classic tough case is the Mexico City airport is located at 2230 m above sea level (Appendix B gives approximately 77,3 kPa for this altitude). ISA+30 at this airport makes the design very challenging.

p_{01}. The pressure at the compressor entry is directly influenced by the flight Mach number M_0 and can then be predicted by isentropic pressure recovery, according to Equation (2.28b) we get:

$$\frac{p_{02}}{p_0} = \left(1 + \frac{\gamma - 1}{2} \cdot M_0^2\right)^{\frac{\gamma}{\gamma-1}} \quad (2.30a)$$

The stagnation temperature in station 2 is obtained from:

$$\frac{T_{02}}{T_0} = 1 + \frac{\gamma - 1}{2} \cdot M_0^2 \quad (2.30b)$$

After establishing estimates for the inlet, we now turn our interest to the next component, **the compressor.** First, we need an efficiency expression. The preferred efficiency for aero engine propulsion modelling is the small stage or so called polytropic efficiency. It is defined by the differential:

$$\eta_{p,c} = \frac{dh_{is}}{dh} \quad (2.31)$$

The formula looks reasonable since the dh_{is}, that is the isentropic energy need for a small stage compression, should be smaller than the real energy need for the same compression dh. Hence the efficiency is less than 100% and relates the ideal process to the real process. To develop the expression further the numerator dh_{is} can be obtained from Gibbs's Equation (2.6a) applied to the stagnation state with $ds = 0$ and the ideal gas law (2.8). The denominator can be replaced by introducing c_p. We get:

$$\eta_{p,c} = \frac{\frac{RT_0 dp}{p_0}}{c_p dT} \quad \Leftrightarrow \quad \frac{dT}{T_0} = \frac{R}{c_p \eta_{p,c}} \frac{dp}{p_0} \quad \Leftrightarrow \quad \frac{dT}{T_0} = \frac{\gamma - 1}{\gamma \eta_{p,c}} \frac{dp}{p_0} \quad \Leftrightarrow$$

$$\frac{T_{03}}{T_{02}} = \left(\frac{p_{03}}{p_{02}}\right)^{\frac{\gamma-1}{\eta_{p,c}\gamma}} \quad (2.32)$$

Notice the similarity between (2.31) and the isentropic process. The only difference is the efficiency in the denominator in the exponent. This will increase the exit temperature T_2 and in turn increase the work needed to reach the pressure ratio $\frac{p_{03}}{p_{02}}$, compared to the isentropic process. A good first estimate for the compressor efficiency is around $\eta_{p,c} = 90\%$, or maybe a few per cent higher for very modern units. The compressor work requirement is obtained directly from the first law for open systems:

$$-\dot{W}_c = \dot{m}(h_{03} - h_{02}) = \dot{m} c_p (T_{03} - T_{02}) \quad (2.33)$$

Here that the work is negative, that is we need to put in work into the fluid going through the compressor.

The combustor is treated by computing a sufficient fuel air ratio, by mass, to achieve a targeted exit temperature T_{04}. The quite high temperatures associated with combustion, modern engines may have temperatures in the range of 1800-1950 K as combustor exit temperature. Such a high temperature level means that a lot of chemical reactions may occur that do not take place at room temperature. Combusting Jet-A, which is the currently the dominating aircraft fuel, mainly produces water and carbon dioxide. At these high temperatures both substances may dissociate into carbon monoxide, hydrogen, hydroxyl radicals and in addition nitrogen oxides with likely form from dissociating nitrogen reacting with the oxygen in the air. Instead of modelling these interrelated and temperature dependent reactions it is customary to simply use charts, see Figure 28 and Figure 29 in Appendix C below, to estimate the relation between fuel use and temperature rise. These charts are based on chemical equilibrium computations performed by specialized codes [3].

Current combustors have very high efficiency, often above 99.9%, so this inefficiency effect is neglected. The loss in stagnation pressure through the combustor is usually in the range 3-5%. Here we use 4%.

Example 5: For a compressor exit temperature T_{03} = 700 K estimate the fuel air ratio to achieve a combustor exit temperature of T_{04} =1800 K.

Solution: The combustor temperature rise needed is 1800 – 700 = 1100 K. Reading off the 700 K inlet air temperature curve we get the fuel air ratio, denoted FAR, as approximately 0.03350. If the air flow into the engine is 100 kg/s the fuel flow is 3.35 kg/s.

The turbine expansion is done analogously to the compressor the only difference being the efficiency definition:

$$\eta_{p,t} = \frac{dh}{dh_{is}} \quad (2.34)$$

Here we get less real power out than we would if the expansion was isentropic. Hence the inverted relation. Integrating using the same line of argument as for the compressor results in:

$$\frac{T_{04}}{T_{05}} = \left(\frac{p_{04}}{p_{05}}\right)^{\frac{\gamma-1}{\gamma}\eta_{p,t}} \qquad (2.35)$$

The power out of the turbine is developed in the same way as for the compressor:

$$-\dot{W}_t = (\dot{m} + \dot{m}_f)c_p(T_{05} - T_{04}) \quad \Rightarrow \quad \dot{W}_t = (\dot{m} + \dot{m}_f)c_p(T_{04} - T_{05}) \quad (2.36)$$

Since the temperature drops during the expansion through the turbine the turbine power output is now positive since the turbine does work on its surroundings. The turbine drives the compressor and the net work on the surrounding is zero. Summing the compressor and turbine work gives:

$$\dot{W}_c + \dot{W}_t = 0$$

or with the expression for the powers introduced:

$$(\dot{m} + \dot{m}_f)c_{pg}(T_{04} - T_{05}) = \dot{m}c_{pa}(T_{03} - T_{02}) \qquad (2.37)$$

To emphasize that we should use different c_p:s for the compressor (air) and after the burner (gas) the indices have been explicitly introduced in equation (2.37). In this treatment we neglect any mechanical losses.

Example 6: The engine studied in Example 4 has a pressure ratio of 8.0 over the compressor. Again, the aircraft flies at 7000 meters at 200 m/s and the turbine exhaust temperature T_{05} remains at 1000 K and the engine entry mass flow $\dot{m}_0$ is 100 kg/s.

Estimate the turbine entry temperature T_{04}.

A way to measure jet engine efficiency is specific fuel burn. It is defined as fuel burn per unit thrust, that is $SFC = \frac{\dot{m}_f}{F}$. Compute this parameter. Use the thrust predicted in Example 4 and the fuel burn predicted in the solution to this example to establish its value.

Solution: The ambient conditions at 7000 meters is determined from Appendix B.

$$T_0 = 242{,}65\ K$$
$$P_0 = 41{,}06\ kPa$$

The speed of sound at this temperature is:

$$a_0 = \sqrt{\gamma R T_0} = 312{,}3\ m/s$$

The flight Mach number M_0 is then:

$$M_0 = \frac{c_0}{a_0} = 0{,}640$$

Due to the relative speed between the engine and the air a stagnation temperature and stagnation pressure builds up. This stagnation process is frequently referred to as “ram”. The process is modelled by Equation (2.30a) and (2.30b):

$$\frac{p_{02}}{p_0} = \left(1 + \frac{\gamma - 1}{2} \cdot M_0^2\right)^{\frac{\gamma}{\gamma-1}} \Rightarrow \ P_{02} = 54{,}1\ kPa$$

$$\frac{T_{02}}{T_0} = 1 + \frac{\gamma - 1}{2} \cdot M_0^2 \ \Rightarrow \ T_{02} = 262{,}56\ K$$

The compression process is modelled using Equation (2.32) with a polytropic efficiency of 90%. This produces a T_{03} according to:

$$T_{03} = T_{02}(8)^{\frac{1.4-1}{0.9\cdot 1.4}} = 508{,}1\ K$$

The temperature at the turbine entry is sought. We only know the exit temperature $T_{05} = 1000\ K$. But we can compute the power required by the compressor since we know the temperature change of the compressor as well as the mass flow. Since the compressor power is equal to the turbine power and we know the turbine exit temperature we should be able to calculate backwards establishing the turbine inlet temperature. From 2.37 we get:

$$(\dot{m}_0 + \dot{m}_f) c_{p,g} (T_{04} - T_{05}) = \dot{m} c_{p,a} (T_{03} - T_{02})$$

The only piece of information missing is the fuel flow. In this case we must iterate using the fuel flow tables (Figure 28 and Figure 29). Looking at the fuel flow tables we see that the fuel air ratio is frequently only a few percent. We should be able to get a good estimate by initially setting the fuel flow to zero in the equation above. We will then have a few percent error in $(T_{04} - T_{05})$ which will result in in an even smaller error in T_{04}. Normally, for the type of preliminary calculations studied here we should be able to accept this error. However, we can of course compute a T_{04} based on the new value of FAR which should then be even more quite accurate. Let’s do this. We first get (from zero fuel flow assumption):

$$(100 + 0) \cdot 1148 \cdot (T_{04} - 1000) = 100 \cdot 1005 \cdot (508{,}1 - 262{,}56)$$

Which gives a $T_{04} = 1214{,}9$ K and a combustor temperature rise $(T_{04} - T_{03}) = 706{,}86\ K$. Looking in Figure 28 we find the FAR=0,01940. The FAR number is a mass flow ratio now we can get the fuel flow:

$$\dot{m}_f = 0{,}01940 \cdot 100 = 1{,}940\ kg/s$$

We now compute T_{04} again using the equation above to get $T_{04} = 1211$ K and see no need for another iteration (1211 K is very close to 1214.9 K). Another iteration would produce an even smaller difference. Notice that we are reading data out of figures and the error from this process is soon larger than the accuracy of our iteration scheme.

From the above results we can now also predict the SFC. Using the thrust established in Example 4 we get

$$SFC = \frac{\dot{m}_f}{F} = 29{,}8\ mg/(\mathrm{N} \cdot \mathrm{s})$$

It customary to state SFC in mg/(N·s) to get reasonably sized numbers.

The useful power to the aircraft is the thrust times its flight speed.

$$P = Fc_0 = 13{,}0\ MW$$

This is an impressive power considering that the exit area is 0.420 m^2 and the corresponding diameter is 0.73 meter. This is despite that the temperature in the turbine entry is a lot lower than can be achieved today. The SFC is also very poor resulting from a combination for the low turbine entry temperature and the low pressure ratio of the engine. In general, being able to run with higher turbine entry temperature increases the optimal pressure ratio for the compressor. State of the art turbofan engines may run with about half the SFC stated in the example above.

For detailed calculations there is also a mechanical efficiency, but these are quite high. Often as high as 99.9%. The large errors made here are the assumption of constant gas properties and that we do not treat turbine cooling. Frequently as much as 25% of the compressor air is often bypassed the combustor and used to cool the turbine blades.

Some efficiency definitions

We can now define an efficiency for this process. As indicated above, the useful power P_{useful} to the aircraft is the thrust F multiplied with the speed at which the aircraft is flying c_0, that is:

$$P_{useful} = Fc_0$$

The overall efficiency is then measured by how the heat content LHV of the fuel flow $\dot{b}$ relates to this efficiency. The overall efficiency η_o is thus:

$$\eta_o = \frac{Fc_0}{\dot{m}_f \cdot LHV}$$

It is customary to split the efficiency into two separate factors, thermal efficiency and propulsive efficiency. The thermal efficiency quantifies the conversion from heat to kinetic energy and the propulsive efficiency relates the conversion of kinetic energy to useful thrust:

$$\eta_o = \eta_{th} \cdot \eta_p = \frac{\dot{W}_{kin}}{\dot{m}_f \cdot LHV} \cdot \frac{Fc_0}{\dot{W}_{kin}}$$

The turbofan & turboprop

To close this section on engine modelling we will discuss the two most common jet engine architectures today the turbofan, and the turboprop. The turbofan dominates the scene, and the turboprops are only used for shorter flight distances and smaller aircraft. A turbofan is shown in Figure 12.

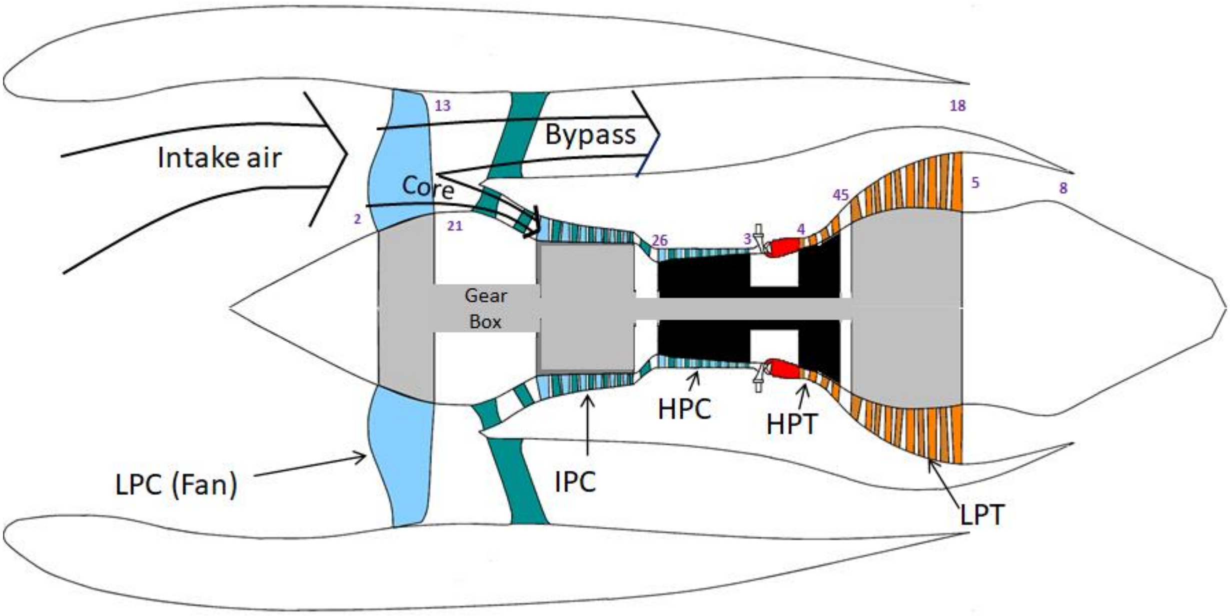

Figure 12: Two-shaft turbofan (geared) engine architecture with station numbering.

The turbofan is more complex than the turbojet in that it has two streams. The inlet flow splits into a large cold stream often referred to as the bypass flow, since it is bypassed the core of the engine ducted around the engine in the bypass duct exiting in the "cold nozzle" denoted by 18 in Figure 12. A much smaller "hot flow" often referred to as the core flow is also indicated in Figure 12. The core flow goes through stations 2, 21, 26, 3, 4, 45, 5 and finally exiting in the core nozzle in station 8. Notice that this numbering is consistent with what we used for the turbojet. The ratio between the bypass mass flow and the core flow is called the bypass ratio, BPR, and is defined as:

$$BPR = \frac{\dot{m}_{bypass}}{\dot{m}_{core}}$$

Modern engines have $BPR{:}s$ around 10.0, and if a mechanical gear is used to reduce the LPC rotational speed it may be above 12.0. Of course, the value varies not only between architectures but also throughout the engine mission.

A number of abbreviations for the turbofan components are in use, as indicated in Figure 7. The LPC is frequently called "the fan". A typical LPC design pressure ratio is around 1.45-1.6. The core flow goes through the same process as we have already discussed with the turbojet. That is first a compressor, then combustion, and finally turbine expansion. The compression is split into the first bit already happening in the LPC, then a second compression step through the Intermediate Pressure Compressor (IPC) and the final compression step occurring in the High-Pressure Compressor (HPC). The turbine expansion occurs through two separate turbine components the High-Pressure Turbine (HPT) and the Low-Pressure Turbine (LPT).

As illustrated in Figure 12, a geared turbofan has two shafts. The low-pressure shaft is comprised of the LPC, IPC and LPT which are connected together mechanically. The IPC/LPT typically runs with a rotational speed 3-4 times higher than the fan. Most of the energy developed in the LPT goes to drive the huge Fan but some is used also for the IPC. The high-pressure shaft is comprised of the HPC and HPT with the combustor placed in between. Typical pressure ratios for the IPC and HPC are 2-4 and 10-20 respectively. A total compression ratio of over 50 is common in large engines today. Thermal efficiencies over 50% are reached and propulsive efficiencies over 80%

resulting in overall efficiencies of above 40%. In addition to geared architectures there are the direct drive two-shafts, and also three-shaft engines where an intermediate pressure turbine drives an intermediate pressure compressor having an independent rotational speed.

The turboprop engine, an example is shown in Figure 13 below, can be designed with different architectures. A common turboprop architecture is to use a free running, not mechanically connected, power turbine. The air enters through the air inlet and is here ducted to an axial/centrifugal compressor, ideal for the much smaller airflows of this engine type. This compression unit is driven by the compressor turbine. Together with the combustor the compressors and turbine generate hot pressurized gas for the free power turbine that is directly linked to the propeller generating the thrust.

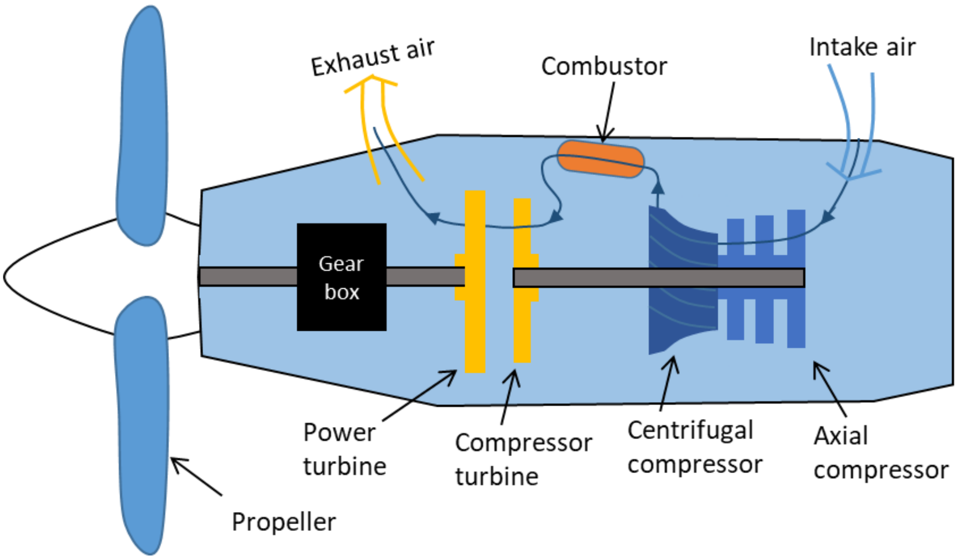

Figure 13: Turboprop architecture

Of course, the power generated onto the shaft by the free turbine could be generated by any other energy source, such as a fuel cell or battery [4, 5].

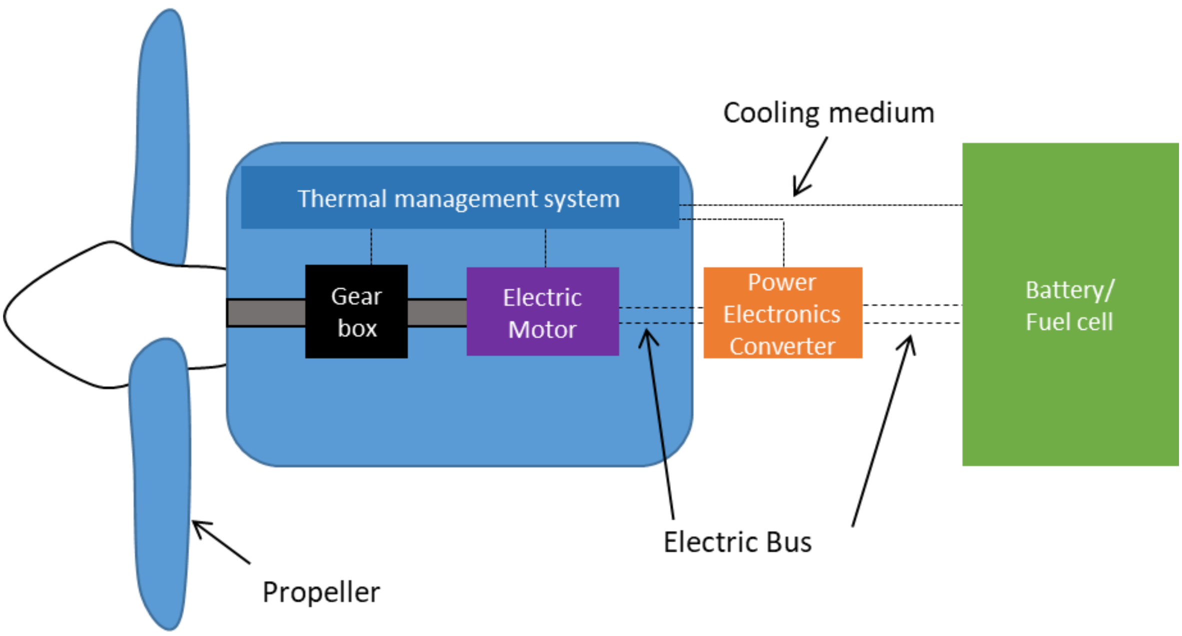

Figure 14: Electric drive system for propeller installation

As illustrated in Figure 14, when electrical energy is adopted, the gas turbine core is replaced by an electric motor integration while the propulsive thrust is still generated by the propeller blades. Primary electric power system elements are the electric motor, power electronics converter, and an electrical energy source device. The energy source is normally represented by batteries or fuel cells. In principle, the electric motor can be designed to drive the propeller either with- or without a gearbox but normally a reduction gear is required as the motor then works more efficiently in a relatively high RPM range. Based on the selection of the type of the motor, a power electronics converter is required to turn the electrical energy from the batteries/fuel cell into a suitable form (current type, voltage level, etc) needed by the motor.

Since a shaft connection is only required between the electric motor and the propeller, this makes the motor integration rather compact compared to the turboshaft engine. However, as the energy densities of batteries of today, up to perhaps 0.3 kWh/kg, are way lower than that of fossil fuels, the resulting high weight of the electrical power system makes it impractical for the medium/ long range flight missions that we usually associate with aviation. For short range smaller aircraft, they may as we will see in this course, become competitive relatively soon. Fuel cells are also constrained by power density but indicate to have a higher potential for compactness than batteries. However, the need for additional pressurized hydrogen increases the compactness of the overall system limiting its the current potential. Having liquified hydrogen on-board changes this story.

The total electric efficiency, from battery to propeller, may reach just over 80% for a typical high-power installation. This is much better than for conventional combustion-based components that may reach 50% for large installations and perhaps 35% for smaller power plants. Fuel cell installations do not seem to have any major efficiency advantage over combustion-based systems, especially when very large powers per unit volume need to be extracted. As a final note, too high or too low component system temperatures may negatively affect the performance and/or life of the components. Hence, a thermal management system is normally considered a critical part of completing the electric drive train. A more comprehensive discussion of electric propulsion is given in the later section of this material.

Engine off-design performance and mission analysis

Fixed geometry limitations and off-design operation

In Example 4 we predicted the nozzle flow exit area that would fit the flow exactly. This can only be achieved in a single condition. What happens if it doesn't fit? Think about it for a while before continuing to read! Clearly, had we done the design for another flight condition with a different forward speed and a different altitude we would have expected a different exhaust area A_8 for choking the flow. Both Example 4 and Example 6 are usually referred to as design point studies. This means that all geometry of the engine and its components being studied, are thought to be adaptable to exactly fit the flows. In other operating points however, we do not have this design freedom. Once we have chosen the design point and have worked out the areas and geometry, we have to live with our choices. For advanced design activities you might strike compromises between multiple design points. Doing this you still face the same challenge, you can choose your areas only once! You might make a more informed and balanced choice considering multiple points, but the fixed area limitations remains.

Actually, engineers have gone to a great length to circumvent the problem of only being able to decide design areas once. A classic example is aircraft wing design. If you could choose freely between operating points, you would like to have a relatively small wing for cruise to keep drag down, however, to allow for a shorter runway you would like to have a larger wing and to be allowed to land at a sufficiently low speed you would likely want an even larger wing. For this reason, engineers have "cheated" and introduced variable geometry using leading edge slats and trailing edge flaps. The different configurations are illustrated in Figure 15 below.

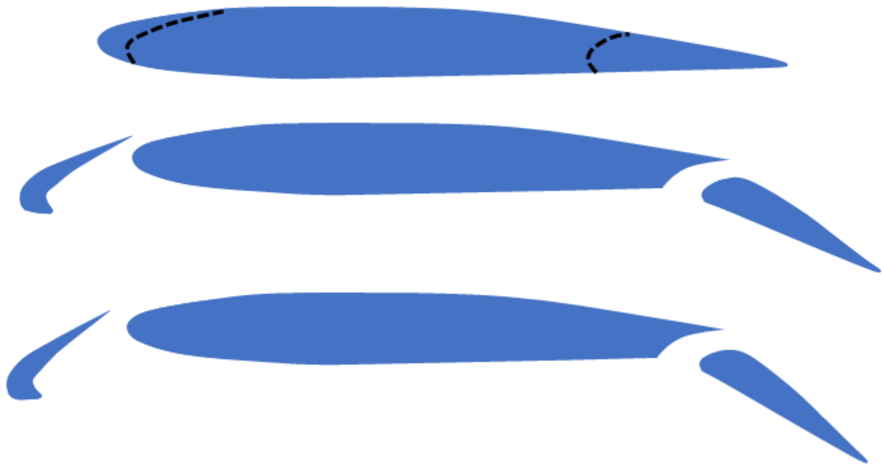

Figure 15: **Top figure:** clean wing for efficient cruise operation. **Middle figure:** application of slat (leading edge) and flap (trailing edge) to aerodynamically increase the wing area. **Lower figure:** extreme condition for landing with maximum position for slat and flap.

This section is not so much about finding remedies for fixed geometry but rather to briefly **discuss how limitations are introduced in propulsion systems** when **fixed geometry components have to be matched together**, that is how several choices of fixed areas constrain each other.

We know that in every operating point of the propulsion system, momentum, mass and energy have to be conserved between components. In addition, the rotational speed of the compressor must be the same as the turbine rotational speed since these two components are hard connected together through a shaft.

For aero engines it is customary to present the whole engine performance using the compressor component data. If we plot compressor pressure ratio over mass flow for a number of rotational speeds, we get something called a compressor map. See Figure 16 below. This map depicts a large number of stable operating conditions in which the compressor could potentially be operating. If you put the compressor in a well-designed test bed you could reach all these points.

To model compressor performance we use the following non-dimensional variables:

$$\frac{p_{03}}{p_{02}} = pressure\ ratio \qquad (2.38a)$$

$$\frac{ND}{\sqrt{\gamma R T_{02}}} = Fixed\ size, fixed\ working\ gas = \frac{N}{\sqrt{T_{02}}} \qquad (2.38b)$$

$$\frac{\dot{m}\sqrt{c_p T_{02}}}{D^2 p_{02}} = Fixed\ size, working\ gas = \frac{\dot{m}\sqrt{T_{02}}}{p_{02}} \qquad (2.38c)$$

First it should be pointed out that the variables used in practical compressor modelling, that is the rightmost ones in Equation (2.38b, 2.38c), are **not** non-dimensional, although they are frequently referred to as non-dimensional variables. The leftmost variants of these variables, as given in Equation (2.38b, 2.38c) are however dimensionless. Because aero engine compressors are intended to be used in air, there is however no need to keep R, c_p and γ present in the variables since they are constants. The same goes for the characteristic size parameter D. The compressor is fixed in size and therefore also D remains constant and can be excluded from the variables. With these provisions made we will allow ourselves to call $\frac{p_{03}}{p_{02}}, \frac{N}{\sqrt{T_{02}}}$ and $\frac{\dot{m}\sqrt{T_{02}}}{p_{02}}$ dimensionless.

In general, the use of non-dimensional numbers allows us to reduce the number of variables we need to describe a physical system. Non-dimensional numbers are introduced in basic courses in physics, and little further will be said here. Only that it can be proven that the degrees of freedom for representing a component is reduced with m number of variables [6], when non-dimensional variables are used. The variable m is the number of fundamental units (time [s], mass [kg], length [m], temperature [K], amount of substance [mol], luminous intensity [cd], electrical current [A]) in the problem at hand. In aerospace we often have $m = 3$ (time [s], mass [kg], length [m]) variables and in some cases where heat transfer and the energy equation play an important role, we have $m=4$ (time [s], mass [kg], length [m], temperature [K]).

For a compressor this process of reducing the number of independent variables by using non-dimensional variables allows us to predict compressor pressure ratio if the non-dimensional rotational speed and the non-dimensional mass flow are given. The same holds for efficiency, that is it also defined from non-dimensional rotational speed and mass flow. See Figure 16 for a typical high speed compressor performance map. Hence, we get a 2-dimensional space (two variables to determine a third). For high-speed compressors, $m = 4$, so if we decide to not use non-dimensional variables we would be stuck with a 6-dimensional space.

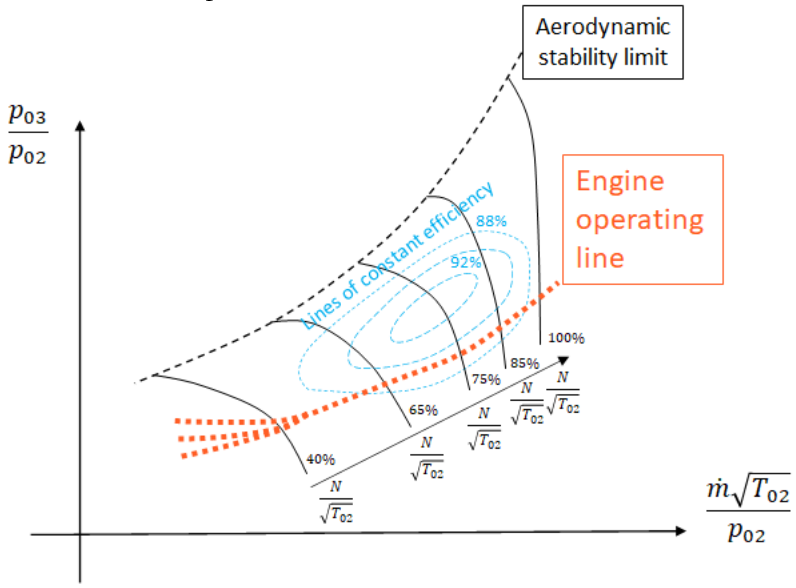

Figure 16: Compressor map plotting a number of rotational speed lines showing pressure ratio as a function of corrected mass flow. Notice the blue cross-hatched lines indicating constant compressor efficiency [7].

Because the performance of aero engines is constrained by how the components limit each other, the points where the whole engine can operate is very constrained! When turbine components are choked, normally the internal flow inside of turbines reach Mach=1.0 for a considerable portion of the engine's envelope, the running line becomes fixed. This means that only one operating point is possible for each rotational speed line as indicated by the orange line in Figure 16. Notice that at lower non-dimensional speeds, in this case around 40%, the engine pressures have dropped down so much that a component may unchoke and it then multiple running lines are possible depending on additional variables such as aircraft speed. Then it gets more complex to predict the engine performance. However, this happens far below the points where most of the fuel is consumed for a normal mission, so we can treat the important part of the engine operation as a 1-dimensional curve!

How do we now connect the engine with the aircraft? The first step is to start to think in terms of missions. Study a typical mission shown in Figure 17 below. The major part of the flight time and also the major part of the fuel burn is incurred by the cruise segment. For longer flights, it is common to climb to higher altitude as the aircraft gets lighter. By climbing to this high altitude the aircraft may then be operated in a region with lower density, hence reducing the aircraft drag, the thrust requirement and the fuel burn.

The last point in the climb phase is usually referred to as top-of-climb (TOC). The same point in the mission but now with engines throttled down to the lower thrust of level flight is called initial cruise. The first point in the descent phase is called top-of-descent. Usually the end of run-way point is taken as the take-off point (TO).

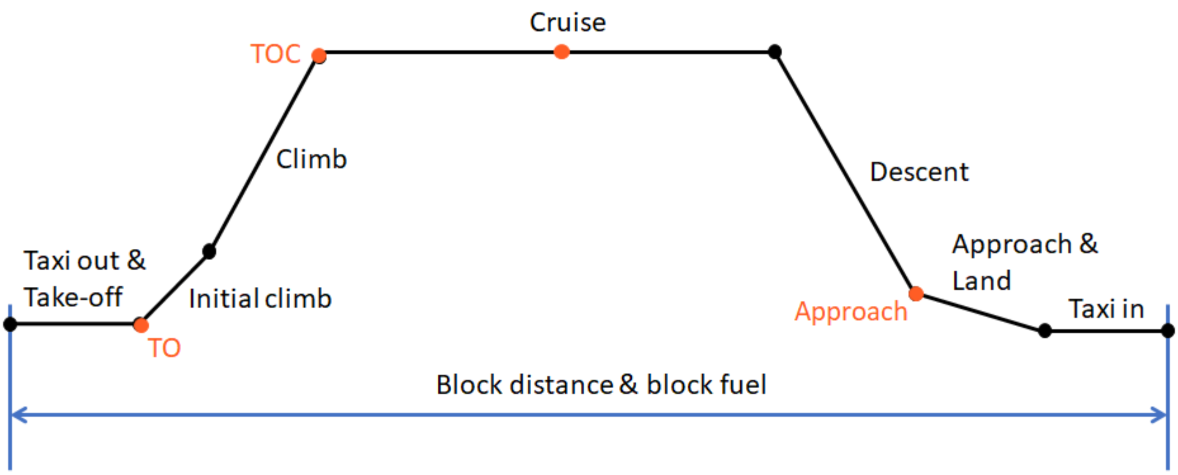

Figure 17: Typical commercial mission for civil aircraft

Returning again to the engine running line and the compressor map we can introduce typical operating conditions into the map:

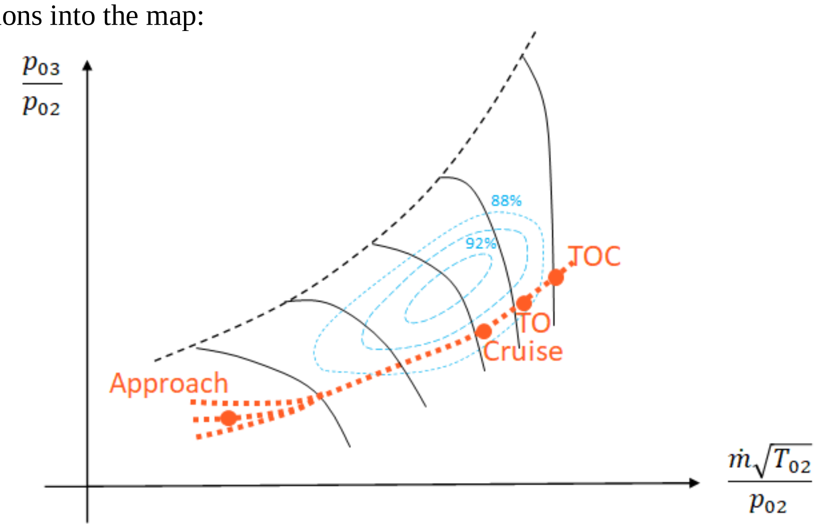

Figure 18: Compressor map with top-of-climb (TOC), take-off (TO), Cruise and the low power point Approach are indicated along the operating line.

In general, the block fuel m_{block} can be approximated quite well through the sum of a number of products multiplying the time spent in a particular phase t_i with the fuel burn for this particular phase $\dot{m}_{f,i}$. We get:

$$m_{f,block} = \sum_{\substack{All\ flight \\ phases\ i}} t_i \dot{m}_{f,i}$$

Several points for each flight phase may be needed to achieve a sufficient accuracy for m_{block}. The total flight time t is then obtained from:

$$t = \sum_{\substack{All\ flight \\ phases\ i}} t_i$$

To approximate the fuel burn during a mission, the major fuel consuming phases may be grouped together and multiplied with time to make a first estimate of the block fuel. It should be pointed out that although the time in take-off and climb is many times much shorter, climb could be done in 15-20 minutes and cruise could go on for 10+ hours, the fuel burn is much higher during take-off and climb and should therefore still be treated separately. A crude approximation for the block fuel b_{block} may therefore be made as:

$$b_{block} = \xi\left(t_{initial\ climb}\dot{m}_{f,\ initial\ climb} + t_{climb}\dot{m}_{f,\ climb} + t_{cruise}\dot{m}_{f,\ cruise}\right)$$

Where $\xi > 1.0$ should approximate the fuel spent by the additional flight phases.

3. ENERGY CARRIERS AND EMISSIONS

Since the early 1950:ies aviation has been characterized by rapid growth and an impressive improvement in vehicle efficiency. The general trends are captured in Figure 19 below. Although CO_2 emissions per passenger kilometre have dropped by a factor of 20 since the 1950:ies growth has been even more rapid and today aviation account for about 2.4% of all CO_2 emissions generated by human activities. In 2018 aviation emitted approximately 918 million tonnes of CO_2. Average emissions from aviation are around 0.125 kg CO_2 / RPK but for economy seated completely full modern aircraft 0.05 kg CO_2 / RPK can be reached despite flying at 1000 km/h!

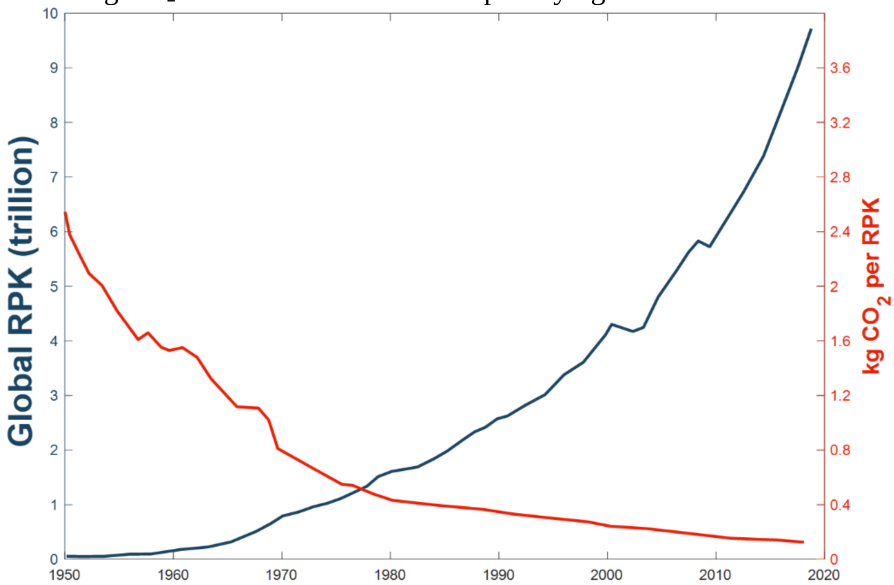

Figure 19: Growth in RPK (revenue passenger kilometers) versus CO_2 emissions per RPK [8].

During COVID aircraft operations dropped back dramatically to levels less than 10% of global RPK! As COVID restrictions were relieved, RPK picked up gradually and in February 2024 an new record value was achieved comparing to pre-covid levels.

For constant speed and level flight, we showed that the thrust of the engines must approximately equal the vehicle drag, through equation (1.5a). Similarly, lift was shown to be approximated well by aircraft weight from equation (1.5b). Thus, mass translates to lift, which translates to drag, which translates to thrust which translates to fuel burn. The amount of fuel carried in an aircraft depends on its mission length. For long-, mid- and short-range aircraft performing design missions, the fuel mass percentage of these aircraft types are around 40%, 25% and 20% respectively! From these numbers and the above argument about constant speed flight it is rather obvious that introducing a fuel with for instance half the energy density will be difficult. For a long range aircraft this would require 80% of the starting weight, which is likely higher than the sum of the payload and fuel, meaning that the aircraft could not even operate empty.

Current operation of commercial aviation is still dominated by use of Jet A. This fuel is fossil, has a density around 0.8 kg/litre, a fuel heating value of around 43 MJ/kg and is chemically often simplified to $C_{12}H_{23}$.

Example 7: One kg of Jet A, represented by $C_{12}H_{23}$ is combusted with air. To stoichiometrically balance the combustion process, this means making sure that the same number of atoms occur on each side (so that no matter is lost) we get:

$$4C_{12}H_{23} + 71O_2 \rightarrow 48CO_2 + 46H_2O$$

You can validate this by verifying that there is 48C, 92H and 142O on both sides. So for every 4 molecules of $C_{12}H_{23}$ we get 48 CO_2. One mole of $C_{12}H_{23}$ has the molar mass of 167,3 grams and a CO_2 molecule has a mass of 44,01 grams. The mass ratio between CO_2 and Jet A is thus:

$$\frac{m_{CO_2}}{m_{C_{12}H_{23}}} = \frac{48}{4} \cdot \frac{44{,}01}{167{,}3} = 3{,}156$$

Hence combusting one kg Jet A gives about 3.156 kg CO_2 emissions.

Example 8: Continuing the turboprop example we estimate the CO_2 emissions per passenger kilometer.

Solution: The SFC is given as 7.2 mg/Ns in cruise. For constant speed, level flight thrust is approximated by drag (1.5a) and lift by the weight of the aircraft (1.5b). The initial mass is given at 8580 kg, hence the lift needs to be:

$$L = mg = 8580 \cdot 9.81 = 84{,}1\ kN$$

The lift over drag was approximated at 19.3 for the entire cruise phase. We get the drag as

$$D = F = \frac{L}{19.3} = 4{,}36\ kN$$

From the SFC we get the fuel consumption of the aircraft

$$\frac{\dot{m}_{fuel}}{F} = 7.2\ mg/Ns$$

We get the fuel flow as:

$$\dot{m}_{fuel} = 31\ grams/s$$

From the velocity we estimate the milage for the aircraft

$$\frac{\dot{m}_{fuel}}{V} = 0{,}330\ kg/km$$

Per passenger we get:

$$\frac{\dot{m}_{fuel}}{V} = 0{,}0173\ kg/km/passenger$$

Multiplying it by 3.156 to get CO_2 emissions we get:

$$\frac{\dot{m}_{fuel}}{V} = 55\ grams\ CO_2/km/passenger$$

If the same analysis is repeated for the final cruise mass 5300 kg we get:

$$\frac{\dot{m}_{fuel}}{V} = 34\ grams\ CO_2/km/passenger!$$

Non-CO_2 emissions

The combustion of Jet A outlined in Example 7 above is an simplification of the real process. Although modern aero engines combustors achieve almost complete combustion a number of byproducts are still formed. The process is illustrated schematically in Figure 20.

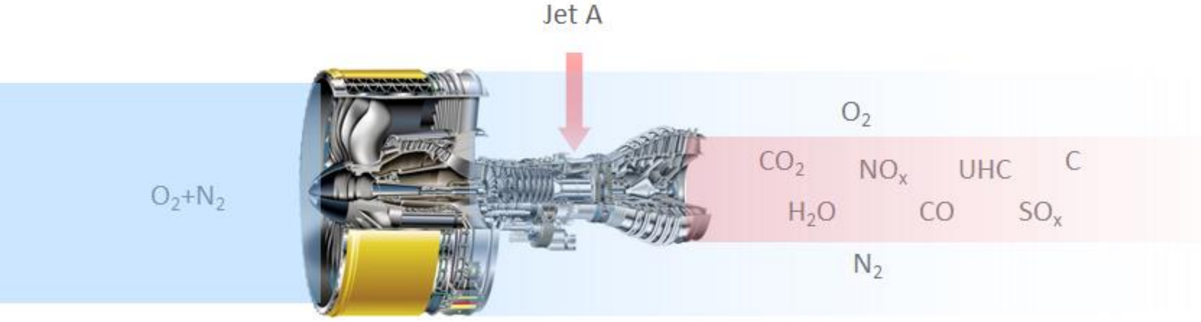

Figure 20: Emissions from Jet A combustion.

Apart from CO_2, we will concentrate our efforts on NO_x and H_2O since they have substantial climate impact. In addition, NO_x also has an important effect on air quality close to airports.

Although water vapor has a direct influence on the radiative forcing balance in the atmosphere [W/m^2], it is the formation of condensation trails, so called contrails, that make water such an important contributor to climate effects. Contrails are line-shaped ice clouds generated from high-altitude flying, see Figure 21 for a schematic view. When retaining their linear shape, they are called persistent contrails, but when they deform and spread out, they are referred to as contrail-cirrus. It should be said the radiative forcing from the contrail-cirrus clouds is quite variable but that the net forcing is generally positive (warming).

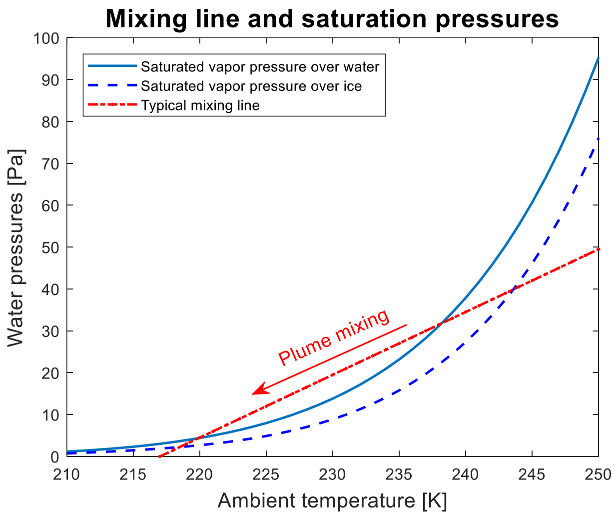

Figure 21: Persistent contrail and contrail-cirrus (left). Conditions for contrail cirrus formation (right).

When a hydrocarbon is combusted water is produced as one of the emissions. Although this exhaust flow is very rich on water it will initially remain gaseous due to the high exhaust temperature. As the jet plume flows downstream of the engine and mixes with the cold ambient and much drier ambient air. At some point of mixing a supersaturated condition with respect to liquid water may be reached. In the rightmost part of Figure 21 this means that the read mixing line crosses the saturated vapor pressure line (solid blue line). Whether the cloud will be persistent depends on the ambient condition which the plume will eventually reach. If the ambient condition is supersaturated with respect to ice (dashed blue line) the contrail will be persistent. However, if it continues below the saturated ice line the contrail will be dispersed.

It can be shown that the slope of the mixing line is:

$$Slope\ of\ mixing\ line = \frac{EI_{H_2O} c_p p}{\frac{M_{H_2O}}{M_{air}} Q(1-\eta)}$$

Where $EI_{H_2O}$is the emission index quantifying how many kilos of water that form per kg of fuel burnt. $P$is the local pressure in the atmosphere and M_{H_2O} and M_{air} are the molar masses for water and air respectively. Q is the heating value of the fuel and η is the total efficiency of the engine. Hence, as engine efficiency increase the slope of the mixing line increases. This could cause the mixing line to completely miss, that is not cross, the liquid saturation line. This would then represent a contrail free flight condition. Furthermore, an efficient engine would also burn less fuel decreasing the partial pressure of water in the exhaust. This also reduced the risk of contrail formation. On the other hand, efficient engines tend to have colder exhausts meaning that the mixing again starts closer to the saturation line. Hence, even from a simple thermodynamic perspective, ignoring the detailed mechanisms of ice formation, contrails modelling has to take a number of aspects into account.

It is known that the formation of ice depends to a large degree on the number of particles formed during combustion. Burning Jet-A gives rise to a much greater number of particles than cleaner fuels such as some biofuels and even more so for hydrogen which is free from particulate matter. For this reason, hydrogen may in the end not be worse than Jet-A with respect to contrail formation. Optical thickness and particle size are also very important factors. These parameters also seem to be in favor for hydrogen. It is still unclear to which extent the water form hydrogen will in the end create a larger or smaller climate warming compared to Jet-A.

NO_x which is created from combustion in air, especially when combustors are designed so that very high local flame temperatures arise. The formation of NO_x influences radiative forcing indirectly by influencing local atmospheric concentrations of both ozone (O_3) and methane (CH_4). NO_x will increase the ozone production which increases radiative forcing. NO_x also leads to the formation of hydroxyl radicals (OH^-) which reduces the lifespan of methane (CH_4) in the atmosphere, a very potent greenhouse gas. Hence, this effect decreases radiative forcing and acts cooling. The net effect of NO_x, although continuously being updated, is generally reported as warming.

A recent analysis of the effect of aviation on the climate net radiative forcing[3] from aviation was estimated at 100.9 mW/m^2 [8]. Key positive contributors were 57.4 mW/m^2 (17,98) from contrail cirrus, 34.3 mW/m^2 (28,40) from CO_2 and 17.5 mW/m^2 (0.6,29) from NO_x. The numbers in parenthesis are 90% likelihood ranges. The net effect of aviation, due to the additional effects of non-CO_2 emissions was estimated at 3.5% of man-made activities.

Depending on the time horizon, you may argue that the climate impact of aviation could become lower in the short future. The warming from the CO_2 emissions will persist for hundreds of years whereas the effect of contrails and NO_x emissions act on much shorter timescales. Thus, if ways to reduce NO_x emissions were found through much improved combustor technology and ways to reduce contrail formation through active avoidance of flying in regions with ice-supersaturated conditions, the negative impact of flying would approach that of the accumulated CO_2 emissions. A radical reduction of NO_x does not seem imminent, whereas contrail avoidance flying might see breakthroughs over the upcoming decade.

Sustainable pathways

Several pathways to curbing the climate impact of aviation exist:

1. Continuous improvement in aircraft and propulsion efficiencies
2. Changing energy carriers to a more sustainable form:
    - Biofuels
    - Hydrogen (combustion/ fuel cell) & electrofuels
    - Electric propulsion

[3] More carefully described the work reports ERF (Effective Radiative Forcing), which includes tropospheric adjustments of the emissions and hence more accurately reflects the warming.

Looking at technology improvement this is an important contributor to greening of future aviation. For the next two decades perhaps an annual improvement in energy efficiency of 1.2%-1.3% can be expected depending on the range of the aircraft [9]. More ambitious technology targets go beyond 2.0% per annum in energy efficiency improvement [10]. However, pre-COVID estimates indicated anticipated growth of the flown passenger kilometers by close to 5% driven by rapid aviation expansion primarily in Asia (China/India) but also in south America. Hence, the game of achieving a net reduction in emissions must come not only from technology improvements but also from going to more sustainable energy carriers.

Continuous improvement on fuel efficiency

A number of ways to improve vehicle energy efficiency exist. Key categories for on-going research are [11]:

1. introduce aircraft drag reduction techniques,
2. increase the use of lightweight structures,
3. make improvement on combustion-based systems,
4. introduce novel engine and aircraft types.

Research wise, Chalmers is very active in categories 2/3 and 4. However, since this is an introductory text, we will not go further into the possibilities of improving technologies. This text has the ambition to reflect state-of-the-art solutions for propulsion and aircraft. The interested reader can find more details in Appendix D, referenced work and as part of more advanced aerospace courses given at Chalmers. The remaining part of this chapter will now overview the possibilities for the use of biofuels, hydrogen and electric propulsion in aviation.

Biofuels

The use of biofuels refers to aviation fuels derived from sustainable feedstocks. They can be originating from waste oils, from plants or animals, domestic waste, food scraps etc. A schematic indicating various production paths can be found in Figure 22. The key elements here are the absorption of atmospheric CO_2 through living organisms and an immediate use of the products to manufacture sustainable fuels. By sustainable we mean in the sense that the captured CO_2 is emitted again, but that this creates a “closed loop” not increasing the CO_2 concentrations in the atmosphere.

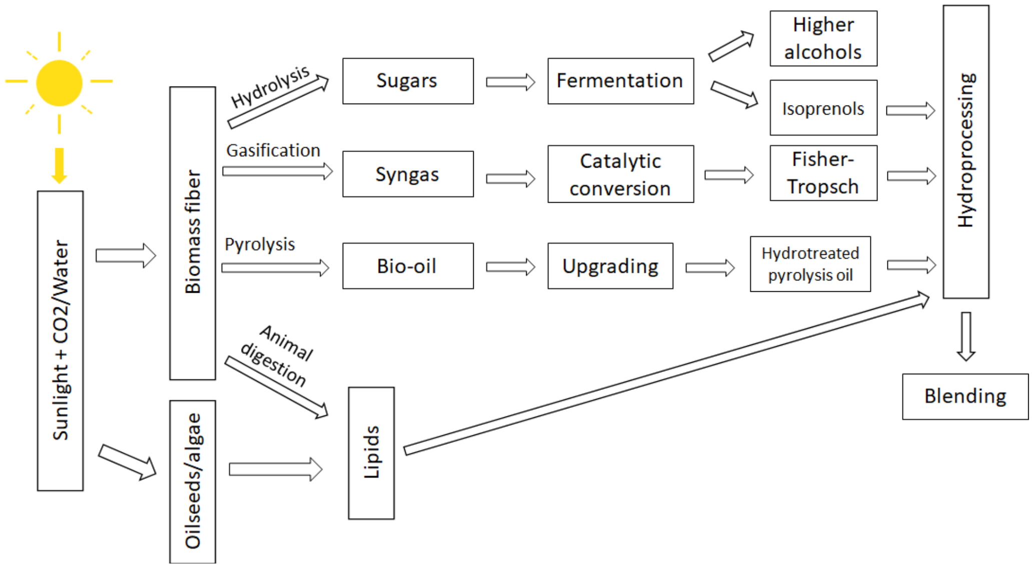

Figure 22: Various paths to bio-produced aviation fuel

Of course, all these pathways require life cycle analysis to assess the true benefit of a given fuel. The emissions reduction potential may be as low as 50% depending on the detailed process.

To be possible to use as an aviation fuel, the production pathways illustrated in Figure 22 need to be certified. Today five types of processes are certified that allow up to 50% blending use:

1. **Fisher-Tropsch:** hydroprocessing and catalytic upgrading of biomass products, such as municipal solid waste, agricultural and forest wastes, energy crops (June 2009)
2. **HEFA:** Oleochemical conversion of for instance oilseed crops. In future this could also become a pathway for algea, a method that potentially could be very productive by allowing more frequent “harvesting” than competing feedstocks (July 2011)
3. **FT-SPK:** Biomass conversion to syngas, which is then converted to synthetic paraffinic kerosen and aeromatics by Fisher-Tropsch (November 2015)
4. **ATJ**: This is a hybrid between thermochemical processing and the use of biochemical technologies. Cellulosic biomass is used (April 2016).
5. **CH-SK**: Catalytic hydrothermolysis synthesized kerosene, from fatty acids or fatty acid esters or lipids from fal oil greases (February 2020)

Additionally four processes allowing either 10% or 5% blend-in are certified in addition to the five processes above.

The first commercial flight on biofuels was conducted in 2008, when a Virgin Atlantic 747 flew from London to Amsterdam using a blend of 20% coconut and babassu oil mixed with 80% conventional jet fuel. Since then, production volumes of biofuels are picking up only slowly. In 2016 less than 0.1% of all aviation jet fuels were biofuel [12].

The Swedish government has introduced a reduction legislation, from 1st of July 2021, to gradually increase the content of biobased fuels in aviation fuels from 0.8% today to 27% in 2030. For Swedish conditions, the availability of biomass would easily cover the need of national as well as internatinoal flying [13]. However, this would require a prioritising the use of biomass for aviation fuel production and also a doubling or tripling of the fuel cost for the airliners. Internationally, the need would be massive and it will be challenging to devote large production volumes to transport, without competing with food production.

Hydrogen & electrofuels

Hydrogen could potentially serve as an aviation fuel. It is feasible to think that large scale production of hydrogen could be done from sustainable energy sources such as solar and wind power, especially considering the rapid drop in production cost for electricity from these sources.

Two common parameters used to describe heat content density are:

$$q_{grav} = heat\ content\ per\ mass\ [kWh/kg]$$
$$q_{vol} = heat\ content\ per\ volume\ [kWh/litre]$$

While analyzing technical solutions it is important to consider installed densities, that is heat density **with** the tank weight included. Hydrogen has a magnificent gravimetric density almost triple that of comparable fossil fuels, 120 MJ/kg compared to 43 MJ/kg for Jet A. Unfortunately, the volumetric density is not as great. To reach reasonable transport performance with respect to volume, gaseous hydrogen is normally compressed to 700 bars, still resulting in only about a 1/10 in volumetric energy density compared to fossil counterparts. The high pressures result in heavy composite tank installations with only 4-6% of the mass fraction being hydrogen. Thus, installed gravimetric densities of only a fraction of the fossil counterpart are achieved despite its very high uninstalled gravimetric value.

For cryogenic hydrogen (liquid form), installed volumetric densities reach about 1/5 of the volumetric energy density of a corresponding fossil fuel [14]. Although real cryo-tank volumetric densities are somewhat better than for compressed tanks, the real benefit comes from its gravimetric values. Due to only modest tank pressures (typically 1.8-3.0 bars) mass fractions up to 35-55% may potentially be reached even going beyond comparable fossil fuels (100% to 150%) in gravimetric densities [14].

Because of the modest volume density of hydrogen, longer range commercial air transport becomes penalized by additional drag caused by aircraft volume increase. A perception of this effect is obtained from reviewing Figure 23.

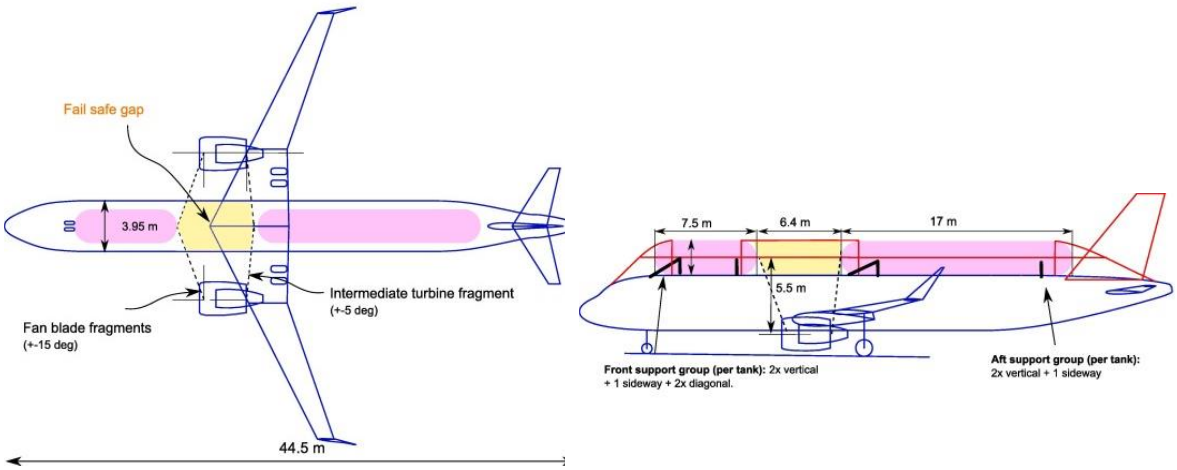

Figure 23: Tank installation concept for medium range hydrogen aircraft. The fail-safe gap refers to that a disc burst in the engine should not result in a turbine projectile going into the tank creating a fire [15].

Producing a kg of hydrogen from electrolysis of water requires approximately 50 kWh electricity. Assuming another 7 kWh for the liquefaction, this could be feasible long term, and ignoring any other energy needs resulting from transport, pumping etc. 57 kWh would thus be needed to generate one kg of cryogenic hydrogen. With a thermal efficiency of perhaps 50% for the engines, the net efficiency from electrical input to mechanical output becomes less than 30%. It is likely that the efficiency of the engine can be improved a few percent by recovering heat in the aero engine exhaust, thereby preheating the fuel before it enters the combustion chamber, but the total efficiency from electricity to useful propulsive power is still quite low. Another disadvantage is that hydrogen combustion creates, is that it produces a relatively large amount of water compared to Jet A. For the same heat release stochiometric analysis can be used to show that hydrogen combustion produces about 1.6 times more water per unit heat than Jet-A. Thus, if one kg water is generated from Jet A combustion, you should expect 2.6 kg from hydrogen combustion in order to create the same heat release.

Although the process from electricity to propulsive energy is rather inefficient for hydrogen it is even worse for more complex electro generated fuels such as electrodiesel. Perhaps the conversion efficiency from hydrogen to the more complex diesel fuel would have an efficiency of 75%, estimated from [16]. Still, not having to handle the complexities of hydrogen, such as increased safety hazard from risks of hydrogen leaks and potential fire, could motivate the introduction of electrodiesel as sustainable alternative for aviation. The real advantage is that the current aircraft would not have to be changed very much, possibly not at all. The major challenge is the production of the large scales of electrodiesel. The downside is that you would emit CO_2 back to the atmosphere. Perhaps the only way this will be allowed on very long term is if the CO_2 was initially captured from the atmosphere?

Electric propulsion - batteries

Today electric energy is challenging the dominating position of fossil fuels in the automotive industry as it can be produced and consumed in a cleaner way. For aerospace applications, however, a lot of technology development is still needed. Comparing to a normal turbofan/turbojet or even piston engine powered aircraft for a normal flight mission, electric propulsion loses in almost all the key aspects such as flight speed, range, and payload. The well-known deficiency of electric propulsion is that none of existing electrical energy storage technologies could achieve the same energy density and power density as burning fossil fuels in the combustion engines. Even with a 95% efficiency electric motor, electric propulsion is not comparable with a gas turbine and jet fuel with an effective energy density about 5 kWh/kg. Still, electric propulsion promises to reduce maintenance cost substantially, achieve zero mission emissions and possibly also reduce noise emissions. It is therefore likely, that electric propulsion will be used for the applications where it is possible to introduce it, which at the time of writing is limited to personal transport and smaller short range aircraft.

Among the state-of-the-art lithium ion (Li-ion) batteries, the NMC (lithium plus nickel, manganese, and cobalt) battery is currently the most widely used battery technology by the automotive industry. Although NMC batteries have a better energy density compared to the nickel-based batteries, with a value approaching 0.3 kW/kg is hardly possible to change the view of the sky. Tesla Model 3, best in class, shows a cell energy density of 247 Wh/kg and a value of 159.5 Wh/kg on pack level [17]. As indicated by several conceptual designs for fully electric aircraft, a minimum of 0.8 kWh/kg is desired for a normal short flight with 150 passengers. Long term targets up to 20 years from now, electric aircraft designers would like to see an energy density above 1.0 kWh/kg for the electrical energy storage.

Thanks to the technological revolution happening in the automotive industry, records for the energy density of batteries are broken quite frequently. For the future, several lithium-based battery technologies have showed great potential. Among them, a theoretical energy density of 3.5 kWh/kg and 2.6 kWh/kg are claimed for lithium-oxygen ($Li\text{-}O_2$) and lithium-sulfur (Li-S) batteries. Solid-state lithium type battery, as one of the most promising candidates for the next generation electrical energy storage, has a more credible target of 0.5 kWh/kg. More importantly, it is considered a safer choice as it replaces the flammable liquid electrolytes with solid-state Li^+ conductors.

Beyond the world of lithium, zinc-air batteries have attracted great attention as they could provide high energy density up to its theoretical limit of 1.2 kWh/kg with low cost and low risk of fire hazard. Even more advanced and energy dense systems may be derived from aluminum-air batteries. These may reach potential energy densities over 8 kWh/kg. Besides this, aluminum-air designs may prove to be low cost and aluminum could even be recovered from the combination of recycling electrolyte and electrolyzing aluminum using clean energy. Then, why is it not widely applied yet? The major problem is the high self-corrosion rate of aluminum anodes as aluminum is a highly active metal. This reduces the practical energy density to far lower than its theoretical value. In addition, zinc/aluminum-air systems are normally not electrically chargeable, therefore mechanical recharging, which is to replace the metal anodes, seems the only solution.

The optimal operating temperature of lithium-based batteries suggested in various literature is limited to 15-40 °C. Generally, increasing the operating temperature increases the degradation rate of the battery while low temperature negatively affects the ionic conductivity hence lowers the performance. Most importantly, limiting the highest working temperature under 130 °C is critical to avoid thermal runaway and explosion of the batteries. Normally, a cooling package has to be integrated with the battery to keep all the battery cells below the acceptable temperature. State of charge (SOC) and discharge rate are also important aspects for batteries as they affect the degradation rate of the device. Both too high and too low SOC are detrimental to the ageing of batteries, whilst higher power requires substantially higher discharge rate is also increasing the degradation rate of the battery.

For the development of hybrid solutions for aircraft, the potential benefits are much smaller than for instance for road vehicle applications. A major part of the fuel consumption is derived from the climb and cruise phases. A general understanding of how this adds up can be derived from Figure 18. In those points the efficiency is relatively close to peak thermal efficiency and substantial improvements from hybridization is much more difficult to achieve than for road vehicle applications [18] where very low power running is common, for instance while driving in cities. Regenerative breaking is another area where little advantage can be derived. Aircraft do very little breaking, rather they recover most of its kinetic and potential energy by extending the airliners range [18].

Parallel hybrids, for which the gas turbine is still the major power source, tries to utilize electric power for improving the gas turbine performance in a short period of critical operating conditions. Here a battery could either supply the power to boost one of the gas turbine shafts or store the excessive power from the gas turbine. In this application, the power density of the battery is as critical as energy density, of which the current technology level is way lower than the desired values. For serial hybrid or turbo-electric configurations, the gas turbine onboard is used to generate electrical power for the motor to drive the propeller.

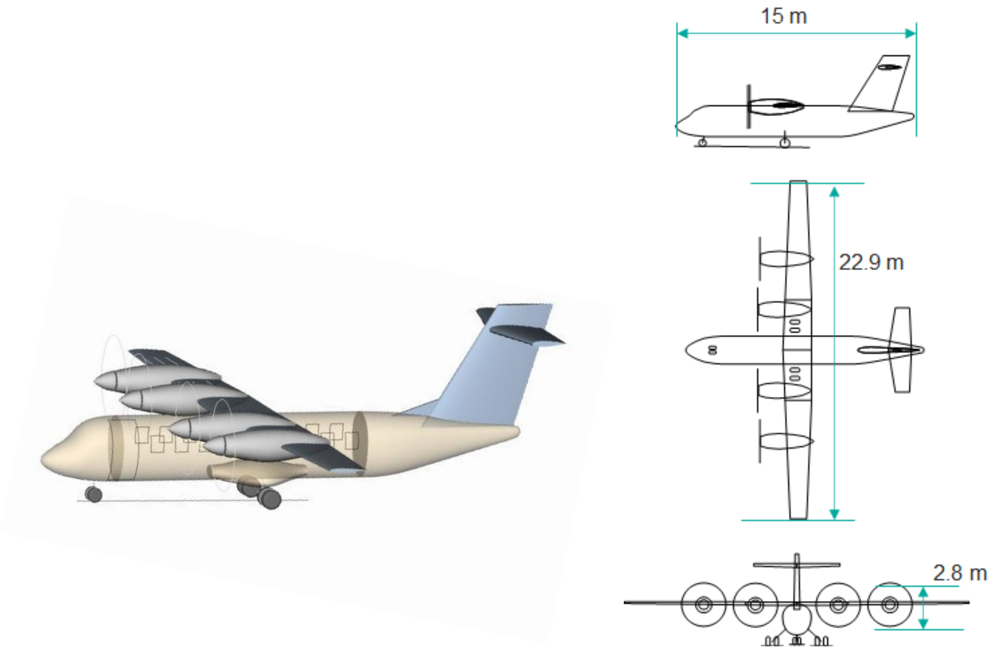

Figure 24: Conceptual design of electric aircraft performed in Chalmers in-house research project.

Even though the current electrical energy storage technologies are still far away from the requirements needed by conventional large aircraft, there are still markets which have a low demand for range, speed, and payload. For example, in 2019, OSM Aviation Academy (one of their training center is located at Västerås, Sweden) ordered 60 two-seats all-electric aircraft for pilots training which may need only an hour flight time and does not require payload other than the pilots. Flying taxi across the cities has been developing by many start-ups. The Swedish start-up Heart Aerospace, which is located in Göteborg, is developing a regional 30 passenger electric aircraft, the ES30. The ES30 will have an all-electric range of 200 km, an extended range of 400 km and a 25-passenger variant flying up to 800 km.

Chalmers is also active to develop a conceptual design platform for electric aircraft, see Figure 24, where different battery technologies and electric drivetrains can be simulated. This aircraft is also the basis for some of the examples given in this text and will be used for labs associated with this course.

Electric propulsion – fuel cells

A fuel cell is actually “burning the fuel” for electricity production in another way. As an alternative to batteries, it could provide high energy density based on the selected fuel, that is hydrogen, and it can be “recharged” as easy as filling the fuel tank. Another advantage is the exhaust, which is just water if using hydrogen. However, the low power density is one obstacle for fuel cell to compete with conventional aircraft propulsion. The highest power density of fuel cell claimed in public until now is 2.5 kW/kg for a solid oxide fuel cell developed by NASA’s Glenn Research Center. Capacitors with high power density potential on the other hand has way too low energy density for being considered in aircraft propulsion. Looking at recent attempts to use fuel cells, it is actually the storage of compressed hydrogen, as discussed above, that constitutes a major part of the weight of the system. Another challenge with fuel cells is to maintain high efficiency when extracting large amount of power. Typical operating conditions do not give any efficiency benefit over combustion-based engines. However, emissions are NO_x-free, and the water produced should be much easier to handle see promising to provide ways to cut non-CO_2 emissions substantially.

4. AERO ENGINE CERTIFICATION

NO_x emission standards

The International Civil Aviation Organization (ICAO), a united nation specialized agency, develops certification procedures for engine emissions. These procedures are then adopted by their member states and sets emission requirements for new engines. A very specific test cycle is used, the so-called Landing-Takeoff (LTO) cycle. The LTO cycle originates from the idea to simulate the operation of the engine close to an airport, as illustrated in Figure 25 below.

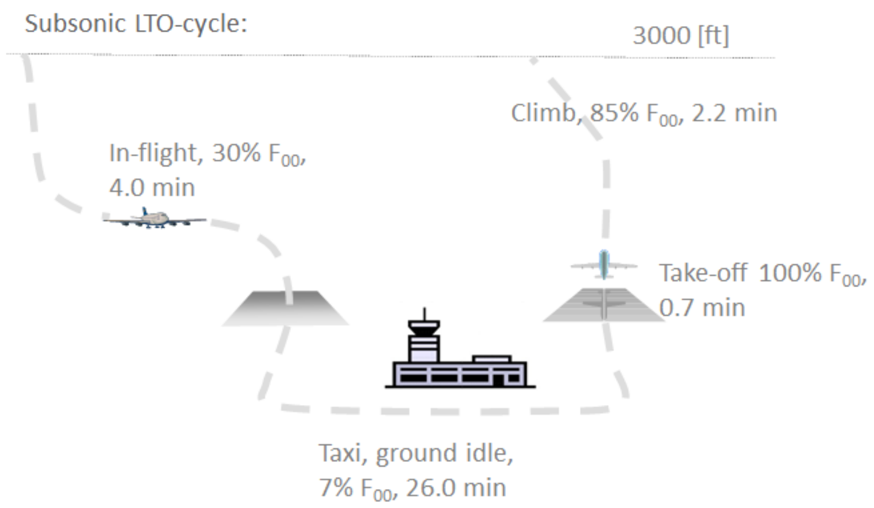

Figure 25: The subsonic LTO cycle as pictured in airport close operation.

As already indicated in Figure 25 the different operating modes are characterized by time flown and thrust settings as summarized in Table 4 below.

Mission phase	Thrust	Time in operating mode [min]
Take-off	100% F_{00}	0.7
Climb	85% F_{00}	2.2
Approach	30% F_{00}	4.0
Taxi/Ground idle	7% F_{00}	26.0

Table 4: The ICAO LTO (Landing-Takeoff cycle)

F_{00} represents the thrust that the engine is set to deliver as specified in its type certificate, for sea level static. Nitrogen Oxides (NO_x), unburned hydrocarbons (UHC) and carbon monoxide (CO) are measured in the different operating modes and summed up to a total emission in grams. In addition, a smoke emission is measured and reported in terms of Smoke Number (SN). Below we only give details for NO_x emission certification.

The metric by which the engines are measured, the emissions index EI_{NOx}, is defined as the total amount of emissions in grams for the four operating modes, divided by the thrust in kilo-Newton.

$$EI_{NOx} = \frac{\sum_i Emission\ rate \cdot Time\ in\ mode}{Sea\ level\ static\ thrust} \quad \left[\frac{gram}{kN}\right]$$

The most recent NO_x standard, CAEP/8 NO_x, sets conditions for engines for which the first individual production model was issued after 1st January 2014 and for which an application for a type certificate was submitted before 1 January 2023. The regulatory levels are defined from the engine overall pressure ratio Π_{00}. For a turbofan, the overall pressure ratio Π_{00} is the pressure ratio between station 3 and station 2 as indicated in Figure 12. A number of thrust and pressure ratio categories are defined, but the most common criteria is engines with pressure ratios between 30 and 104.7 and with a thrust F_{00} greater than 89 kN. For such engines Then the EI_{NOx} must be below:

$$EI_{NOx} < -9.88 + 2.0 \cdot \Pi_{00}$$

and engines with the same range in pressure ratio but a thrust less than 89.0 kN and greater than 26.7 kN. Then the engine must obey:

$$EI_{NOx} < 41.9435 + 1.505 \cdot \Pi_{00} - 0.5823 \cdot F_{00} + 0.005562 \cdot \Pi_{00} \cdot F_{00}$$

The procedure to certify engines for NO_x emission just in the vicinity of the airport is rather questionable. In particular, considering the previous discussions about NO_x emissions and climate impact.

CO_2 emission standards

Relatively recently, in February 2016, the Committee on Aviation Environmental Protection (CAEP), adopted a CO_2 fuel efficiency standard. The key parameter is Specific Air Range (SAR) which measures the km traveled per kg of fuel for a given aircraft. To allow regulations to be tightened by reducing the regulatory value, ICAO uses the inverted value, that is 1/SAR. Three different aircraft masses are used based on the Maximum Take-off Mass (MTOM):

1. High gross mass (92% of MTOM)
2. Low gross mass ($0.45\text{MTOM} + 0.63\text{MTOM}^{0,924}$)
3. Mid gross mass, which is the arithmetic mean of the high gross mass and the low gross mass as specified above.

1/SAR is measured in all three points and averaged. To make the comparison fairer between different size classes a scaling factor is introduced, a so called Reference Geometric Factor (RGF), determined by multiplying the pressurized fuselage length by the fuselage width. The parameter used for regulation called MV is:

$$MV = \frac{\frac{1}{3}\left(\frac{1}{SAR_1} + \frac{1}{SAR_2} + \frac{1}{SAR_3}\right)}{RGF^{0,24}}$$

This metric is then compared against a regulatory curve parameterized on MTOM. The curve is found in Figure 26 below. The standard applies to new type designs from year 2020 as well as from in production aircraft from 2023 that are modified. Of course, the plan is to successively lower the curve and tighten the pressure to create more efficient aircraft.

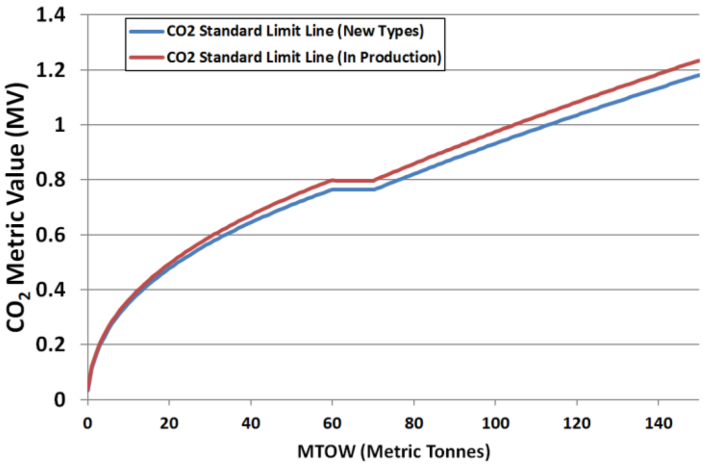

Figure 26: Aircraft CO2 standard regulatory curve.

APPENDIX A - derivation of speed of sound

The speed of sound is derived by a so-called Lorentz transformation, that is you analyze the flow by travelling with the wave rather than as a bystander, see Figure 27 below.

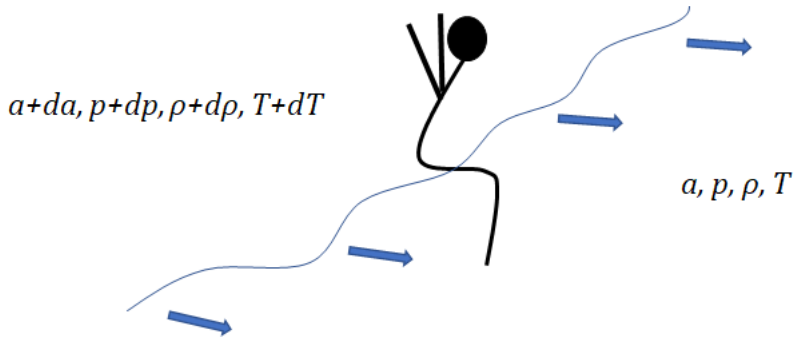

Figure 27: A happy wave rider

As we sit on top of the wave, we see the air moves towards us with a speed a, but that downstream of the wave the velocity is somewhat different $a+da$. The same is true for the pressure p, the density ρ and the temperature T. Applying the continuity (1.18) over the wave we get:

$$\rho a = (\rho + d\rho) \cdot (a + da)$$

Simplifying and neglecting higher order terms give:

$$\rho da = -d\rho a \quad \Longrightarrow \quad a = -\rho \frac{da}{d\rho}$$

Performing the same exercise with the momentum equation (1.3b) gives:

$$\rho a^2 + p = (\rho + d\rho)(a + da)^2 + (p + dp)$$

Developing and ignoring higher order terms give:

$$0 = \rho 2ada + d\rho a^2 + dp$$

Then, da is:

$$da = -\frac{a^2 d\rho + dp}{\rho 2a}$$

Use this in the continuity-based expression to get:

$$a = \rho \frac{\frac{a^2 d\rho + dp}{\rho 2a}}{d\rho} = \frac{a^2 d\rho + dp}{2ad\rho}$$

We get a^2 from as:

$$a^2 = \frac{dp}{d\rho}$$

APPENDIX B – ISA standard for altitudes up to 25000 m-

Altitude	Pressure [Pa]	Temperature [K]	Density [kg/m3]	Speed of sound [m/s]
0	101325	288,15	1,22499	340,29526
500	95460,773	284,9	1,16726	338,37075
1000	89874,448	281,65	1,11163	336,43523
1500	84555,833	278,4	1,05806	334,48851
2000	79495,003	275,15	1,00648	332,5304
2500	74682,287	271,9	0,95685	330,56068
3000	70108,27	268,65	0,90911	328,57916
3500	65763,787	265,4	0,86322	326,58562
4000	61639,921	262,15	0,81912	324,57983
4500	57727,997	258,9	0,77676	322,56157
5000	54019,578	255,65	0,73611	320,5306
5500	50506,465	252,4	0,6971	318,48668
6000	47180,688	249,15	0,65969	316,42955
6500	44034,509	245,9	0,62383	314,35897
7000	41060,411	242,65	0,58949	312,27466
7500	38251,099	239,4	0,55661	310,17634
8000	35599,496	236,15	0,52516	308,06373
8500	33098,736	232,9	0,49508	305,93653
9000	30742,166	229,65	0,46634	303,79444
9500	28523,337	226,4	0,43889	301,63713
10000	26436,003	223,15	0,4127	299,46429
10500	24474,117	219,9	0,38772	297,27556
11000	22632	216,65	0,36391	295,0706
11500	20916,113	216,65	0,33632	295,0706
12000	19330,32	216,65	0,31082	295,0706
12500	17864,756	216,65	0,28726	295,0706
13000	16510,307	216,65	0,26548	295,0706
13500	15258,547	216,65	0,24535	295,0706
14000	14101,693	216,65	0,22675	295,0706
14500	13032,547	216,65	0,20956	295,0706
15000	12044,46	216,65	0,19367	295,0706
15500	11131,287	216,65	0,17899	295,0706
16000	10287,348	216,65	0,16542	295,0706
16500	9507,394	216,65	0,15288	295,0706
17000	8786,574	216,65	0,14128	295,0706
17500	8120,403	216,65	0,13057	295,0706
18000	7504,74	216,65	0,12067	295,0706
18500	6935,754	216,65	0,11152	295,0706
19000	6409,907	216,65	0,10307	295,0706
19500	5923,929	216,65	0,09525	295,0706
20000	5474,795	216,65	0,08803	295,0706
20500	5059,713	216,65	0,08136	295,0706
21000	4676,102	216,65	0,07519	295,0706
21500	4321,575	216,65	0,06949	295,0706
22000	3993,927	216,65	0,06422	295,0706
22500	3691,12	216,65	0,05935	295,0706
23000	3411,271	216,65	0,05485	295,0706
23500	3152,639	216,65	0,05069	295,0706
24000	2913,616	216,65	0,04685	295,0706
24500	2692,715	216,65	0,0433	295,0706
25000	2692,715	216,65	0,0433	295,0706

APPENDIX C – Fuel use charts – Jet A

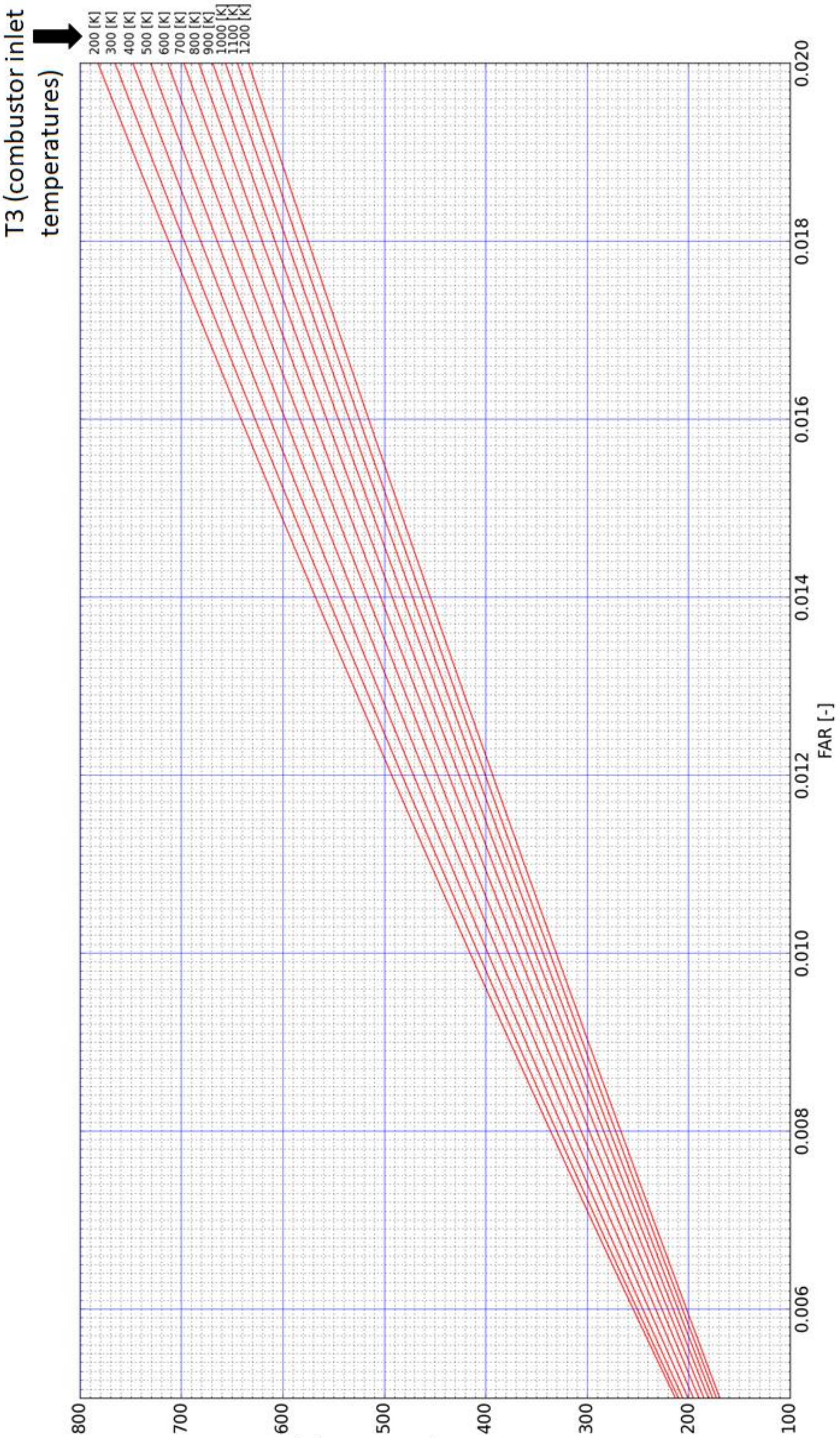

Figure 28: Combustor temperature rise - lower range

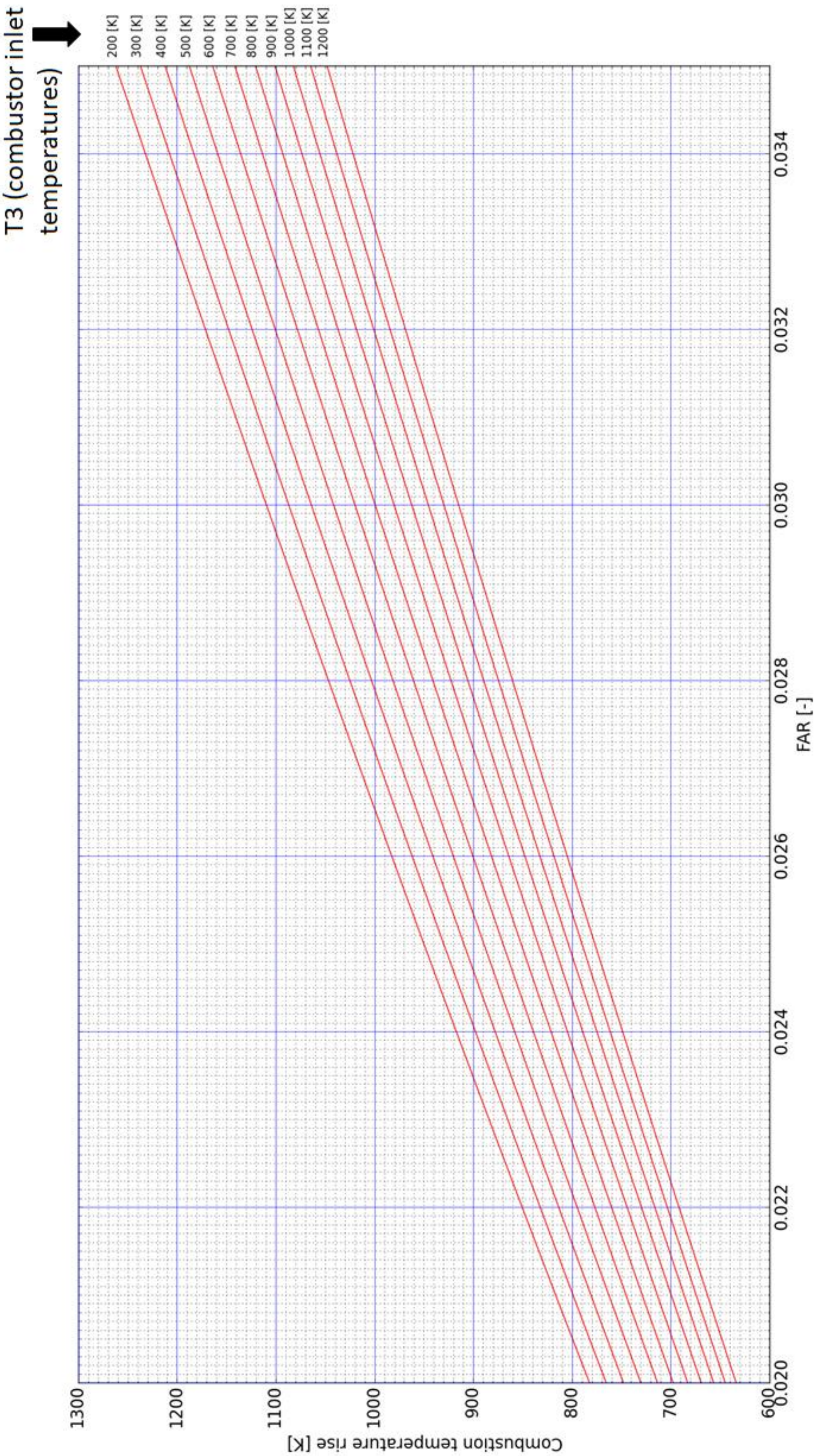

Figure 29: Combustor temperature rise - higher range

APPENDIX D – pathways to technology improvement

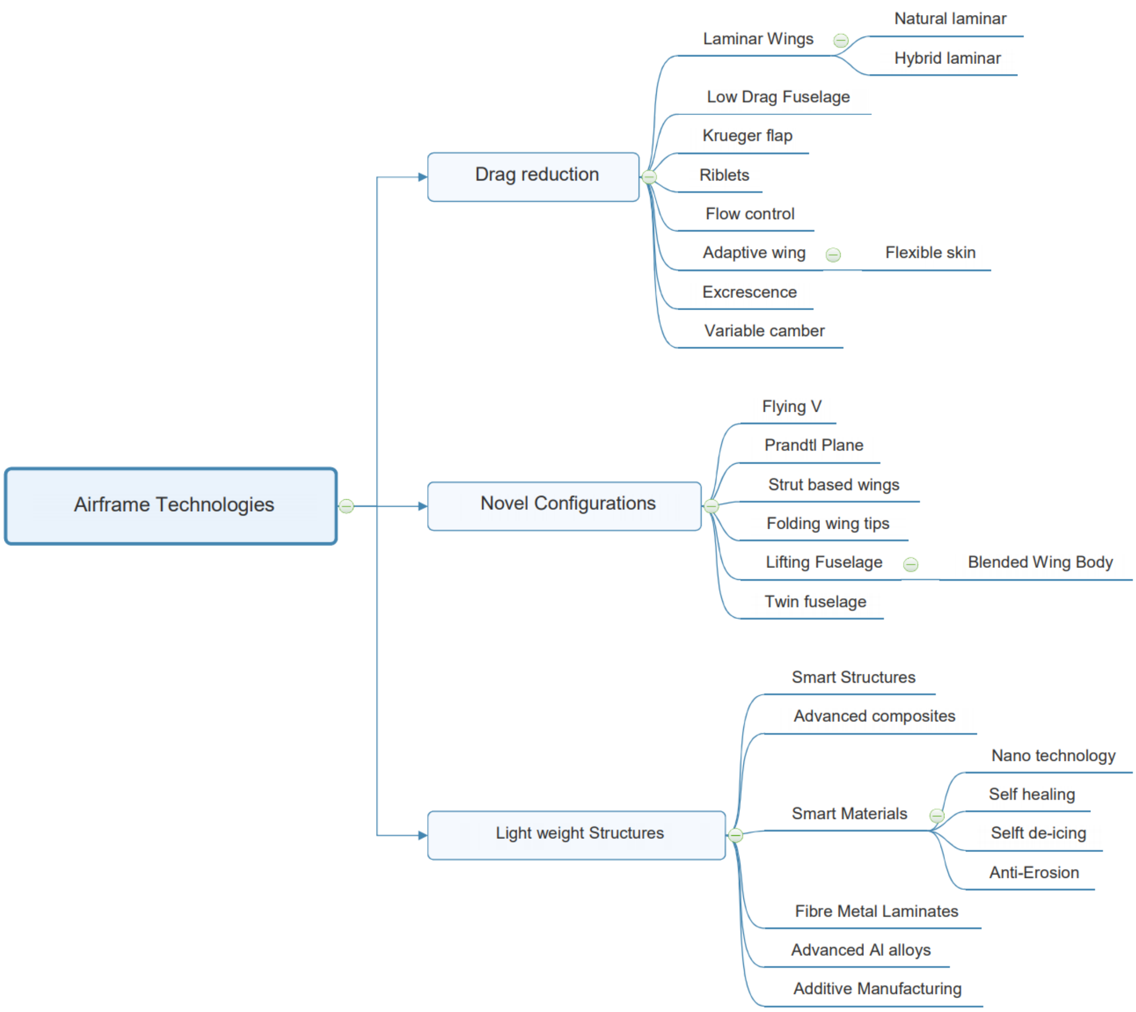

Figure 30: Breakdown of promising airframe technologies, see supplementary material of [11] for more detail.

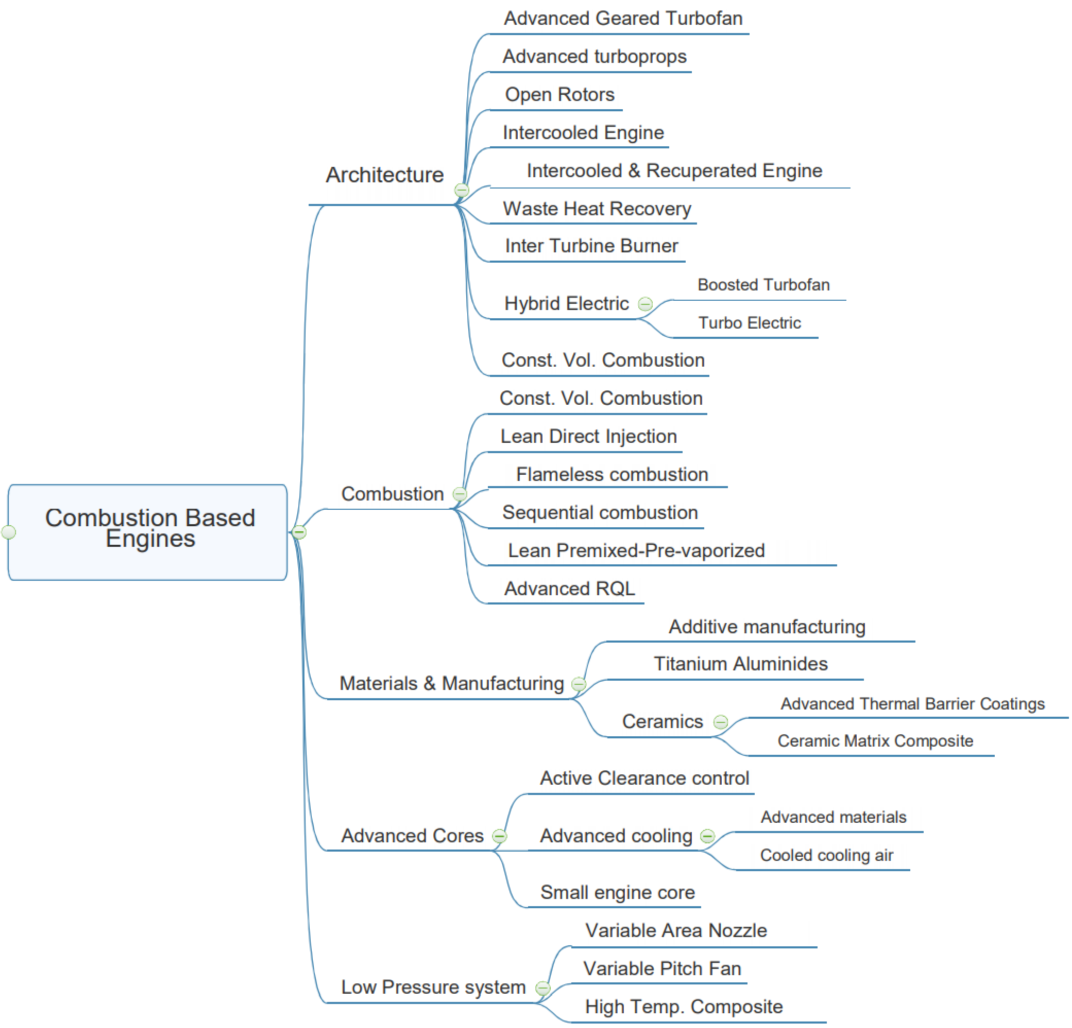

Figure 31: Breakdown of promising combustion engine technology improvements, see supplementary material of [11] for more detail.

APPENDIX E (not in MMS196) – the Schmidt/Appleman theory[4]

First, we introduce the **specific mass content** of water and the **specific enthalpy content** by m and h respectively.

$$m_{H_2O} = mass\ of\ water\ divided\ by\ total\ gas\ mass$$
$$h = enthalpy\ per\ kilogram\ gas$$

Here we also use the concept of emission index. The emission index gives the amount of emissions in kg resulting from the combustion of 1 kg of a given fuel. For instance, burning a hydrocarbon in air produces an emission index of water equal to:

$$EI_{H_2O} = \frac{m_H M_{H_2O}}{2M_H} \qquad \text{(E1)}$$

Where M_{H_2O} is the molar mass of water and M_H is the molar mass of hydrogen. Equation (E1) is motivated in the end of this appendix.

If the mass of fuel consumed is assumed to be 1 kg/s and the exhaust mass flow is assumed to be N, then the mass of the air going into the engine must have been N-1. Following the analysis of [19] we call N the dilution factor. The mass fraction of water in the exhaust plume, must then be:

$$m_{H_2O,P} = \frac{EI_{H_2O}}{N} \qquad \text{(E2a)}$$

Equation (E2a) assumes completely dry air. However, the air coming into the engine from the environment is normally not completely dry. We can include this water content using a specific water content $m_{H_2O,E}$ for the environment air. We then get:

$$m_{H_2O,P} = \frac{EI_{H_2O} + (N-1)m_{H_2O,E}}{N} \qquad \text{(E2b)}$$

The change in water mass fraction Δm from the environment to the exit plume becomes:

$$\Delta m_{H_2O} = m_{H_2O,P} - m_{H_2O,E} = \frac{EI_{H_2O} + (N-1)m_{H_2O,E}}{N} - m_{H2O,E} = \frac{EI_{H_2O} - m_{H_2O,E}}{N} \approx \frac{EI_{H_2O}}{N} \quad \text{(E2c)}$$

Where the last approximation is due to that normally $EI_{H_2O} \gg m_{H_2O,E}$.

A fraction of the heat released during combustion, Q, is converted into work ηQ to propel the aircraft. The remainder is lost as heat, hence the heat loss per unit of fuel must be:

$$Q(1-\eta)$$

For bypass engines the mixing between the core and bypass streams are assumed to be rapid. The increase in enthalpy Δh from the environment to the exhaust plume then becomes:

$$\Delta h = h_P - h_E = \frac{Q(1-\eta) + (N-1)h_E}{N} - h_E = \frac{Q(1-\eta) - h_E}{N} \approx \frac{Q(1-\eta)}{N} \quad \text{(E3)}$$

Where the last approximation is due to that $Q(1-\eta) \gg h_E$.

By forming the ratio of the change of specific mass content of water to the change of specific enthalpy content we approximately have:

[4] The derivation outlined here follows the trail of thought presented in [19]

$$\frac{\Delta m_{H_2O}}{\Delta h} = \frac{\frac{EI_{H_2O}}{N}}{\frac{Q(1-\eta)}{N}} = \frac{EI_{H_2O}}{Q(1-\eta)} \qquad \text{(E4a)}$$

We now re-write the ratio of E4a by looking at temperature change rather than enthalpy change also including partial pressures instead of the specific water content. Remember that the partial pressure of water p_{H_2O} in the exhaust plume is related to the specific mass content of water in the exhaust plume through:

$$m_{H_2O,P} = \frac{M_{H_2O}}{M_{air}} \cdot \underbrace{\frac{p_{H_2O,P}}{p}}_{\substack{molar\ fraction \\ of\ water}}$$

For a correctly computed average c_p we then get the sought ratio:

$$\frac{\Delta p_{H_2O}}{\Delta T} = \frac{p_{P,H_2O} - p_{E,H_2O}}{T_P - T_E} = \frac{\frac{EI_{H_2O}}{N}\frac{p}{\frac{M_{H_2O}}{M_{air}}}}{\frac{Q(1-\eta)}{c_p N}} = \frac{EI_{H_2O} c_p p}{\frac{M_{H_2O}}{M_{air}} Q(1-\eta)} = G \qquad \text{(E4b)}$$

This ratio plays a central role in the Schmidt-Appleman work and therefore it has deserved its own denotation G, herein simply referred to as the Schmidt-Appleman constant. Hence, there is a linear relation in the partial pressure of water with the temperature in the plume:

$$p_{P,H_2O} = G(T_P - T_E) + p_{E,H_2O} \qquad \text{(E4c)}$$

Clearly, there will be no contrails in the plume immediately downstream of the engine exhaust. The exit temperature of the core engine is of the order 800 K. To predict if contrails may arise, we need to follow the dilution of exhaust air with ambient air from the core nozzle exit to downstream in the plume. For a turbofan the dilution is here modelled in two steps. The first dilution step occurs when the core air is mixed with the bypass air. Although the bypass air is assumed to have the same humidity as the ambient air, the temperature and hence the enthalpy is higher because of the work performed by the fan component. After the mixing of the core and bypass flows, Equation (E4b) can be used to dilute the flow down to the condition needed to predict whether contrails will occur or not.

Since the methods used in this text simplify modelling by using constant heat ratios $(\gamma{:}\,s)$ and constant specific heats $(c_p{:}\,s)$, energy is generally not conserved, only approximated. To achieve accurate conservation, integrals for these properties would be needed. In addition to energy conservation, a direct computation of the plume properties from engine exit conditions actually introduces new complexity. The plume energies are established depending on stagnation states relative to earth rather than relative to the engine, and the nozzle choking pressures need to be considered as they influence the plume energies as well.

A much simpler way to predict the exit condition is then to set the stagnation temperature from the fact that energy not transferred to the aircraft, will be transferred to the fluid exiting the engine. This is also the argument originally used by Schmidt/Appleman as stated above, that is the fluid energy increase relative to the surrounding is:

$$Q(1-\eta)$$

Where the efficiency η is readily determined from the flight speed, the net thrust and Q. The numbers are found in the table above. More specifically:

$$T_{0,plume} = \frac{Q(1-\eta)}{c_{pa}(\dot{m}_{bypass}+\dot{m}_{core})} + T_{0,ambient} \quad \text{(E5)}$$

As an input to study the mixing process we give some data in Table 5 below. The ambient conditions are computed for an altitude of 10668 meters and ISA condition. Since the dilution process is extensive it is more accurate to use c_{pa} for the calculations.

Table 5: Turbofan cruise conditions.

Ambient conditions	
p_ambient	23.84 kPA
t_ambient	218.8 K
Relative humidity	0%
Energy balance	
Fuel flow	0.3426 kg/s
Q (added heat, 43 MJ heating value)	14.73 MW
Net thrust (F)	23.6 kN
Flight speed (c_0)	231.4 m/s
Energy to aircraft ($F \cdot c_0$)	5.462 MW
Energy to gas - $Q(1-\eta)$	9.270 MW
Total efficiency η	37.1%
Schmidt-Appleman constant G	1.762
Emission index, EI_{H_2O}	1.238
Engine core exit	
$\dot{m}_{core}$	14.06 kg/s
FAR	0.025
Engine bypass exit	
$\dot{m}_{bypass}$	171.3 kg/s
Mixed condition (initial plume conditions)	
m_H2O (mass fraction)	0.00229
$T_{0,plume}$ (from E5)	268.7 K

If 100% humid ambient air is assumed, the output mass fraction changes from 0.00229 to 0.00239. Hence, the water content in the plume just exiting the engine is completely dominated by the combustion products.

To be able to predict if contrails may be created, the plume air is now mixed successively with air of the ambient condition. For this, we need to review saturated conditions over ice and water with temperature. Accurate analytic approximations are for instance found in [20]:

$$p_{ice} = e^{9.550426 - \frac{5723.265}{T} - 3.53068 ln(T) - 0.00728332T}$$

$$p_{water} = e^{54.842763 - \frac{6763.22}{T} - 4.210 ln(T) + 0.000367T + \tanh(0.0415(T-218.8))\left(53.878 - \frac{1331.22}{T} - 9.44523 \ln(T) + 0.014025T\right)}$$

However, here we use a simpler polynomial approximation according to:

$$p_{ice} = c_1\left(\frac{T_a}{100}\right)^6 + c_2\left(\frac{T_a}{100}\right)^5 + c_3\left(\frac{T_a}{100}\right)^4 + c_4\left(\frac{T_a}{100}\right)^3 + c_5\left(\frac{T_a}{100}\right)^2 + c_6\left(\frac{T_a}{100}\right) + c_7 \quad \text{(E6a)}$$

$$c_1 = 0.0110599 \cdot 10^6, c_2 = -0.1454453 \cdot 10^6, c_3 = 0.7986358 \cdot 10^6, c_4 = -2.3428980 \cdot 10^6$$

$$c_5 = 3.8716784 \cdot 10^6,\ c_6 = -3.4161722 \cdot 10^6,\ c_7 = 1.2570587E6 \cdot 10^6$$

$$p_{water} = c_1\left(\frac{T_a}{100}\right)^6 + c_2\left(\frac{T_a}{100}\right)^5 + c_3\left(\frac{T_a}{100}\right)^4 + c_4\left(\frac{T_a}{100}\right)^3 + c_5\left(\frac{T_a}{100}\right)^2 + c_6\left(\frac{T_a}{100}\right) + c_7 \quad \text{(E6b)}$$

$c_1 = 0.0331372 \cdot 10^5, c_2 = -0.4024138 \cdot 10^5, c_3 = 2.0391213 \cdot 10^5, c_4 = -5.5159271 \cdot 10^5,$
$c_5 = 8.3970790 \cdot 10^5, c_6 = -6.8182806 \cdot 10^5, c_7 = 2.3061883 \cdot 10^5$

The water approximation has the largest relative error of 0.062% as compared to the data. The ice approximation is even more accurate with a max relative error of 0.032%. The two polynomial approximations are valid in the range 200 to 273 K. The two curves are plotted in the Figure below:

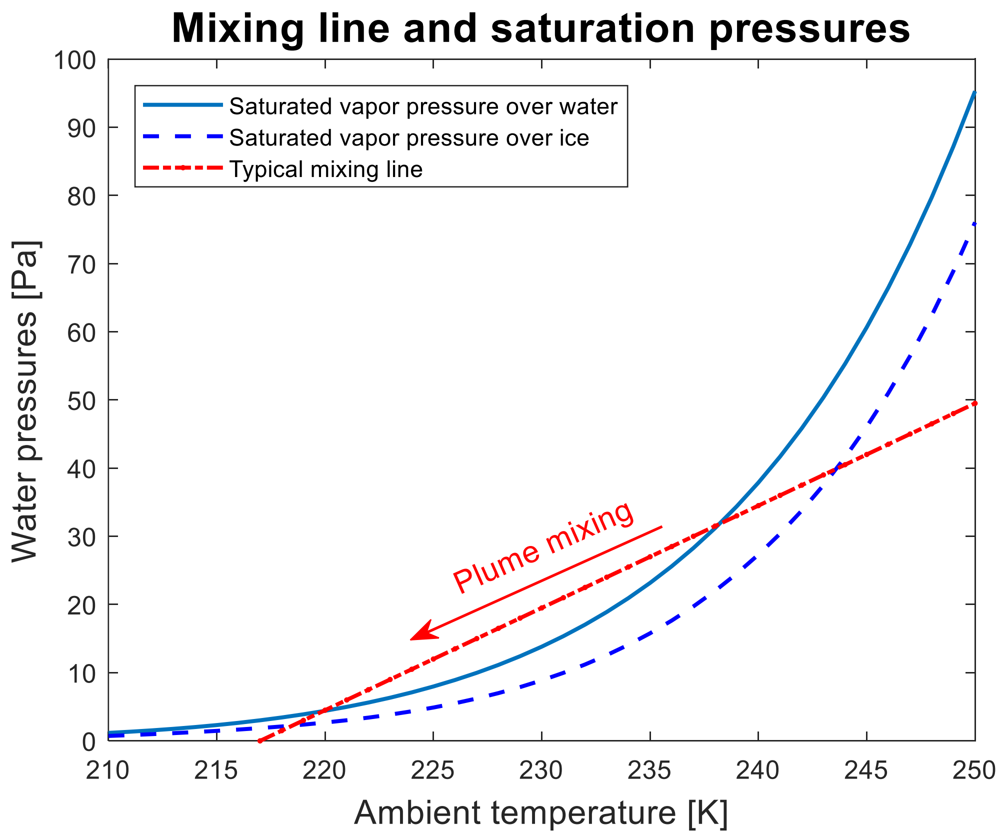

Figure 32: Saturated water pressures over water (full, blue) and ice (dashed blue) with typical mixing line (dashed dotted, red). The mixing line is drawn for a Schmidt/Appleman coefficient of 1.5.

In addition, a typical plume mixing curve is added in red. **If the plume mixing line crosses the saturated vapor pressure over water contrails may form.** Liquid water then starts to fall out which subsequently freezes.

Carrying out the expansion from the mixed condition stated in Table 5, i.e. $\left(T_P = 268.7\ K, m_{H_2O} = 0.00229\right)$ we obtain:

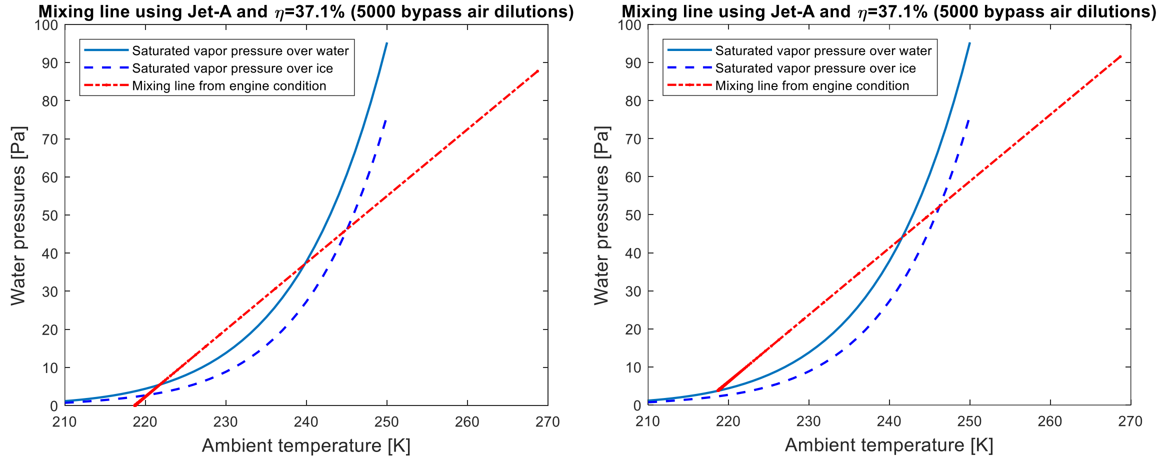

Figure 33: Dilution for engine exit condition as stated in Table 5. The rightmost graph is calculated assuming 100% ambient humidity.

Figure 30 was computed using successive dilution starting from the initial plume conditions of the exhaust air, as stated in Table 5. Water content and energy was conserved for these calculations. It confirms that the linear approximation proposed by Schmidt-Appleman is sound.

Establishing the Schmidt-Appleman diagrams

As we have shown, the slope of the mixing line depends on the fuel type, the engine efficiency (E4b) as well as the altitude that influences the pressure. Clearly there is one particular limiting line where the mixing line does not cross the saturated vapor pressure but precisely is a tangent. The matching point, that is the point where the mixing line tangents the saturated water line, can be found by forming the derivative of the water vapor saturation line and setting it equal to the Schmidt-Appleman constant G, that is:

$$\frac{dP_{water}}{dT_a}(T_a) = G$$

The solution to this match equation is denoted T_{LM}. Since we have chosen to use polynomials, we readily get the derivative from the expressions. A simple iteration is needed to establish the correct T_a that solves the equation. This solution now uniquely defines the line since now both the derivative and point on the line is known. To establish the limit temperature the line has to be followed down to the final dilution point, the threshold temperature T_{LC}.

Example 7: Establish the limiting temperature for a Schmidt/Appleman constant Gequal to 1.5 and a dry air.

First find in which point the saturated water line has the derivative equal to 1.5, i.e. we determine the matching temperature T_{LM}. This is achieved by equating the derivative of E6b with 1.5:

$$\frac{dP_{water}}{dT_a} = \frac{1}{100}\left(6c_1\left(\frac{T_a}{100}\right)^5 + 5c_2\left(\frac{T_a}{100}\right)^4 + 4c_3\left(\frac{T_a}{100}\right)^3 + 3c_4\left(\frac{T_a}{100}\right)^2 + 2c_5\left(\frac{T_a}{100}\right) + c_6\right) = 1.5$$

An iteration in T_a results in that the equation is satisfied by: $T_{LM} = T_a = 230.222\ K$. The threshold temperature T_{LC} can thus be found from the line that crosses $(T_{LM}, p_{water}(T_{LM}))$ and has the slope G=1.5. Using the equation of a straight line the crossing with the x-axis occurs at 220.8 K. This crossing represents the threshold temperature, denoted T_{LC}. For higher temperatures than the threshold temperature T_{LC} contrails cannot form. Notice that for humid air the limiting condition is located above the x-axis and a slightly more elaborate iteration scheme is needed.

The resulting limit condition is illustrated below:

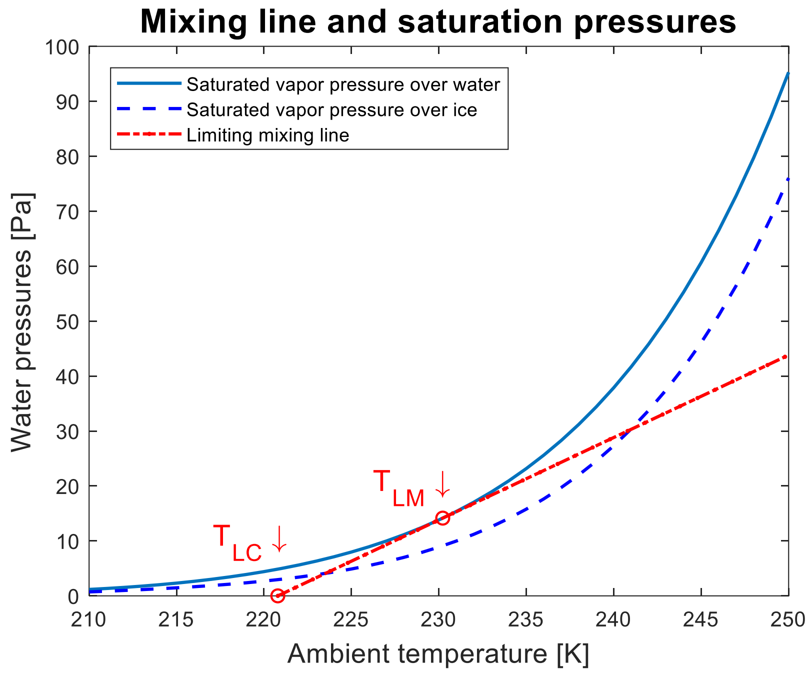

The iteration outlined in example 7 can easily be extended to the humid case by the following expression [19]:

$$T_{LC} = T_{LM} - \frac{P_{water}(T_{LM}) - RH \cdot P_{water}(T_{LC})}{G} \qquad (E6)$$

Notice that for U = 0.0, dry air, the equation simplifies to the equation used in example 7. The added term $RH \cdot P_{water}(T_{LC})$ represents the ambient vapor pressure at threshold conditions.

For the 0% humidity case, see Figure 30, the mixing will eventually reach a point below the ice-saturated curve. Then, the contrail will dissipate by sublimation. If the ambient condition is such that the humidity is higher than for saturated ice, the contrail would persist.

Obviously, it is possible to repeat the calculation illustrated in Example 7 above, determining T_{LC} for every altitude and repeat this for a set of humidities. Non-zero humidities require the use of Equation (E6). If then the computed T_{LC}:s are compared with the local temperature, for instance the ISA temperature profile, necessary conditions for contrail formation are obtained. Such charts are called Appleman-Schmidt charts. Below such a chart is established for Jet-A combustion assuming an efficiency of 30.0% for the engine.

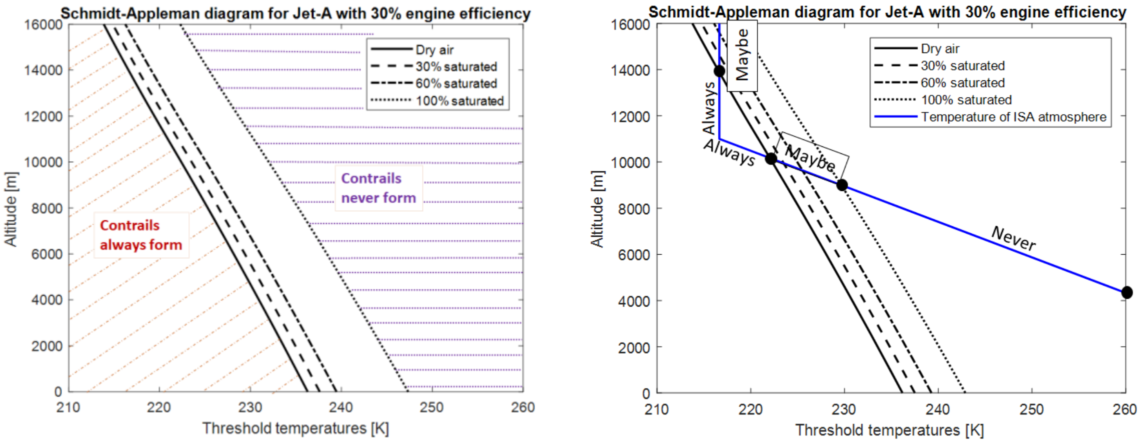

Figure 34: Schmidt-Appleman diagram for engine efficiency of 30%. Threshold temperatures for four different humidities (left) and same chart with ISA condition included. For this case the model predicts that contrails never from zero altitude to 8180 meters. From 8180 to 10150 contrails may form depending on the local air humidity. From 10150 up to 13950 meters contrails will always form and above 13950 up to 16000 meters contrails may again form depending on the local air temperature.

If the simplifying assumptions used to establish the Schmidt-Appleman constant are not made, but a numerical calculation is made the G constant is found to vary only slightly, increasing along the mixing line. This is driven party by the change of c_p along the mixing line. Also, remember that the Schmidt-Appleman constant was derived neglecting the effect of the ambient humidity. For very large dilution, the amount of water from the ambient air eventually gets comparable to the water in the exhaust air. At that point the original assumption is not valid. In the case above it increases from 1.752 to 1.779. A final point is worth making, if the initial conditions are given a straight line could not strictly fulfil a combination of ambient temperature and ambient humidity. It could be drawn to a specific ambient temperature but then the water pressure would not match that of the surrounding. The slight non-linearity adjusts for this.

Motivation for Equation (E1)

For instance, for methane, CH_4 we have:

$$CH_4 + 2O_2 \rightleftharpoons 2H_2O + CO_2$$

First, we compute the mass of hydrogen (m_H) in 1 kg of methane to plug in to E1. The molar mass of methane is 16.042 g/mol. Hence the mass of hydrogen in 1 kg of methane is:

$$m_H = \underbrace{\overbrace{\frac{1000}{16.042}}^{Number\ of\ moles\ of\ CH_4} \cdot 4}_{Number\ of\ moles\ of\ H} \cdot \overbrace{1.008}^{\substack{Molar\ mass\ of\\ hydrogen}} = 251.3\ grams$$

This is the mass of the hydrogen in 1 kg of methane. Since all of the hydrogen goes to produce water, there are no other products of the combustion that contains hydrogen atoms, we get:

$$EI_{H_2O} = \underbrace{\overbrace{\frac{m_H}{M_H}}^{\substack{Number\ of\ moles\\ of\ hydrogen\ from\ 1\ kg\\ methane}} \cdot \frac{1}{2}}_{\substack{Number\ of\ moles\ of\\ water}} \cdot M_{H_2O} = 2.246\ [kg\ H_2O\ per\ kg\ combusted\ CH_4]$$

The expression just above confirms the stated form of (E1). For Jet-A the emission index is 1.238 and for hydrogen we get 8.937.

APPENDIX F (not in MMS196) - NOx emissions prediction methods

There are many NOx emissions prediction methods for turbofan engines available in open literature. Among them, some methods require proprietary information which largely rely on specific engine performance models and combustor designs to determine the emissions levels. On the other hand, emissions at sea level for modern existing engines are publicly available in the ICAO emissions databank [21]. Some emissions prediction methods have been developed to **extrapolate the emission databank results to other operating conditions.** Here we present two such simple extrapolation methods, the European Association of Aerospace Industries method (AECMA) and the Boeing Fuel Flow Method 2 (BFFM2).

The AECMA correlation

Calculation of the NO_x emissions index from the AECMA method is rather straightforward, and is computed from the expression below:

$$EINO_X = 2.0 + 28.5\sqrt{\frac{P_3}{3100}}\exp\left(\frac{T_3-825}{250}\right) \qquad \text{(F1)}$$

where p3 and T3 are the compressor outlet pressure and temperature in kPa and K, respectively, and $EINO_x$ is in g NO_x per kg fuel combusted. This correlation is said to provide a good estimate of the emissions of modern large engines [22, 23] and for single annular type combustors [24].

The Boeing Fuel Flow Method 2 (BFFM2)

The BFFM2 method [25, 26] is now outlined. The method allows the estimation of NOx emissions for any aircraft altitude and ambient condition. The first step is to make an initial mapping of the flight level (FL) fuel flow $W_{f_{FL}}$ to the corresponding sea level (SL) fuel flow $W_{f_{SL}}$ including temperature and pressure corrections.

$$W_{f_{SL}} = W_{f_{FL}}\left(\frac{\theta_{amb}^{3.8}}{\delta_{amb}}\right)e^{0.2M^2} \qquad \text{(F2)}$$

where M is the flight Mach number and amb denotes the ambient conditions for which:

$$\theta_{amb} = T_{amb}/288.15 \qquad \text{(F3)}$$

$$\delta_{amb} = \frac{P_{amb}}{101.325} \qquad \text{(F4)}$$

where T_{amb} should be in [K] and P_{amb} in [kPa]. Then, the $EINO_x$ value for the sea level fuel flow $W_{f_{SL}}$ is interpolated using the known certification data points. A log-log interpolation is normally applied. The obtained value is denoted $EINO_{X_{SL}}$. The process is then completed by scaling the obtained value back to the particular altitude condition under study:

$$EINO_{X_{FL}} = EINO_{X_{SL}}\left(\frac{\delta_{amb}^{1.02}}{\theta_{amb}^{3.3}}\right)^{0.5}e^{H} \qquad \text{(F5)}$$

The parameter H in the exponent above (F5) is introduced to increase the accuracy by correcting for humidity variation. The H parameter is obtained from:

$$H = 19(h_{SL} - h_{FL}) \qquad \text{(F6)}$$

For which a sea level reference humidity h_{SL} is set to 0.00634 kg water/kg dry air. This corresponds to 60% relative humidity at sea level ISA condition. Tests are made at a number of conditions and sometimes also varying locations, making it difficult to state an exact number to use. The local term

h_{FL} is obtained from the local temperature estimating the amount of water per kg dry air, from local humidity and the saturation pressure of water:

$$h_{FL} = \frac{(0.622 \cdot RH \cdot P_{sat})}{(P_{amb} - (RH \cdot P_{sat}))} \qquad \text{(F7)}$$

Where the saturation pressure is obtained from the ambient temperature. Oftentimes the relative humidity for the particular flight condition is not measured, then assuming the same (60%) relative humidity is customary. The saturation vapor pressure P_{sat} can be calculated from for instance equation (E6b). Notice the limitation in range of validity for this.

In Table 6 below, the LTO cycle fuel flow and EINOx of two modern representative engines, the PW1100G and the Trent772 have been extracted from the ICAO emissions databank [21]. A log-log plot of the data in Table 6 is also presented in Figure 35.

Table 6: LTO cycle fuel flow and $EINO_x$ [21] for PW1100G series (1127G1-JM) and RR Trent772.

	Pratt&Whitney 1100G		**Rolls-Royce Trent 772**	
	Fuel flow [kg/s]	*EINOx [g NOx/kg Fuel]*	*Fuel flow [kg/s]*	*EINOx [g NOx/kg Fuel]*
Take-off	0.800416	17.76	3.139	35.56
Climb-out	0.661263	14.18	2.53	26.82
Approach	0.232194	8.85	0.821	10.42
Idle	0.089743	6.55	0.27	4.66

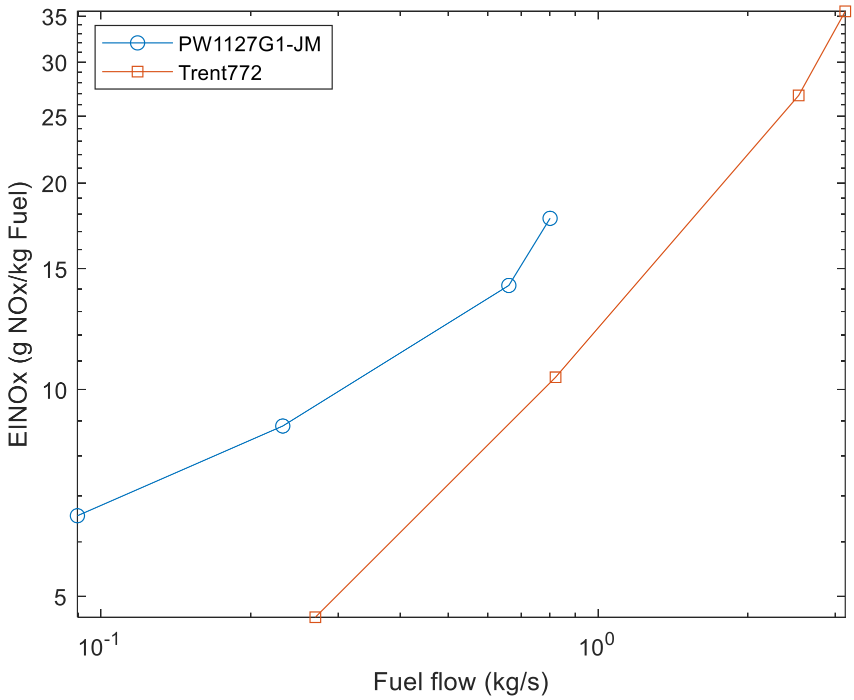

Figure 35 Log-log plot of PW1127G1-JM and Trent772 ICAO emissions data points

Appendix G – sample evaluation of turbofan engine

Exercise: Assume a turbofan engine like the one presented in the figure. Such an engine is, for example, the PW1100G, which is a high bypass geared turbofan engine. For this exercise, the following data can be assumed.

Overall pressure ratio	45
Fan pressure ratio	1.48
Bypass ratio	12.5
HPC pressure ratio	10
Turbine inlet temperature	1650 K
Fan, IPC, HPC polytropic efficiency	0.90
HPT polytropic efficiency	0.85
LPT polytropic efficiency	0.90
Combustor pressure loss	0.04
Total air mass flow	185 kg/s

For an aircraft flying at 10668 meters altitude at a Mach number of 0.78, predict the engine thrust and the SFC, under ISA conditions.

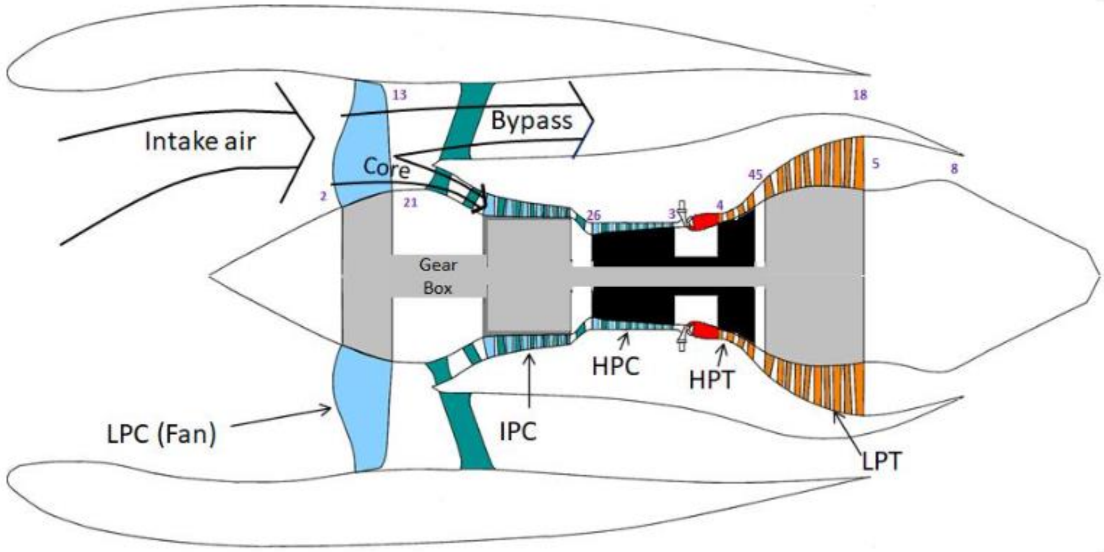

Solution: Firstly, the ambient conditions at 10668 m can be found either from the table in Appendix B or from Equations (2.29a) and (2.29b). Here, the table is used, and a linear interpolation is performed to calculate the atmospheric temperature and pressure:

$$T_0 = 218.81\ K$$

$$p_0 = 23.86\ kPa$$

At the fan entry (station 2), Equations (2.30a) and (2.30b) can be used to calculate the stagnation pressure and temperature:

$$p_{02} = p_0 \cdot \left(1 + \frac{\gamma_a - 1}{2} \cdot M_0^2\right)^{\frac{\gamma_a}{\gamma_a - 1}} = 35.66\ kPa$$

$$T_{02} = T_0 \cdot \left(1 + \frac{\gamma_a - 1}{2} \cdot M_0^2\right) = 245.43\ K$$

The pressure at station 21 is calculated from the FPR as:

$$p_{021} = p_{02} \cdot FPR = 52.77\ kPa$$

Using Equation (2.32), the stagnation temperature at station 21 can be computed with polytropic efficiency:

$$T_{021} = T_{02} \cdot \left(\frac{p_{021}}{p_{02}}\right)^{\frac{1}{\eta_{p,fan}} \cdot \frac{\gamma_a - 1}{\gamma_a}} = 277.96\ K$$

The IPC pressure ratio is calculated from the OPR, FPR and HPC pressure ratio as:

$$r_{IPC} = \frac{OPR}{FPR \cdot r_{HPC}} = 3.04$$

Then, the pressure and temperature at station 26 are given by:

$$p_{026} = p_{021} \cdot r_{IPC} = 160.45\ kPa$$

$$T_{026} = T_{021} \cdot \left(\frac{p_{026}}{p_{021}}\right)^{\frac{1}{\eta_{p,IPC}} \cdot \frac{\gamma_a - 1}{\gamma_a}} = 395.64\ K$$

Similarly, for the HPC:

$$p_{03} = p_{026} \cdot r_{HPC} = 1604.50\ \ kPa$$

$$T_{03} = T_{026} \cdot \left(\frac{p_{03}}{p_{026}}\right)^{\frac{1}{\eta_{p,HPC}} \cdot \frac{\gamma_a - 1}{\gamma_a}} = 821.79\ K$$

The loss in stagnation pressure in the combustor is assumed 4 % and thus, the pressure in station 4 is given by:

$$p_{04} = p_{03} \cdot (1 - dp) = 1540.32\ kPa$$

The turbine inlet temperature is given equal to 1650 K. Then, from the chart in Appendix C the fuel air ratio can be estimated:

$$FAR = 0.0250$$

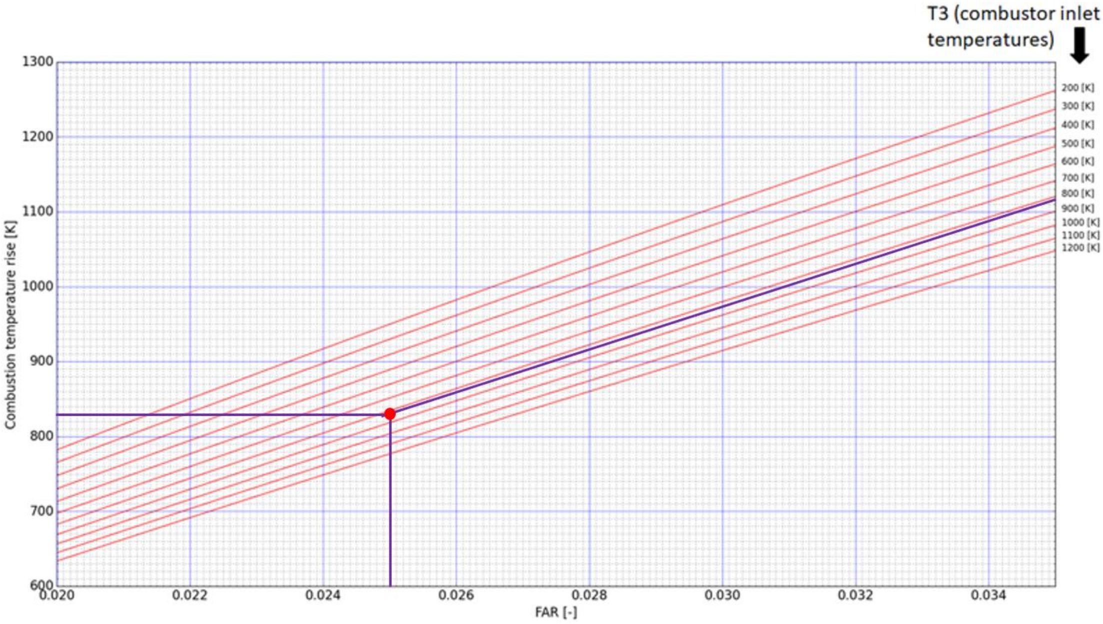

It is then possible to compute the fuel flow:

$$\dot{m}_{bypass} + \dot{m}_{core} = \dot{m} => \dot{m}_{bypass} = \frac{\dot{m}}{1 + \frac{1}{BPR}} = 171.2963\ kg/s$$

$$\dot{m}_{core} = 13.7037\ kg/s$$

$$\dot{m}_f = \dot{m}_{core} \cdot FAR = 0.3426\ kg/s$$

Since the HPC is driven by the HPT, Equation (2.37) can be used to compute the temperature at station 45:

$$\left(\dot{m}_{core} + \dot{m}_f\right) \cdot c_{pg} \cdot (T_{04} - T_{045}) = \dot{m}_{core} \cdot c_{pa} \cdot (T_{03} - T_{026})$$

$$T_{045} = T_{04} - \frac{c_{pa} \cdot (T_{03} - T_{026})}{(1 + FAR) \cdot c_{pg}} = 1286.03\ K$$

The stagnation pressure at this point is calculated from the polytropic efficiency:

$$p_{045} = p_{04} \cdot \left(\frac{T_{045}}{T_{04}}\right)^{\frac{\gamma_g}{(\gamma_g - 1) \cdot \eta_{p,HPT}}} = 476.32\ kPa$$

In the same way the fan and the IPC are driven by the LPT:

$$\left(\dot{m}_{core} + \dot{m}_f\right) \cdot c_{pg} \cdot (T_{045} - T_{05}) = \dot{m} \cdot c_{pa} \cdot (T_{021} - T_{02}) + \dot{m}_{core} \cdot c_{pa} \cdot (T_{026} - T_{021})$$

$$T_{05} = T_{045} - \frac{C_{pa}}{C_{pg} \cdot (1 + FAR)} \cdot \left((1 + BPR) \cdot (T_{021} - T_{02}) + (T_{026} - T_{021})\right) = 810.47\ K$$

The pressure is calculated as before:

$$p_{05} = p_{045} \cdot \left(\frac{T_{05}}{T_{045}}\right)^{\frac{\gamma_g}{(\gamma_g - 1) \cdot \eta_{p,LPT}}} = 61.10\ kPa$$

To check if the nozzles are choked the critical pressure ratio should be calculated for the cold and hot nozzle respectively:

$$\frac{p_{018}}{p_{18}} = \left(\frac{1+\gamma_a}{2}\right)^{\frac{\gamma_a}{\gamma_a-1}} = 1.893$$

$$\frac{p_{08}}{p_8} = \left(\frac{1+\gamma_g}{2}\right)^{\frac{\gamma_g}{\gamma_g-1}} = 1.852$$

Then,

$$\frac{p_{013}}{p_0} = \frac{p_{021}}{p_0} = 2.212 > 1.893$$

$$\frac{p_{05}}{p_0} = 2.561 > 1.852$$

Hence, both nozzles are choked and the speed at the exit is sonic. Then, the limit can be used to compute p_{18}, T_{18}, p_8 and T_8. Starting with the cold stream:

$$p_{18} = \frac{p_{018}}{1.893} = 27.88\ kPa$$

$$T_{18} = \frac{2}{1+\gamma_a} T_{021} = 231.63\ K$$

The speed of sound at this temperature is:

$$a_{18} = \sqrt{\gamma_a \cdot R \cdot T_{18}} = 305.07\ m/s$$

And the exhaust velocity:

$$c_{18} = M_{18} \cdot a_{18} = 305.07\ m/s$$

The density can be calculated from Equation (2.8):

$$\rho_{18} = \frac{p_{18}}{R \cdot T_{18}} = 0.4193\ kg/m^3$$

Then, the cold nozzle required area is obtained from Equation (2.18):

$$A_{18} = \frac{\dot{m}_{bypass}}{c_{18} \cdot \rho_{18}} = 1.3390\ m^2$$

The same parameters are calculated for the hot stream:

$$p_8 = \frac{p_{08}}{1.852} = 32.98\ kPa$$

$$T_8 = \frac{2}{1+\gamma_g} T_{05} = 694.79\ K$$

$$a_8 = \sqrt{\gamma_g \cdot R \cdot T_8} = 515.56\ m/s$$

$$c_8 = M_8 \cdot a_8 = 515.56\, m/s$$

$$\rho_8 = \frac{p_8}{R \cdot T_8} = 0.1654\, kg/m^3$$

$$A_8 = \frac{\dot{m}_{core} + \dot{m}_f}{c_8 \cdot \rho_8} = 0.1647\, m^2$$

The thrust is finally calculated by:

$$F = (\dot{m}_{core} + \dot{m}_f) \cdot c_8 + A_8 \cdot (p_8 - p_0) + \dot{m}_{bypass} \cdot c_{18} + A_{18} \cdot (p_{18} - p_0) - \dot{m} \cdot c_0 = 23603\, N$$

And the specific fuel consumption:

$$SFC = \frac{\dot{m}_f}{F} = 14.51\, mg/Ns$$

Schmidt-Appleman Theory[5]: With the models of appendix E an estimate whether the engine will produce persistent contrails can be made. For Jet-A the emission index of water, EI_{H_2O}, is 1.238. This is based on an assumed composition of $C_{12}H_{23}$. This can be confirmed from Equation (E1). The mass of hydrogen in 1 kg of $C_{12}H_{23}$, that is m_H, is:

$$1\ kg\ C_{12}H_{23} \Leftrightarrow \frac{1000}{M_{C_{12}H_{23}}} = 5{,}97\ mole\ \Longrightarrow 5{,}97 \cdot 23 = 137{,}5\ mole\ H\ \Longrightarrow$$

$$m_H = 138{,}5\ gram$$

Thus Equation (E1) gives:

$$EI_{H_2O} = \frac{m_H M_{H_2O}}{2M_H} = \frac{138{,}5 \cdot 18{,}01468}{2 \cdot 1{,}00784} = 1238 \text{ gram } H_2O \text{ per kg } C_{12}H_{23}$$

Assuming that the ambient air is dry, we can then compute the mass fraction in the exhaust plume. The total amount of water originates from the combustion only, according to $m_{H_2O,\,tot} = 1.238 \cdot 0.3426 = 0.424\ kg/s$ water in the exhaust. The specific mass content is then:

$$m_{H_2O,P} = \frac{m_{H_2O,\,tot}}{\dot{m}_{bypass} + \dot{m}_{core}} = 0.002293$$

A corresponding partial pressure of water can be established:

$$m_{H_2O,P} = \frac{M_{H_2O}}{M_{air}} \cdot \underbrace{\frac{p_{H_2O,P}}{p}}_{\substack{molar\ fraction \\ of\ water}} \Longrightarrow p_{H_2O,P} = \frac{m_{H_2O,P}\, p M_{air}}{M_{H_2O}} = 87.9\ Pa$$

It would be possible to compute the appropriate temperature for the plume by introducing the stagnation temperature relative to the earth and correct for energy transferred through potentially choked nozzles. However, it is much easier to follow the steps outlined by Schmidt/Appleman and use:

[5] For the MMS196 course, you are not required to be able to perform such calculations, read what is in the main text on contrails and what's in the lecture notes.

$$Q(1-\eta)$$

The added heat per unit time is:

$$Q = \dot{m}_f \mathrm{LHV}_{C_{12}H_{23}} = 0.3426 \cdot 43.0 = 14.7 \text{ MW}$$

The overall efficiency η is then:

$$\eta = \frac{Fc_0}{Q} = 0.371$$

The energy lost in the exhaust is then:

$$Q(1-\eta) = 14.7 \cdot 0.629 = 9.273 \text{ MW}$$

A consistent exhaust condition is then established from this energy loss using Equation (E5):

$$T_{0,plume} = \frac{Q(1-\eta)}{c_{pa}\left(\dot{m}_{bypass} + \dot{m}_{core}\right)} + T_{0,ambient} = 268.6\ K$$

Now we compute the Schmidt/Appleman constant:

$$G = \frac{EI_{H_2O} c_{pa} p}{\frac{M_{H_2O}}{M_{air}} Q(1-\eta)} = 1{,}76\ Pa/K$$

Introducing the mixing line together with the mixing curves produces:

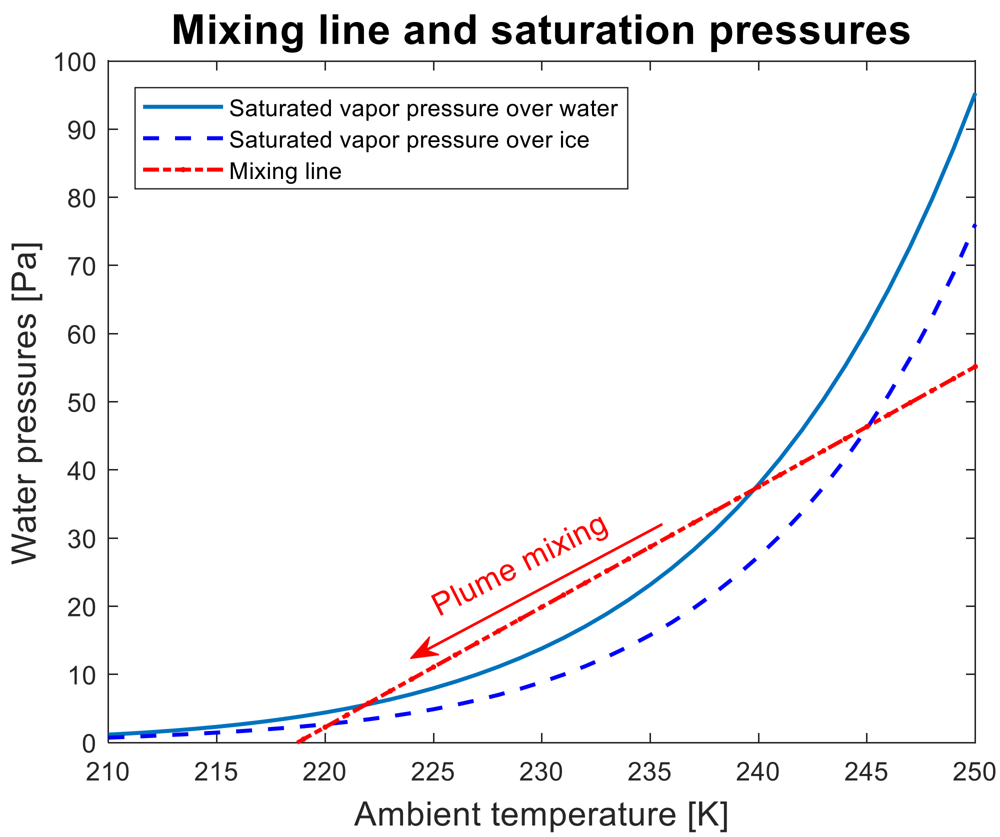

NOx emissions prediction – The Boeing Fuel Flow Method 2 (BFFM2)[6] With the method BFFM2 detailed in appendix F, the NO_x emissions index for the engine at cruise could be estimated. As the aircraft is flying at 10668 meters altitude and at a Mach number of 0.78, we have:

$$\theta_{amb} = \frac{T_0}{288.15} = \frac{218.81}{288.15} = 0.7594$$

$$\delta_{amb} = \frac{p_0}{101.325} = \frac{23.86}{101.325} = 0.2355$$

We can then estimate the corresponding sea level fuel flow using Equation (F2):

$$W_{f_{SL}} = W_{f_{FL}} \left(\frac{\theta_{amb}^{3.8}}{\delta_{amb}}\right) e^{0.2M^2} = 0.3426 * \left(\frac{0.7594^{3.8}}{0.2355}\right) e^{0.2*0.78^2} = 0.5773 \text{ kg/s}$$

For the PW1100G engine series a number of data can be found in the database. See the compendium for a reference. Here we use the particular variant PW1127G1-JM. The EINOx and fuel flow data from the ICAO data have been reproduced in Table 6 of appendix F.

The $EINO_{X_{SL}}$ factor needed for equation (F5) could then be obtained from a log-log linear interpolation. For a general interpolation between two points (x_1, y_1) and (x_2, y_2) we have:

$$\log(y) = \log(y_1) + \frac{(\log(y_2) - \log(y_1))}{(\log(x_2) - \log(x_1))}(\log(x) - \log(x_1))$$

Since the fuel flow is between the climb-out and approach point we then interpolate according to:

$$\log(EINO_{X_{SL}}) = \log_{10} EINO_{X_{approach}} + \frac{\log_{10} EINO_{X_{climb-out}} - \log_{10} EINO_{X_{approach}}}{\log_{10} W_{f_{climb-out}} - \log_{10} W_{f_{approach}}} \cdot \left(\log_{10} W_{f_{SL}} - \log_{10} W_{f_{approach}}\right)$$

Plugging in values gives:

$$EINO_{X_{SL}} = 10^{\left(\log_{10} 8.85 + \frac{\log_{10} 14.18 - \log_{10} 8.85}{\log_{10} 0.661263 - \log_{10} 0.232194} \cdot (\log_{10} 0.5773 - \log_{10} 0.232194)\right)} = 13.2554 \text{ g NOx/kg Fuel}$$

To calculate the humidity adjustment, firstly we need to compute the P_{sat}, where we have

$$T_{ambc} = T_0 - 273.15 = -54.34 \text{ °C}$$

Since the ambient temperature is within the valid range of equation E6b in appendix E we get:

$$P_{sat} = 0.041514 \, mbar$$

The humidity ratio is then:

$$h = \frac{(0.622*0.6*0.041514)}{(23860-(0.6*0.041514))} = 0.000064937 \text{ kg water/kg dry air}$$

The humidity adjustment H is then:

$$H = 19 * (0.00634 - 0.000064937) = 0.1192$$

Finally, we could get the NOx emissions index at the cruise point:

[6] For the MMS196 course, you are not required to be able to perform such calculations, read what is in the main text on NOx emissions and what's in the lecture notes.

$$EINO_{X_{FL}} = EINO_{X_{SL}}\left(\frac{\delta_{amb}^{1.02}}{\theta_{amb}^{3.3}}\right)^{0.5} e^{H} = 11.2486 \text{ g NOx/kg Fuel}$$

istent due to

References

[1] J. D. Mattingly, W. H. Heiser and D. T. Pratt, Aircraft Engine Design, Reston, VA: AIAA, 2002.

[2] Rolls-Royce, The Jet Engine, London: Wiley, 2005.

[3] B. J. McBride and S. Gordon, "Computer Program for Calculation of Complex Chemical Equilibrium Compositions and Applications II. Users Manual and Program Description," NASA, Cleveland, Ohio, 1994.

[4] A. D. Anderson, N. J. Renner, Y. Wang, S. Agrawal, S. Sirimanna, D. Lee, A. Banerjee and K. Haran, "System Weight Comparison of Electric Machine Topologies for Electric Aircraft Propulsion," in *AIAA Propulsion Energy Forum*, Cincinnati, Ohio, 2018.

[5] J. B. Bird, "A Review of Electric Aircraft Drivetrain Motor Technology," *IEEE*, 2005.

[6] J. Bertrand, "Sur l'homogénéité dans les formules de physique"," *Comptes Reundus.*, vol. 86, no. 15, pp. 916-920, 1878.

[7] S. Dixon and C. Hall, Fluid Mechanics and Thermodynamics of Turbomachinery, Oxford: Butterworth-Heinemann, 2014.

[8] D. S. Lee, D. Fahey, A. Skowron, M. R. Allen, U. Burkhardt, Q. Chen, S. J. Doherty, S. Freeman, P. M. Forster, J. Fuglestvedt, A. Gettelman, R. De Leon, L. L. Lim, M. T. Lund, R. J. Millar, B. Owen, J. E. Penner, G. Pitari, M. J. Prather, R. Sausen and L. M. Wilcox, "The contribution of global aviationto anthropogenic climate forcing for 2000 to 2018," *Atmospheric Environment*, vol. 244, 2021.

[9] N. Cumpsty, D. Mavris, J. Alonso, F. Catalano, C. Eyers, M. Guitines, T. Grönstedt, J. Hileman, A. Joselzon, I. Khaletskii, O. F., M. Ralph, S. J., R. Wahls and D. Zingg, "INDEPENDENT EXPERT INTEGRATED TECHNOLOGY GOALS ASSESSMENT AND REVIEW FOR ENGINES AND AIRCRAFT," ICAO, Quebec, Canada, 2019.

[10] European Commission, "Flightpath 2050 Europe's Vision for Aviation," Publications of the Office of The European Union, Brussels, Belgium, 2011.

[11] V. Grewe, A. G. Rao, T. Grönstedt, C. Xisto, L. F., J. Middel, B. Ohlenforst, S. Blakey, S. Christie, M. S. and K. Dahlmann, "Valuating the climate impact of aviation emission scenarios towards the Paris Agreement including COVID-19 effects," *Nature communications, 12, 3841,* 2021.

[12] IRENA, "BIOFUELS FOR AVIATION," International Renewable Energy Agency, Abu Dhabi, 2017.

[13] P. Kågeson, "Flygets klimatutmaningar – en analys," Nature Associates, 2018.

[14] K. Dahal, S. Brynolf, C. Xisto, J. Hansson, M. Grahn, T. Grönstedt and M. Lehtveer, "Techno-economic review of alternative fuesl and propulsion systems for the aviation sector," *Renewable and Sustainable Energy Reviews,* vol. 151, 2021.

[15] A. Capitao-Patrao, I. Johnsson, C. Xisto, A. Lundbladh and T. Grönstedt, "Compact heat exchangers for hydrogen-fueled aero engine intercooling and recuperation," *Applied Thermal Engineering,* vol. 243, 2024.

[16] M. Grahn, M. Taljegard and S. Brynolf, "Electricity as an Energy Carrier in Transport," in *EVS 31 & EVTeC,* Kobe, Japan, 2018.

[17] K. Field, "Tesla Model 3 Battery Pack & Battery Cell Teardown Highlights Performance Improvements," 2019. [Online]. Available: https://cleantechnica.com/2019/01/28/tesla-model-3-battery-pack-cell-teardown-highlights-performance-improvements/. [Accessed 27 August 2021].

[18] A. H. Epstein and S. M. O'Flarity, "Considerations for Reducing Aviation's CO2 with Aircraft Electric Propulsion," *Journal of Propulsion and Power,* vol. 35, no. 3, pp. 572-582, 2019.

[19] U. Schumann, "On conditions for contrail formation from aircraft exhausts," *Meteorologische Zeitschrift,* vol. 5, pp. 4-23, 1996.

[20] D. M. Murphy and T. Koop, "Review of the vapour pressures of ice and supercooled water for atmospheric applications.," *Q. J. R. Meteorol. Soc.*, vol. 131, p. 1539–1565, 2005.

[21] EASA, "ICAO Aircraft Engine Emissions Databank," [Online]. Available: https://www.easa.europa.eu/en/domains/environment/icao-aircraft-engine-emissions-databank. [Accessed 22 August 2023].

[22] J. E. Green, "Greener by design—the technology challenge," *The Aeronautical Journal* , vol. 106, no. 1056, pp. 57-113, 2002.

[23] "Influence of Engine Cycle on Emissions, Aeronet Working Paper Nr 2," in *Results of a workshop held at Munich on 14 September 1999,* Munich, 1999.

[24] N. Chandrasekaran and A. Guha, "Study of prediction methods for NOx emission from turbofan engines," *Journal of Propulsion and Power,* vol. 28, no. 1, pp. 170-80, 2012.

[25] D. DuBois and G. C. Paynter, ""Fuel Flow Method2" for Estimating Aircraft Emissions," *SAE Technical Paper Series 2006-01-1987,* 2006.

[26] S. L. Baughcum, T. G. Tritz, S. C. Henderson and D. C. Pickett, "Scheduled Civil Aircraft Emission Inventories for 1992: Database Development and Analysis," NASA Contractor Report 4700, 1996.

[27] S. Farokhi, Aircraft propulsion, West Sussex: Wiley, 2014.

[28] M. James, "mikejamesmedia.com," [Online]. Available: http://www.mikejamesmedia.com/genx_1b_engine_02.html. [Accessed 28 August 2021].

[29] S. A. S. AIRBUS, "A321 AIRCRAFT CHARACTERISTICS AIRPORT AND MAINTENANCE PLANNING," Airbus, Tolouse, 2020.

[30] P. Minnis, J. K. Ayers, R. Palikonda and D. Phan, "Contrails, cirrus trends, and climate," *Journal of Climate,* vol. 17, pp. 1671-1685, 2004.